UNIVERSITE LOUIS PASTEUR

INSTITUT DE MECANIQUE DES FLUIDES ET DES SOLIDES

UMR CNRS 7507

THESE

Présentée en vue de l'obtention du grade de

DOCTEUR DE L'UNIVERSITE LOUIS PASTEUR DE STRASBOURG

Spécialité : Mécanique des fluides

Par

Taef ZUHAIR SALMAN ASWED

MODELISATION DE LA POLLUTION DE LA NAPPE D'ALSACE PAR SOLVANTS CHLORES

Soutenue le 13 novembre 2008 devant le jury constitué de :

MM.	REMOND Yves	Rapporteur interne
	BUES Michel	Rapporteur externe
	VAUCLIN Michel	Rapporteur externe
	ACKERER Philippe	Directeur de Thèse
	MERHEB Fadi	Examinateur

à mes parents…

REMERCIEMENTS

Je tiens à remercier en tout premier lieu Monsieur Philippe ACKERER, Directeur de Recherche CNRS et Directeur Adjoint de l'IMFS, qui a dirigé cette thèse dans la continuité de mon stage de DEA. Tout au long de ces années, il a su orienter mes recherches aux bons moments et il a toujours été disponible pour d'intenses et rationnelles discussions. Pour tout cela, je le remercie vivement.

Pour reprendre un ordre plus chronologique, je voudrais remercier deux amis qui ont joué un rôle fondamental dans ma formation: Mohamed HAYEK et Hussein HOTEIT. Merci à eux d'avoir partagé leurs idées et expériences.

Je remercie tous particulièrement Monsieur Michel VAUCLIN, Directeur de Recherche CNRS du LTHE Grenoble et Monsieur Michel BUES, Professeur à l'Université de Nancy, qui ont accepté de juger ce travail et d'en être les rapporteurs externes. Je remercie également Monsieur Fadi MERHEB Expert référent au BURGEAP, d'avoir accepté d'être examinateur de cette thèse.

Je remercie mon président du jury, Monsieur Yves REMOND, professeur à l'ULP, d'être rapporteur interne, mais aussi pour m'avoir accueillie au sein de l'institut qu'il dirige.

Plusieurs collègues m'ont fait partager leurs compétences scientifiques, techniques, ou linguistiques. Je pense en particulier à: Anis YOUNES, Ingrid POLLET, Marwan FAHS et Romain ARMAND.

Je remercie mes amis et camarades de l'institut: Benjamin, Charbel, Hussein, Jérôme et Selim. Un merci particulier à Monsieur François LEHMANN, Maître de Conférences à l'ULP, pour ces qualités humaines et pour sa disponibilité aux moments où j'avais des problèmes techniques avec mon PC.

Je remercie aussi l'ensemble du personnel administratif et technique qui contribue souvent à entretenir et améliorer nos conditions de travail.

Ainsi je remercie l'ambassade de France à Bagdad de m'avoir accorder une bourse d'étude (BGF) pour mon DEA et ma thèse afin que je puisse achever ce travail. Je remercie en particulier Monsieur Christian COUTURAUD attaché culturel à l'ambassade.

Mes plus profonds remerciements vont à ma famille: mes parents, mes sœurs Arwa, Hanadi et Zahaa, mon frère Mustapha, qui m'ont soutenue, encouragée et aidée tout au long de mon cursus. Ils ont su me donner toutes les chances pour réussir.

Enfin, mes dernières pensées vont à mon mari Mohamed HAYEK et ma petite fille Naya, née durant cette aventure.

CONTENTS

LIST OF FIGURES

LIST OF TABLES

ABBREVIATIONS

ANN: artificial neural network

ASTM: American society of testing and materials

ATSDR: agency for toxic substances and disease registry

$BC_{(S)}$: boundary condition(s)

BRGM : bureau de recherche géologique et minière

BTC: breakthrough curve

BURGEAP: bureau de géologie appliquée

BUA: Beratergremium für umweltrelevante Altstoffe

CCl_3. : trichloromethyl radical

CCl_4: carbon tetrachloride

CEREG: centre d'études et de recherches eco-géographiques

CF: chloroform

CH_4: methane

CIENPPA: commission interministérielle d'étude de la nappe phréatique de la plaine d'Alsace

CM: chloromethane

CO_2: carbon dioxide

CPHF: California public health foundation

1D, 2D, 3D: one-, two-, three-dimensional

DCM: dichloromethane

DDA: direction départmentale de l'agriculture

DDASS: direction départementale des affaires sanitaires et sociales

DG: discontinuous Galerkin

DIREN : direction régionale de l'environnement

$DNAPL_{(S)}$: Dense non-aqueous phase $liquid_{(S)}$

EPA: environmental protection agency

FD: finite difference

FV: finite volume

GA: genetic algorithm

GAC: granular activated carbon

HCl: finite difference

HSG: health and safety guide

IMFS: institut de mécaniques des fluids et solids

IPCS: international programme on chemical safety

MC: Monte-Carlo

MCL: maximum contaminant level

MCLG: maximum contaminant level goals

ME: mean error

MHFE: mixed hybrid finite element

$NAPL_{(S)}$: non-aqueous phase $liquid_{(S)}$

NIOSH: national institute for occupational safety and health

OH^-: hydroxide

OSHA: occupational safety and health administration

PIREN: programme interdisciplinaire de recherche en environnement du CNRS

SD: standard deviation

SEMA: service des eaux et des milieux aquatiques de la DIREN

SGAL: service géologique d'Alsace-Lorraine

TCE: trichloroethylene

TRACES: Transport of RadioACtiver Elements in the Subsurface

UNEP: united nations environment programme

VOC: volatile organic chemical

WHO: world health organization

RESUME

Introduction

Les eaux souterraines représentent une grande part des réserves en eau potable de la terre. Elles constituent une ressource de qualité, généralement supérieure à celle des eaux de surface, du fait de la protection relative due aux couches de couverture et aux propriétés filtrantes de l'aquifère. Cependant, face à l'accroissement des phénomènes de pollution, celles-ci deviennent de plus en plus vulnérable, et se pose alors le problème de la qualité de la ressource en eau souterraine, qui devient vital à long terme.

Pour protéger et préserver l'aquifère, il faut être capable de comprendre son mode de fonctionnement. La quantification des paramètres qui régissent l'écoulement de la nappe est devenue un impératif tant pour l'évolution et la gestion des ressources en eau, que pour les études d'environnement. Etant donnée la grande complexité des processus hydrogéologiques, due à l'interaction entre le terrain et l'eau, la connaissance des variations, dans l'espace et dans le temps, d'un grand nombre de paramètres physiques, essentiellement hydrodynamiques et structuraux, est nécessaire. La représentation de tous ces paramètres dans un modèle est donc très utile. Malheureusement, les paramètres d'un modèle sont très incertains. Ces incertitudes sur les paramètres doivent être prises en compte afin de garantir une meilleure modélisation de la pollution dans l'aquifère.

Cette thèse entre dans le cadre de la modélisation de la pollution de la nappe d'Alsace par un solvant chloré, le tétrachlorure de carbone (CCl_4). En effet, suite à un accident en 1970, un camion citerne contenant du CCl_4 s'est renversé à Benfeld, ville située à l'amont hydraulique d'Erstein, entraînant une pollution de la nappe phréatique par ce solvant chloré. Pour protéger les ressources en eau, beaucoup d'études ont été effectuées afin de connaître l'état hydrodynamique et la qualité de l'eau de la nappe. Cette thèse a pour but principal d'étudier le comportement de la source du contaminant et d'estimer sa migration dans l'aquifère à long terme.

Le manuscrit est organisé comme suit: au premier chapitre, nous présentons le contexte de l'étude et les principaux mécanismes liés à ce polluant (dissolution, volatilisation, sorption, dégradation). Dans le deuxième chapitre, nous rappelons les équations classiques de l'hydrodynamique et du transport monophasique par convection et dispersion d'un soluté en milieu poreux saturé. Nous présentons également et d'une façon générale, la méthode numérique de résolution des équations correspondantes, par le code TRACES développé à l'IMFS. Le troisième chapitre concerne la modélisation de la pollution de l'aquifère rhénan par le CCl_4. Le quatrième chapitre est consacré à la méthode utilisée pour déterminer la source et à l'analyse des résultats. Une analyse des incertitudes de la source liées aux incertitudes sur les paramètres a été effectuée dans ce chapitre afin d'améliorer les résultats. Finalement, nous terminons le manuscrit par une conclusion et quelques perspectives.

Chapitre 1: CCL_4 Pollution history of the Alsatian aquifer

La nappe d'Alsace est située dans le Nord-Est de la France et atteint la frontière avec l'Allemagne. L'aquifère alsacien s'étend sur une superficie de 3000 km^2 et est constitué d'un volume d'alluvions d'environ 250 milliards de m^3. Cet aquifère est l'une des plus grandes réserves d'eau en Europe. Il contient environ 50 milliards de m^3 d'eau souterraine avec un renouvellement annuel de 1.3 milliards de m^3. Le problème a commencé en 1970, quand un camion citerne contenant du tétrachlorure de carbone (CCl_4) s'est renversé à Benfeld, ville de l'Alsace située à une trentaine de kilomètre au sud de Strasbourg. Après un certain nombre d'années, les analyses montrent des concentrations de CCl_4 très élevées au niveau du captage d'eau à Erstein, une ville située à une dizaine de kilomètre au nord de Benfeld. L'état de pollution sérieuse est affirmé en 1992 avec des teneurs en CCl_4 de 60 μg/l dans les puits qui alimentent la population. Cette quantité est trop élevée selon le code de la santé publique révisé en 1989 qui fixe le danger à 1 μg/l. Dès lors, des mesures d'urgence s'imposèrent pour protéger les utilisateurs. Une recherche de l'origine de la pollution fut engagée et des dispositions pour enrayer la situation s'avérèrent nécessaire puisque celle-ci semblait se prolonger.

Plusieurs travaux ont été effectués dans le passé pour étudier la migration de CCL_4 dans l'aquifère alsacienne. Parmi ces travaux on peut citer Vigouroux et al. (1983) qui ont utilisé un modèle numérique 2D afin d'étudier quelques cas de pollution de la nappe. Hamond (1995) a utilisé un modèle 2D pour l'écoulement et un modèle 3D pour le problème couplé (écoulement et transport) pour modéliser la pollution en utilisant des données recueillies entre les années 1970 et 1993. En 1999, Beyou (1999) a complété le travail de Hamond en utilisant des nouvelles données obtenues entre les années 1993 et 1999. Il est important de signaler qu'aucun de ces travaux n'a mené à des résultats entièrement satisfaisants.

Notre travail a pour but d'améliorer les résultats de ces modélisations en adoptant une nouvelle technique d'estimation de la source de contaminant, en tenant en compte des incertitudes sur cette source et en utilisant des nouvelles données récoltées entre les années 1999 et 2004. Les principales difficultés du travail peuvent être résumées ainsi :

- La quantité exacte du polluant infiltrée dans le sol est inconnue, une partie est enlevée juste après l'accident et une autre partie a disparu par vaporisation.
- L'évolution de la source est inconnue en espace et en temps.
- Il y a des problèmes d'incertitudes liées aux paramètres de la nappe comme la porosité, la perméabilité, la dispersivité,…
- Les propriétés du polluant comme la solubilité dans l'eau, la diffusion, la volatilisation, les coefficients de dégradation,… sont mal connues.

Face à ces difficultés, nous avons effectué une étude bibliographique approfondie sur le polluant CCl_4 afin d'aboutir à des hypothèses qui nous permettent de résoudre le problème. Ces recherches bibliographiques montrent que ce solvant chloré peut être considéré comme un traceur dans l'eau car :

- La dégradation du CCl_4 est négligée puisque notre aquifère est typiquement aérobie, et les études bibliographiques montrent qu'il n'y a pas de dégradation de CCl_4 sous condition d'aérobie.
- L'adsorption n'est pas importante due de la faible valeur du coefficient de distribution K_d (environ 0.11 l/kg),
- la volatilisation peut être négligée puisque le domaine d'étude est un milieu saturé en eau.

Chapitre 2: Basic equations of flow and transport in porous media

Dans ce chapitre, nous présentons le modèle mathématique utilisé pour modéliser la pollution de la nappe ainsi que les méthodes numériques adoptées pour résoudre les équations. La migration du contaminant est décrite par l'équation de l'écoulement et l'équation de transport. L'équation de l'écoulement est régie par deux équations principales qui sont loi de Darcy et l'équation de continuité. La loi de Darcy exprime la vitesse de filtration en fonction du gradient de charge. L'équation de continuité exprime le principe de la conservation de la masse d'un fluide en mouvement. Dans un volume élémentaire, la masse du fluide prélevé ou injecté est égale à la somme de la variation de la masse du fluide durant un intervalle de temps élémentaire et des flux massiques traversant la surface de ce volume. Le transport de polluant est décrit par l'équation de convection-dispersion.

Le model numérique TRACES (Transport of RadioACtive Elements in the Subsurface) est un code numérique (2D-3D) développé au sein de l'équipe HTMP (Hydrodynamique et Transfert en Milieu Poreux) de l'IMFS qui permet de simuler l'écoulement et le transport réactif dans un milieu poreux saturé. Dans TRACES, l'équation de l'écoulement est résolue par la méthode des Eléments Finis Mixtes Hybrides (EFMH) qui est basée sur l'espace de Raviart-Thomas de l'ordre le plus faible. Avec la méthode EFMH, la charge hydraulique et la vitesse de Darcy sont approchées simultanément avec le même ordre de convergence. L'équation de transport est résolue en utilisant la technique de séparation d'opérateurs. L'intérêt de cette technique est de séparer l'équation de transport en différentes sous équations, qui sont traitées chacune de manière spécifique. Cette technique permet ainsi de traiter des processus différents comme la convection et la diffusion avec des méthodes appropriées pour chaque type d'équation aux dérivées partielles. Avec cette technique, le terme de diffusion est résolu par la méthode EFMH et le terme de convection est résolu par la méthode des éléments finis discontinus de Galerkin (EFDG). La méthode des EFDG est très largement répandue pour le calcul numérique des solutions des lois de conservation, en particulier les équations de convection. Elle permet de traiter de façon naturelle et robuste les lois de conservation et peut s'appuyer sur des structures à géométrie complexe. Afin d'éviter les oscillations non-physiques, la méthode des EFDG est stabilisée par un schéma

de limitation de pente. Finalement, notons que la combinaison des méthodes EFMH et EFDG permet de conserver la masse à l'échelle de la maille.

Chapitre 3: The CCl_4 modelling pollution in the Alsatian aquifer

Dans ce chapitre, nous nous intéressons au modèle numérique utilisé pour modéliser la pollution dans la nappe d'Alsace. La modélisation du système se fait en deux phases. La première phase consiste à l'utilisation d'un modèle d'écoulement à grande échelle entre Kogenheim et Strasbourg. La description des processus se fait dans un cadre bidimensionnel (modèle hydrodynamique 2D). La deuxième phase se base sur les résultats acquis de la modélisation 2D pour constituer un modèle couplé d'écoulement et de transport d'approche tridimensionnelle (modèle hydrochimique 3D), prenant en compte les variations de paramètres sur toute l'épaisseur de l'aquifère. Le domaine d'étude, dans ce cas, est réduit au secteur géographique contaminé, et susceptible de l'être en moyen terme, c'est-à-dire entre Benfeld et Illkirch.

Le calage du modèle 2D se fait en régime permanent. Le domaine d'étude a été étendu sur sa partie Ouest jusqu'à la limite de la nappe. Il concerne ainsi une superficie de 25 km de large en moyenne et d'un peu moins de 35 km du Nord au Sud. Une telle extension permet d'imposer des conditions aux limites de débit conformes au milieu naturel, d'inclure davantage de points de mesures piézométriques pour le calage du modèle et de rendre négligeable l'influence des conditions aux limites sur la piézométrie dans le domaine Benfeld-Erstein. Chaque extrémité du domaine 2D présente des caractéristiques hydrologiques naturelles spécifiques. Celles-ci constituent trois types de conditions aux limites :

- A l'amont et à l'aval du domaine, les frontières sont définies par des conditions aux limites de Dirichlet (charges hydrauliques imposées).
- Des limites de Neumann (flux imposés) sont attribuées à l'Ouest, en bordure vosgienne qui représente la limite d'alluvions.
- A l'est, la limite du domaine d'étude suit le cours du Rhin. La condition introduite dans le modèle sur cette limite est du type échange nappe-rivière.

La discrétisation du domaine 2D à modéliser se fait par des mailles triangulaires. Ce type de maillage permet de bien décrire la géométrie de la nappe et de suivre les rivières.
Le modèle 3D comporte dix couches d'épaisseurs variables entre 5m et 15m. Elles sont fragmentées en zones ayant des propriétés hydrodynamiques (porosité, dispersivité, conductivité hydraulique) différentes afin de restituer la structure complexe de l'aquifère. Le domaine d'étude établi pour l'approche tridimensionnelle de la pollution est orienté approximativement dans le sens de l'écoulement de la nappe entre Benfeld et Erstein, c'est-à-dire Sud-Ouest/Nord-Est. La zone concernée se situe à l'intérieur d'un rectangle de 6 km de large et 20 km de long sur des dizaines de mètre (environ 110 m) en profondeur. Les charges hydrauliques calculées dans le modèle 2D sont utilisées comme conditions aux limites du modèle 3D. Afin de résoudre l'équation de transport, un maillage non-uniforme prismatique de 45460 mailles (en fonction de la structure topographique de la nappe) a été utilisé.

Les données utilisées dans ce travail sont constituées de l'ensemble des mesures de concentration réalisées entre les années 1992 et 2004. Sur les 24 stations de mesures (284 valeurs) sont retenues 16 stations procurant 236 valeurs mesurées sur cette période. Il faut noter que ces mesures sont récoltées d'une manière irrégulière à l'échelle de l'espace et à l'échelle du temps. A titre d'exemple, sur les 236 valeurs mesurées retenues 161 valeurs proviennent d'une seule station appelée Negerdorf ! Cette irrégularité s'ajoute aux difficultés du problème et peut fortement influencer les résultats.

Comme nous l'avons signalé, un des objectifs principaux de la thèse est de comprendre le comportement de la source du contaminant dans l'aquifère à différentes profondeurs et éventuellement de prédire sa migration dans l'aquifère. Pour ceci, il est nécessaire de définir la localisation de la source dans l'aquifère ainsi que sa profondeur dans le sol.
Pour localiser la source dans l'aquifère, nous nous sommes basés sur les mesures de concentrations de CCl_4 collectées en 2004 et le maillage du domaine 3D. En effet, l'extension latérale de la source a été déterminée par les deux mailles comprenant les valeurs de concentrations mesurées les plus élevés. La profondeur de la source a été déterminée en tenant compte des analyses réalisées en 1997 dans un

piézomètre multi-niveaux près de la source de pollution. Ces analyses montrent que la concentration de CCl_4 est faible au dessous de 35m. En conclusion, la source a été discrétisée par les quatre premières couches dans le modèle numérique (chaque est constituée de deux mailles prismatiques). Les épaisseurs des couches de la source sont 16, 4, 5 et 5 m du haut vers le bas, respectivement.

Chapitre 4: Applications and results

Ce chapitre comporte deux parties principales. Dans la première partie, nous présentons la méthode adoptée pour atteindre l'objective de l'étude qui est la détermination du comportement de la source à l'endroit de l'accident. Dans la deuxième partie, nous présentons une analyse sur les incertitudes de la source en considérant plusieurs scénarios.

Dans ce chapitre, le modèle tridimensionnel est utilisé pour étudier le comportement de la source de contaminant à différentes profondeurs. Afin d'estimer son comportement, la source a été localisée aux endroits contenant les concentrations de CCl_4 les plus élevées. Elle a été discrétisée ensuite en quatre couches comme nous l'avons mentionné au chapitre 3. La profondeur de la source a été estimée à environ 35 m. La concentration de CCl_4 a été imposée dans les huit mailles (chaque couche comprenant deux mailles) situées verticalement au dessous de l'endroit de l'accident.

Dans la première partie de ce chapitre, nous avons mis au point une méthode inverse originale permettant d'estimer la concentration à la source à partir des concentrations mesurées dans la nappe à différents temps et en différents points. Cette concentration est estimée à partir d'un calcul préliminaire permettant de déterminer les rapports de concentration entre les différents points du domaine et la source ainsi que le temps de parcours source-point de mesure qui définit le temps d'apparition de cette concentration à la source.

La technique utilisée pour estimer la source aux quatre couches est la suivante: Tout d'abord, nous fixons la concentration de CCl_4 dans chaque élément (maille) représentant la source dans les quatre couches. Ensuite, le code TRACES est utilisé

afin de calculer la concentration dans le domaine et en particulier aux points de mesures (aux piézomètres). Les concentrations pour chacune des mailles représentant la source sont obtenues à l'aide de la formule suivante:

$$C_s\left(t-t_c\right)=C_{ini}\left(t-t_c\right)\frac{C_{mes}\left(t\right)}{C_{cal}\left(t\right)}$$

où, C_{ini} est la concentration initiale à la source (valeur arbitraire supposée égale à 100μg/l dans ce travail), $C_{cal}\left(t\right)$ est la concentration calculée au point de mesure correspondante à la concentration à la source. Le temps de parcours du contaminant t_c entre la source et les points de mesure est estimé en utilisant les moments temporels. Le temps à la source est ensuite calculé par $t_s=t-t_c$.

Les résultats numériques montrent que les concentrations à la source calculées en utilisant l'approche ci-dessus sont très oscillantes. Afin de résoudre ce problème, nous procédons au lissage de ces résultats en deux étapes :
Dans la première étape, les concentrations calculées à la source sont lissées en utilisant une interpolation de valeur moyenne. L'intervalle de temps est divisé en un certain nombre de sous intervalles d'une durée uniforme (6 mois). Dans chacun de ces sous-intervalles, nous remplaçons les concentrations par leur valeur moyenne. Puisqu'il n'y a pas de points de mesures avant l'année 1992, la concentration est supposée constante à partir de la date de l'accident et égales à celles estimées en 1992.
La deuxième étape consiste à utiliser une interpolation exponentielle des valeurs des concentrations moyennes utilisées à la première étape.

Dans la deuxième partie de ce chapitre et afin d'améliorer les résultats, nous avons étudié les incertitudes sur la source du contaminant. Ces incertitudes sont liées aux paramètres du problème. Ces paramètres sont : la porosité, les coefficients de dispersivité (longitudinal et transversal) et la perméabilité.

- Pour la porosité : plusieurs études hydrogéologiques ont été effectuées sur cette nappe, ces études ont montré que les porosités varient entre 10% et 20 %.

- Pour la dispersivité : en l'absence de mesures, le coefficient de dispersivité a été estimé par essais-erreurs en utilisant des informations a priori obtenues pour des formations géologiques similaires.
- Pour les perméabilités : les perméabilités sont déterminées en utilisant une approche de type Monte-Carlo qui consiste à réaliser de nombreuses simulations en tirant au hasard une valeur d'un paramètre dans un intervalle pré-défini. Ces intervalles sont déterminés par couche à l'aide des coupes lithologiques.

La méthode consiste à faire varier un paramètre tout en laissant fixes les deux autres et en commençant successivement par la porosité, la dispersivité et la perméabilité. Pour chaque valeur du paramètre courant (le paramètre qui varie) nous associons un scénario de la source. Chaque fonction source est ensuite considérée dans le code TRACES pour simuler les concentrations dans le domaine associé à cette source. Pour chacun des valeurs du paramètre courant, nous comparons les concentrations calculées et les concentrations mesurées et la source retenue est celle correspondante aux meilleurs résultats.

Les résultats numériques ont conduit à une restitutions globalement satisfaisante des concentrations mesurées, avec des écart types (σ) très acceptables et ce, pour une porosité fixée à 10% $(\sigma = 37.8\ \mu\text{g/l}, \text{CV}=0.30)$, pour des dispersivités longitudinale et transversale estimées à 20 m et 3 m, respectivement $(\sigma = 24.53\ \mu\text{g/l}, \text{CV}=0.30)$, et pour des perméabilités (conductivités hydrauliques) $(\sigma = 15.27\ \mu\text{g/l}, \text{CV}=0.2)$ résultant des simulations Monte Carlo spatialement distribuées et prenant en compte les hétérogénéités du milieu souterrain.

Conclusion et recommandations

Les conclusions de ce travail peuvent être résumées ainsi :

- Un nouveau modèle 3D de migration de CCl_4 dans la nappe d'Alsace du type convection-diffusion-dispersion a été utilisé afin d'estimer la concentration à la source du polluant.

- De nouvelles données récoltées entre 1999 et 2004 ont été intégrées dans ce nouveau modèle.

- Nous avons mis au point une méthode inverse originale permettant d'estimer la concentration à la source à partir des concentrations mesurées dans la nappe d'Alsace à différents temps et en différents points.

- La caractérisation de la source est évidemment liée à l'hétérogénéité de l'aquifère.

- Nous avons effectué une estimation des incertitudes sur la source liées aux paramètres du problème: trois paramètres incertains (porosité, dispersivité et conductivité hydraulique) ont été étudiés afin d'améliorer l'estimation de la concentration à la source.

- Différents scénarios de la source ont été obtenus en variant successivement les paramètres incertains. La source retenue est celle restituant au mieux les concentrations mesurées dans la nappe.

- Les résultats obtenus sont satisfaisants et montrent la fiabilité de la méthode d'estimation des concentrations à la source.

Les conclusions de ce travail nous mènent aux perspectives suivantes:

- Etudier l'effet de la discrétisation sur le problème d'estimation de la source en raffinant le maillage à la source.

- Prendre en compte l'évolution de la concentration dans la source pendant les premières années après l'accident.

- Utiliser un modèle multiphasique (CCl_4 n'est pas considérer comme un traceur) pour l'estimation de la source.

- Appliquer la méthode d'estimation de la source sur d'autres problèmes de pollution d'aquifères.

INTRODUCTION

The importance of studying groundwater and its movement is related to the importance of groundwater itself. Groundwater is the main source of drinking water, and therefore has a vital importance in our society. Beside, sensible management of water resources and protection of groundwater quality are a necessity.

Groundwater is an important resource globally endangered both in its quantity and quality. Computational models for prediction and risk assessment of groundwater are required to ensure its sustainable management. Such models are helpful to design remediation strategies and prediction of this natural resource.

To ensure reliability and faith in predictive computational models, it is essential to accurately represent the physics of the problem. Unfortunately, aquifers being in the invisible subsurface are very complex, and aquifer characterization is generally expensive and prone to error. Therefore, the parameters in computational models are mostly uncertain. If one does not rigorously quantify the uncertainty of model parameters, the unquantified uncertainty of model output may render the model useless. Successful practice for model calibration should, therefore, account for aquifer heterogeneity and uncertainty.

The work in this thesis is devoted to study the assess the spreading of a dangerous chemical that contaminated a part of the Alsatian aquifer as a result of a tanker accident in 1970.

The Alsatian aquifer lies in the north-eastern of France and reaches out the border with Germany. The aquifer surface is over 3000 km^2 and contains a volume of alluvial about 250 billion m^3. It is one of the largest fresh water reserves in Europe. The groundwater reservoir contains about 50 billion m^3 of water, with an annual renewal of 1.3 billion m^3. It provides 75% of the drinking water requirements, 50% of the industrial water requirements and 90% of the irrigation water requirements in the region.

In 1970, a tanker containing carbon tetrachloride (CCl_4) capsized at 35 km south of Strasbourg city. According to a note from SGAL (1971), about 4000 l of CCl_4 were leaked on the accident site, where a part of which could have been infiltrated into the subsurface and another part disappeared by evaporation. In 1992, measurements

carried out by BRGM, showed abnormal quantities of CCl_4 in the pumping wells in Erstein, see Figure 1.2. The high level of CCl_4 concentrations has caused a serious problem in the region and contaminated the most important drinking water source in the area. Carbon tetrachloride is a very toxic chemical that may cause cancer to humans.

The Alsatian aquifer has been the subject of several studies that addressed the hydrodynamic state of the aquifer and the pollution migration. Vigouroux et al. (1983) studied some cases of pollution in the aquifer of the Rhine Graben by using a 2D numerical model taking into account convection, dispersion and retention. Hamond (1995) presented a numerical approximate of the hydraulic and transport problems. His study was based on data measured between 1970 and 1993. Beyou (1999) completed the study by adding measured data during the period between 1993 and 1999. None of the previous works showed satisfactory matching of the measured data.

Our work is provide to improve the simulation model to adopt a new techniques for estimation the behavior of the contaminant source and account for uncertainty and also to inquire new data that were measured between 1999 and 2004. These data were not considered in the pervious studies. We used a 2D/3D numerical model (TRACES) that is developed at the IMFS to describe the water flow and mass transfer problems.

The main difficulties of the problem are illustrated in the following points:

- The exact amount of the chemical infiltrated in the underground is unknown since some of the tanker volume was recovered and another part could have been disappeared by vaporization.
- Carbon tetrachloride has low solubility in water. Some of the chemical could be trapped underneath of the accident site because of several physical and chemical mechanisms such as gravity, capillarity, and adsorption. The trapped CCl_4 may continue to release miscible quantities due to the rain or the contact with the underground water flow. Therefore, the initially trapped CCl_4 may act as a continuous source of contamination for the underground water.
- The source behavior of the contaminant that continued to feed the contamination and, which is space and time dependent, is unknown.

- High uncertainty in the aquifer formation properties such as porosity and permeability. The aquifer is heterogeneous and has different permeable layers.
- Uncertainty in the chemical properties such as the solubility in water, diffusion, volatilization, and degradation coefficients.
- Complexity in defining a proper coupling between the water flow and pollutant transfer in the permeable medium and the corresponding boundary conditions.
- The aquifer geometry is complex and cannot be properly modeled by the conventional finite difference method on structured (Cartesian) gridding, see section 2.4.

Measured data showed jumps in the CCl_4 concentration that might be an indication of a convection dominated transfer problem owing to potential sharp propagating fronts. Higher-order numerical schemes are, therefore, crucial in order to improve the accuracy of the numerical solution.

As will be shown later, we have set a consistent workflow to attack the problem: 1) The source function is estimated by using an inverse method coupled with a smoothing technique and the temporal moments method; 2) Different schemes such as the Monte-Carlo and trial and error methods are used to asses the uncertainty in the formation and formation-fluid properties; 3) Various source scenarios are tested 4) The combined mixed hybrid finite element and discontinuous Galerkin methods are used to insure logically accurate numerical solutions. Theses methods are superior to the conventional methods in reducing the numerical diffusion and improving the flow velocity approximation.

An outline of this thesis is as follows:

Chapter 1 is essentially informative that provide some information about the Alsatian aquifer related its hydrogeology, geography situation and vulnerability to pollution. The story of the famous accident of 1970 that caused high level of carbon tetrachloride is outlined. Some physical and chemical properties of the CCl_4 that are useful in our study are provided. Chapter 2 reviews the fundamental mathematical equations describing flow and solute transport in porous media that are used in this study. In addition, the numerical model, TRACES, is briefly presented. Chapter 3

includes an overview of the workflow and the adopted numerical techniques related to the main assumptions and simplifications, uncertainty analysis, and the model design and boundary conditions. The location and dimensions of the contamination source are presented. Chapter 4 sets the different procedure steps on the track. We present the measured concentrations that are used in the numerical model and the methodology adopted to estimate the contamination source. The uncertainty on the source behavior by assuming different parameter values are presented. Comparisons between the computed and measured data are preformed. We finally end with conclusions and suggestions for future work.

CHAPTER 1

CHAPTER 1
CCL_4 POLLUTION HISTORY OF THE ALSATIAN AQUIFER

In this chapter, we give a brief description of the Alsatian aquifer and its vital role in the region. We also outline some of the main contamination sources in the aquifer and in particular the carbon tetrachloride tanker accident occurred in 1970. Some physical and chemical properties of carbon tetrachloride will be illustrated. The sections that follow describe the DNAPL migration and its dissolution. Fluid properties such as volatilization, sorption, and degradation will be defined with particular focus on the properties of carbon tetrachloride (CCl_4). In this study, the scenario of CCl_4 migration in the aquifer is discussed. This work will lead to some hypothesis of CCl_4 transport processes.

1.1. General description of the aquifer

1.1.1. Geographic location

The Rhine Graben forms a part of a rift that crosses the west European plate (Villemin and Bargerat, 1987), extending into eastern France and western Germany. The Upper Rhine plain is a rift valley that extends over a distance of 300 km between Basel in the South and Frankfurt in the North with an average width of about 40km (Bertrand et al., 2006). The water table of the Rhine valley between Basel to Mainz is an essential compartment of the Upper Rhine hydrosystem that contains about 250 billion m^3, which makes it the largest alluvial aquifer in Europe (Guilley F., 2004).

The Upper Rhine valley is a broad valley bordered by mountains; on the east side by the Black Forest and on the west side by the Vosges (Bertrand et al., 2006). In the south, the Swiss Jura leads an exit of the valley to the southwest through the "Burgundische Pforte", while the Rhine River is deflected to the east. A sketch of aquifer area is shown in Figure 1.1.

The phreatic aquifer of Alsace forms an integral part of this immense hydrogeological system. It is located in the southern part of the Upper Rhine valley in the north-eastern of France and extends to the border between France and Germany. The Alsatian aquifer is surrounded by the Jura Alsatian Mountains in the south, the Vosges Mountains in the west, the Rhine in the east, and the Haguenau-Pechelbronn basin in the north-west (Hamond, 1995).

In the north, the aquifer is obstructed artificially at the height of Lauterbourg close to borders with Germany. The plain slopes smoothly from south to north, and from the edge of Vosges towards the Rhine. The altitudes range from +250 m in Basel to +130 m in Lauterbourg, at a distance of 160 km (Hamond, 1995). A map of the aquifer in the French side is given in Figure 1.2.

1.1.2. Structure and dimensions of the aquifer

The basin of the aquifer is a result of the tectonic history, sediment, hydrographic, and the climatic of the open rift valley between the Vosges and Black-Forest. The aquifer is filled with up to 200 m of tertiary and quaternary sediments, mainly fluvial gravels and sands deposited from various origins (Vosgean alluvium and Rhine alluvium). This immense rift has variable thickness because of an irregular morphology of the marls substratum that supports the Rhine alluvium. This permeable alluvial has a thickness of a few meters at the Vosgean edge, and 150 m to 200 m in the center of the Rhine plain. In Strasbourg region, the average thickness is around 80 m (Hamond, 1995).

Globally, the Alsatian aquifer extends on a surface over 3000 km^2 and contains a volume of alluvium about 250 billion m^3. The aquifer, which lies in the heart of these alluvium, represents an immense reserve of ground water whose estimated volume is about 50 billion m^3, with an annual renewal of 1,3 billion m^3. The exploitation of the aquifer for collectives, industry and agriculture is almost the third of renewal volume,

which is about 0.5 billion m^3. These numbers are extracted from the note of CIENPPA (1984), which shows the importance of the phreatic aquifer and its economic role in the region.

1.1.3. Hydrodynamic characteristics of the aquifer

Several studies of the Alsatian aquifer, that have been carried out since 1950, described the hydrodynamic characteristics of the aquifer. The aquifer is defined as an extensive alluvial aquifer, which is fed especially by meteoric deposits and drained mainly by rivers and human activities.

The groundwater in the aquifer flows mostly from south to north and with some local variations mainly due to heterogeneity in the permeable formation. The hydraulic gradient, however, is not uniform over the aquifer. It is about 0.7% to 0.9% in the center of the plain and is higher at the edge of the aquifer, where the sediments are less thick (Hamond, 1995).

The hydraulic conductivity is relatively constant across the vertical trench of the aquifer, which is about 10^{-3} to 10^{-2} m/s. The geophysical analysis performed to the aquifer (resistivity measurement) showed a layered structure with a random superposition of different alluviums (clay, sand fine to rough, gravels, coarse…), and presented the hydrodynamic and hydrogeology characteristics (permeability, porosity, transmissivity), of the porous medium. The porosity is up to 15%.

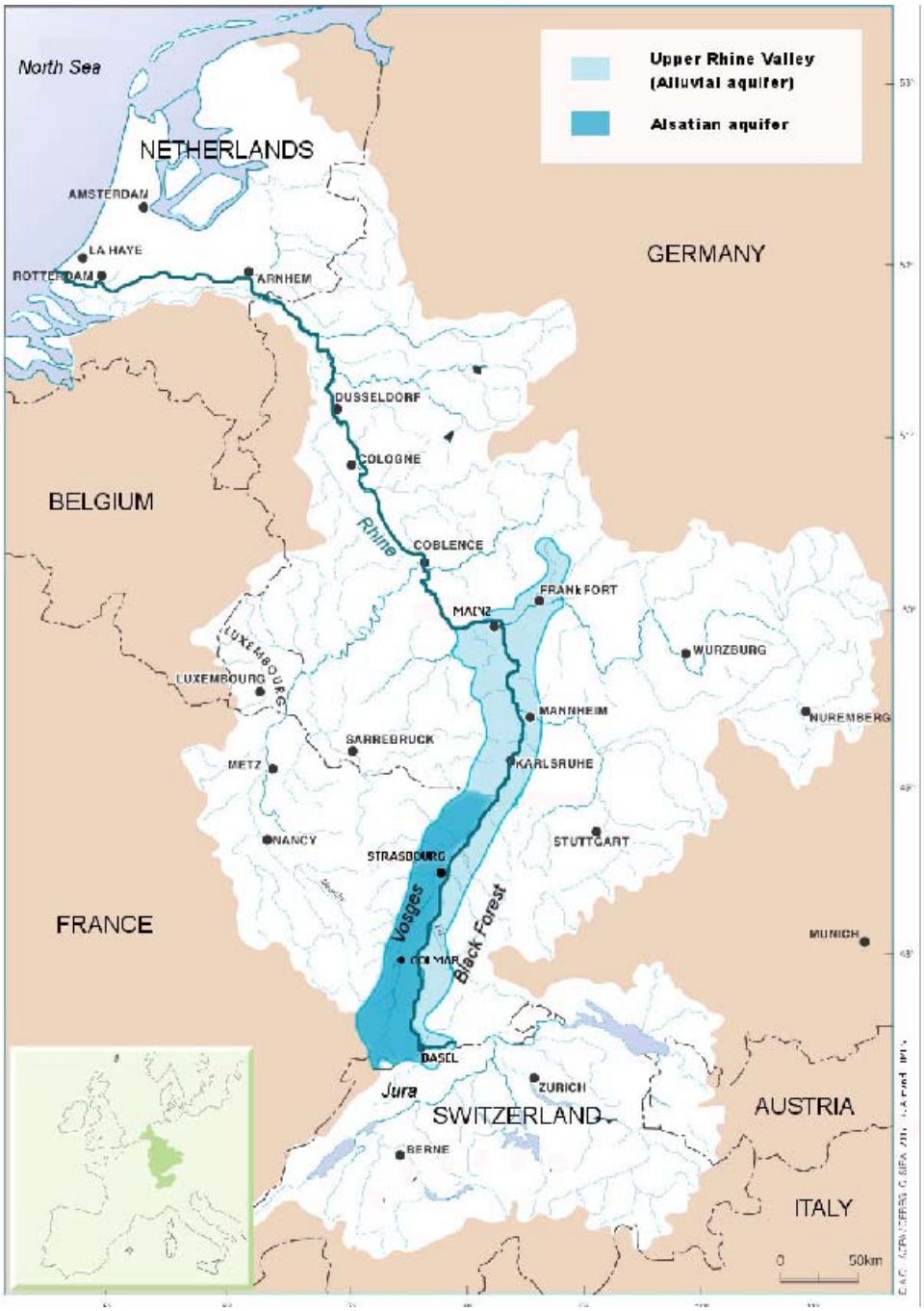

Figure 1.1. The Rhine valley.

Figure 1.2. The map of Alsace region showing the Alsatian aquifer.

1.1.4. The hydrographical system of the Alsace plain

1.1.4.1. Description

The Rhine valley is dominated by two main rivers: the Ill River with a discharge flow rate ranging between 5 and 10 $m^3 s^{-1}$ at Strasbourg, and the channeled Rhine with a flow rate typically between 700 and 1500 $m^3 s^{-1}$, (Eikenberg et al., 2001).

The Ill River is sourced from Jura and runs northward through the Alsace. The flow direction of the Ill River is almost parallel to the Rhine. Before joining the Rhine aquifer at the north of Strasbourg, all the smaller rivers carrying the discharge water from the Vosges mountains flow directly into it (Eikenberg et al., 2001). These rivers have a classic hydraulic system. The precipitation of the basins varied with time: high water level in winter and spring, and low water level in the end of summer.

The Rhine River, sourced from the Swiss Alps, flows through Germany, France, and the Netherlands in to the North Sea with a length over 1320 km and a catchment area of about 200.000 km^2 including the parts in Switzerland, Germany, France, Luxembourg, Belgium, and the Netherlands (Middelkoop, 1998), (see Figure 1.1). It takes a north-east direction flowing through the plains of Alsace and passes through the cities of Strasbourg, Mainz and the schistose massif of the Rhineland near Cologne. It has a characteristic Alpine regime conducted by melting snow that explains the high water level in summer and the low level in the winter.

1.1.4.2. Aquifer interaction with the rivers

River-aquifer interactions are governed by the fluctuating water level of the rivers. The groundwater reservoir is a part of a complex hydrosystem. It includes frequent exchanges between the rivers and the aquifer that vary with the seasons caused by the proximity between the surface and the groundwater. The aquifer is highly exposed to contamination from the neighboring rivers. The Rhine River with an average annual flow of 35 billion m^3 plays a dominant role as it supports the level of the aquifer, from the eastern side where the local deposits are scanty (Hamond, 1995). In addition to the natural exchanges, there are artificial exchanges with the Rhine River through a system of transfer canals. The embankment and the hydroelectric managements of the Rhine control the aquifer level, that overshadow the supply coming from the Alps. The pollution of the Rhine contributing to the contamination of the aquifer is of unknown extent.

The aquifer also interferes with the fluvial system of the Ill and its tributaries. The watercourses result in a high water level in the aquifer when they are flooded. In the southern part of the aquifer, the Ill River supplies around 100 million m^3 to the aquifer, while further downstream, the aquifer contributes to the flow of the same river, (Stenger, 1998).

1.1.5. Vulnerability and pollutions

In general, groundwater benefits from the natural protections provided by deep soil cover, and by the slow rate of recharge and water flow. On the other hand, the slow movement of groundwater, while favorable to its protection, works against rehabilitation.

The Alsatian aquifer, considered as unconfined aquifer because of its physical characteristics, is highly vulnerable to various sources of pollution. These contamination threats come also from the proximity between the groundwater and the surface.

The use of pesticides and fertilizers in agriculture, waste dumping by industries and municipalities, and traffic increase, all threaten the quality of groundwater in Alsace. In the past, a number of accidents have caused local pollution in the aquifer, leading local authorities to shut down several wells. The degradation of groundwater quality revealed a possible number of pollution sources.

Pollution of industrial origin is generated by the dissolution of the slag heaps of the potash basins located in the north of Mulhouse. Rainfall and the infiltration of water containing chloride cause huge salt plume, that extends to the north. After 1960, concentration exceeding 200 mg/l could be observed until Colmar, whereas a less sensitive zone of pollution, with concentration ranging between 60 and 200 mg/l has been detected in the upstream of Strasbourg (Hamond, 1995). De-pollution operations such as dissolution of slag heaps and pumping, may allow to reduce the pollution of the aquifer.

Another example of the impact of the industrial activities on the water quality of the aquifer is the spilling of hydrocarbons. The leakages of kerosene detected in 1971 close to the airport of Strasbourg-Entzheim, and the rupture of the South-European

pipeline in Issenheim (Haut-Rhin) in December 1989, have contaminated the aquifer by thousands of m^3 of hydrocarbons.

Agricultural pollution was observed by abnormal quantities of nitrate that exceeded 50 mg/l at the border of the Vosges. These concentrations are explained by the agricultural activities relying on vines and cereals crops which are cultivated on the Vosges Mountains and the agriculture in the Rhine valley. The intensive use of pesticides in agriculture also threatens the quality of groundwater in the region.

During the last decades, the situation in Alsace has become serious, with several important accidents, releasing dangerous pollutants such as chlorinated solvents in the groundwater. Such accidents drew the attention to pollution problems because of its irreversible character and its long life time that make the cleaning up a very difficult and expensive process.

1.2. History of the pollution in the aquifer by CCl_4

1.2.1. The accident of 1970

On December 11th, 1970, a tanker truck containing a chlorinated solvent appended to a Dutch company, capsized in the north of Benfeld, which is a small town about 35 km to south of Strasbourg (Figure 1.2). In spite of the efforts of the fire and help services to control the spilling of the chemical by installing a pneumatic tank, an important quantity of the chemical could not be recovered. According to a note of SGAL, on December 21th, 1971, some 4000 l (nearly 1056 gallons) of carbon tetrachloride (CCl_4), were spread on the area of the accident, infiltrating into the ground or disappearing by evaporation (Hamond, 1995).

After a couple of years of the accident, the SGAL showed a possibility that the chemical could reach the aquifer and described the probable mechanisms of CCl_4 migration. The hypotheses of the propagation of the product in the ground refers to the analogy of the observed processes of the salty solutions (pollution comes from slag heaps of the potash of Alsace). Initially, the infiltration of the pollutant may reach the unsaturated medium, while the above loess layers can play the role of a screen. The chemical may migrate quickly towards the aquifer because of its high density.

The phenomenon of convection, diffusion, dispersion, and solubility of the product, may lead to the creation of pollution plume of about 21 000 m^3 of the aquifer area. In addition to the uncertainties concerning the behavior of the product in the aquifer, the migration of the chemical to several kilometers downstream was unpredicted. The prevailing idea was that the pollution would be relatively limited and it would be diluted and dispersed with time before reaching the supplies of drinking water located downstream of Benfeld. However, the final recommendations of SGAL included the installation of piezometers and monitoring wells to evaluate the water quality and follow-up the pollution propagation in the zone of the accident.

These suggestions were transmitted to mine services and to the DDA (Direction department of agriculture) but without getting much attention, since they assumed that the chemical would be removed before being able to threaten the supplies of water downstream.

1.2.2. Pollution discovery

The first analysis of the drinking water wells was carried out in 1991 in Erstein (Figure 1.2), where an abnormal quantity of CCl_4 (about 15.6 μg/l) was discovered (Beyou, 1999).

Regular analyses of the drinking water wells showed that the level of CCl_4 has always been exceeding the safe limits recommended by WHO (2 μg/l). In 1992, the pollution was confirmed with CCl_4 levels between 62.4 μg/l and 56.2 μg/l (Beyou, 1999). This high level of CCl_4 concentrations has caused a serious problem in the region by contaminating the most important drinking water source in the area.

1.2.3. Cleanup approach

Since 1992, after the discovery of abnormal quantities of CCl_4, the authorities have worked to educate the community and recommended to stop using the drinking water wells. They suggested a treatment in two stages: immediate actions and long-term actions.

The immediate actions have been started after the discovery of pollution in 1992, by installing a treatment system plant on one residential well (Negerdorf) in Erstein town.

To remove CCl_4 from groundwater, the treatment technologies used for soil and/or ground water remediation include: air stripping and granular activated carbon absorption.

The first step in the treatment is the air-stripping by an insulating two packed towers. The towers are a forced draft system with air blown at up to 1700 m^3/h. Ground water is pumped through the towers and the blown air is used to separate CCl_4 from water by evaporating. CCl_4 has a high Henry's constant, which indicates that CCl_4 is very volatile therefore, it may be transferred from aqueous to vapor phase. The volatilization is the dominant removal mechanisms as it removes about 90% of CCl_4, (Hamond, 1995).

The second step in the treatment is by granular activated carbon (GAC) which is installed on a bed where the contaminated water is pumped through. The contaminant gets absorbed by GAC. This process is to remove 100% of CCl_4. The final processing step before distributing water to consumers, water is disinfected with Chlorine. Figure 1.3 shows a simple diagram of the treatment system.

Water pumped from the wells between 1992 and 1995 showed that a level of CCl_4 above the standard drinking water, (DDASS, 1992). This indicates continuous source of pollution, furthermore, the pollution may pollute a wider region in particular in the north of Strasbourg.

The long-term plans addressed the identification and remediation of sources of contamination. A study carried by BRGM in 1993 established that the source of pollution is located in Benfeld, which corresponds to the accident location.

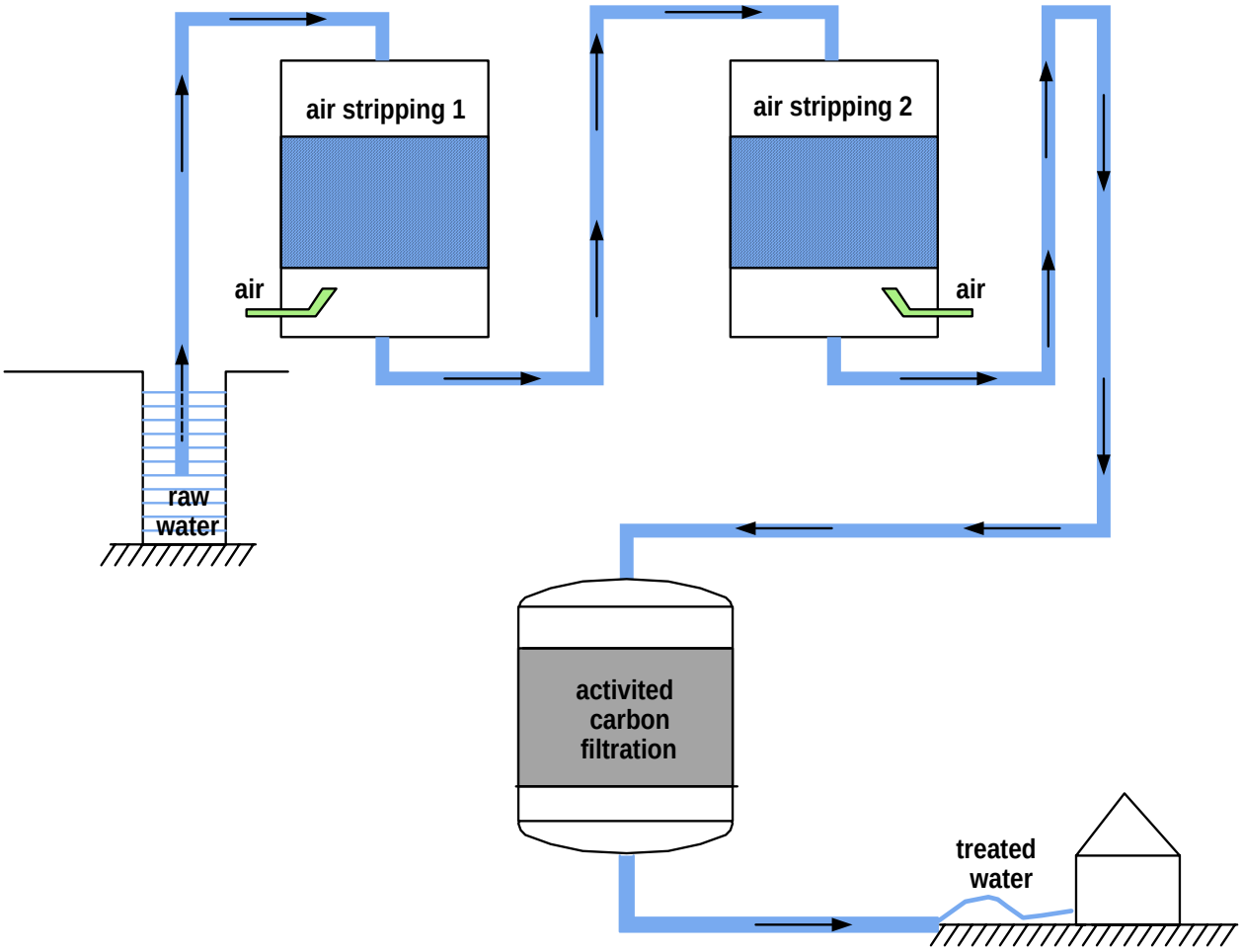

Figure 1.3. Schematic diagram of the treatment plant installed on Negerdorf well in Erstein.

1.3. Properties of CCl_4

Carbon tetrachloride acts as a chlorinated solvent which is toxic and harmful for human and for environment. The physiochemical properties of CCl_4 are discussed in the following sections.

1.3.1. Physical and chemical properties of CCl_4

Carbon tetrachloride, which is a volatile organic chemical (VOC), does not naturally occur in the environment. It is commonly found as a man-made chemical in liquid state. It is miscible with most aliphatic solvents but has low solubility in water. Carbon tetrachloride is highly toxic, clear and heavy (more dense than water) with a sweet smell that can be detected at low levels. Decomposition of CCl_4 may produce phosgene, carbon dioxide, hydrochloric acid, methane tetrachloride, perchloromethane, tetrachloroethane, and benziform (HSG 108, 1998). Some of the physical and chemical properties of carbon tetrachloride are listed in Table 1.1.

Table 1.1. Physical and chemical properties of carbon tetrachloride

Property	Value or Information	References
Molecular weight	153.84 g/mol	CPHF, 1998
Color	Colorless	NIOSH, 1994
Phase state	Liquid	NIOSH, 1994
Odor	Sweet, ether-like odor	NIOSH, 1994
Odor threshold (in water)	0.52 mg/l	U.S.EPA, 1998
Boiling point	76.7°C	CPHF, 1998
Melting point	-23°C	U.S.EPA, 1998
Solubility at 25°C	1160 mg/l	CPHF, 1998
Solubility at 20°C	800 mg/l	CPHF, 1998
Density	1.59 g/ml at 20°C	NIOSH, 1994
Log K_{ow}	2.64	CPHF, 1998
Soil Sorption Coefficient K_{oc}	K_{oc} = 71 (moves readily through soil)	U.S.EPA, 1998
Bioconcentration Factor	Log BCF = 1.24-1.48, not significant	U.S.EPA, 1998
Vapor Pressure	91.3 mm Hg at 20°C	CPHF, 1998
Henry's Law Constant	3.04×10^{-2} atm-m^3/mol at 24.8°C	U.S.EPA, 1998
Henry's Law Constant (dimensionless)	1.25 at 24.8	U.S.EPA, 1998

1.3.2. Usage

Carbon tetrachloride is a synthetic chemical compound that is widely used in the production of refrigeration fluid and propellants for aerosol cans, in fabricating nylon, grain fumigant, petrol additives, and semi-conductors. It is used as a solvent for fats, oils, and greases, for dry cleaning and for degreasing metals, and is used at home as a spot remover for clothing (EPA, 1998). It was also used in agriculture through the mid-1980s as a fumigant to kill insects in grain. All these uses are now banned and its usage is limited to some industrial applications, (ATSDR, 1995), because of its toxicity and its effect on the ozone layer. The Montreal Protocol on substances that deplete the Ozone layer (1987) and its amendments (1990 and 1992) established a timetable for the phase out of the production and consumption of carbon tetrachloride. The manufacture of CCl_4 has, therefore, dropped and will continue to drop (UNEP, 1996; IPCS, 1999). Carbon tetrachloride was used as a pesticide, but this was stopped in 1986.

1.3.3. Regulation and recommendation

The public health code of 1989 set a limit for carbon tetrachloride at 1 μg/l of water quality. If carbon tetrachloride is present above that level, the system must continue to monitor this contaminant.

The Environmental Protection Agency (EPA) has set a Maximum Contaminant Level Goals (MCLG) for carbon tetrachloride at zero parts par billion (ppb) of drinking water. Based on this MCLG, EPA has set an enforceable standard called a Maximum Contaminant Level (MCL). The MCL has been set at 5 ppb for general water usage.

In Germany in 1976, high levels of carbon tetrachloride were measured in Rhine River (160-1500 μg/l) and in Main River (about 75 μg/l). The contamination was a result of direct waste release by industrial effluents (BUA, 1990; IPCS, 1999). Water quality criteria based on fish/shellfish and water consumption set by the EPA is 0.23 μg/l and if based on fish/shellfish consumption is only 1.6 μg/l.

For air in the workplace, the Occupational Safety and Health Administration (OSHA) has identified a limit of 10 ppm for an 8-hour workday over a 40-hour work.

The world health organization (WHO), 1999 recommended the level of carbon tetrachloride in air to be less than 0.11 part per million (ppm). Humans cannot smell carbon tetrachloride if its level is less than 10 ppm.

1.3.4. Toxicity

Carbon tetrachloride and some of its degradation products are considered carcinogens or suspected carcinogens, and are regulated substance and hazardous material. Exposure to high concentrations of carbon tetrachloride may cause liver, kidney, and central nervous system damage (ATSDR, 1995). Toxic effects of CCl_4 are initiated by enzymatic reactions that transform it into trichloromethyl radicals (CCl_3.), resulting in damage hepatic cells, (Macdonald, 1982). These effects can occur after ingestion or breathing carbon tetrachloride, and possibly from exposure to the skin. The EPA has determined that carbon tetrachloride is a probable human carcinogen.

1.3.5. Environmental impact

Due to carbon tetrachloride relatively high evaporation rate when released to the environment, most of its quantity moves quickly into air. Carbon tetrachloride is stable in air (30-100 years) (ATSDR, 1995) and may react with other chemicals that have the potential to destroy upper atmosphere ozone layer. Only a small amount sticks to soil particles; the rest evaporates or moves into the groundwater. Releases or spills on soil should result in rapid evaporation due to high vapor pressure and leaching in soil resulting in groundwater contamination due to its low adsorption to soil. Evaporation from water is a significant removal process (half-life minutes to hours). Based upon field monitoring data, the estimated half-life in rivers is 3-30 days, and in lakes and groundwater is 3-300 days.

1.4. CCl_4 migration in the subsurface

Carbon tetrachloride can be classified as a dense non-aqueous phase liquid (DNAPL). Generally, DNAPL's have different behavior than other contaminants in the subsurface, as they are normally observed in more complex distributions which are strongly influenced by aquifer heterogeneity (Feenstra et al., 1996). DNAPL may remain a long term source of contamination. Plumes developing from these source zones often travel large distances to eventually impact water supply wells or surface waters. Once in the aquifer, DNAPL migrates in two different phases: (1) dissolved in water (aqueous) and (2) liquid (non-aqueous phase).

The rate of migration of a DNAPL through a porous medium can be highly irregular (Kueper et al., 1993), and depends on several factors: 1) the DNAPL density and viscosity; 2) the pressure driving the DNAPL; 3) the intrinsic permeability of the medium, and 4) the degree of DNAPL saturation, (Feenstra et al., 1996). Higher density and lower viscosity result in faster migration. More permeable media and higher DNAPL saturations will also cause faster infiltration.

In general, residual and mobile DNAPL may present above or below water table. In the vadose zone (unsaturated), DNAPL flows downward with relatively little spreading (Schwille, 1988; Pankow and Cherry, 1996) under the force of gravity and soil capillarity. Some of the contaminant may be retained by capillary forces in pores and fractures formations. This fraction, which is not mobile under static conditions, is termed as residual saturation. Infiltration through the DNAPL zone dissolves some of the soluble organic constituents in the DNAPL, carrying organics to the water table and forming a dissolved organic plume in the aquifer. Migration of gaseous vapors can also act as a source of dissolved organics to ground water (Mendoza and McAlary, 1990).

Given sufficient quantity, DNAPL may move vertically downward, penetrate the water table, and continue to move vertically downward until gravitational movement is restrained by physical barriers (e.g., an impermeable geologic stratum) or until the DNAPL volume has been depleted by residual containment in the zone through which the DNAPL is descending (Domenico and Schwartz, 1990). As a result of these migration patterns, DNAPL may present in the saturated zone as pools (mobile) and disconnected globules within relatively coarse-grained pathways bounded by fine-grained materials. A finite DNAPL source will eventually be

immobilized by residual saturation or in stratigraphic traps. Mobile and immobile DNAPL in the saturated zone may dissolve into flowing groundwater, giving rise to aqueous phase plumes which act as a source of long term groundwater contamination. Risks posed to groundwater resources and supplies are most often concerned with the migration of the dissolved-phase plume formed by the contact of flowing groundwater with the spilt DNAPL.

There are four partitioning processes which are of interest when addressing DNAPL behavior in the subsurface: 1) solubility of DNAPL in water; 2) volatilization of dissolved chemicals from water into air; 3) vaporization of DNAPL into air; 4) sorption of dissolved chemicals from water to solids (Feenstra et al., 1996).

1.4.1. Dissolution of DNAPL

The dissolution is the process by which soluble components from DNAPL dissolve in groundwater or dissolve in infiltration water and form a groundwater contamination plume. DNAPL and water do not mix freely but when a DNAPL comes into contact with water, mass is transferred across the DNAPL-water interface. This mass transfer results in the contamination of groundwater. Dissolution of contaminants from residual saturation or bulk liquid into water may occur in either the unsaturated or saturated portions of the subsurface.

In the unsaturated zone, dissolution of contaminants from residual DNAPL occurs as groundwater flows through the residual zone. The processes governing dissolution from DNAPLs are generally complex and depend upon many variables (Feenstra et al., 1996). The rate of mass transfer of a DNAPL into groundwater depends on the solubility of the compound in water, the groundwater velocity, the pore structure of the soil, the distribution of the DNAPL in the soil, and the diffusion coefficients of the compound (Feenstra and Guiger, 1996). Chemicals are initially dissolved and transferred into the flowing groundwater by means of molecular diffusion due to the concentration gradient at the DNAPL-water interface (Feenstra and Guiger, 1996).

In general, the rate of mass transfer from NAPL is given as the product of a mass transfer coefficient, a concentration difference, and an interfacial contact area. The concentration difference can be approximated using the effective solubility of a compound and either the measured concentration of the compound in groundwater

adjacent to the DNAPL, or a calculated groundwater concentration. Because of complex pore geometry that exists in natural porous media, determining the interfacial contact area is impractical. As a result, the mass transfer coefficients and the interfacial area are often represented mathematically using a lumped mass transfer rate coefficient that takes into account the properties of the porous media, fluid properties, flow conditions and interfacial area (Sleep and Sykes, 1989; Miller et al., 1990; Powers et al., 1992; Imhoff et al., 1994). This process is described by:

$$\frac{\partial C_w}{\partial t} = -\lambda \left(C_w - C_s \right) \tag{1.1}$$

where,

λ : is the lumped mass transfer coefficient, [LT^{-1}];

C_w: is the concentration of the contaminant in the aqueous phase, [ML^{-3}];

C_s: is the aqueous solubility of the contaminant, [ML^{-3}].

In general, models for dissolution of DNAPL in porous media either assume local equilibrium between phases, or assume that dissolution is a first-order process governed by Eq. (1.1) (Feenstra et al., 1996, Miller et al., 1990; Guiguer et al., 1994; Shiu et al., 1988; Mackay et al.,1991).

Dissolution of water-soluble constituents from the residual DNAPL may act as a continuous source of contamination to local groundwater. DNAPL, such as CCl_4, has slow dissolution rate and can persist in the subsurface for long periods of time.

1.4.2. Volatilization

Volatilization is the process of a compound partitioning into a gaseous phase from a liquid or solid phase. In general, factors affecting the volatilization of contaminants from groundwater into soil gas include the contaminant concentration, the change in contaminant concentration with depth, the diffusion coefficient of the compound, mass transport coefficients for the contaminant in both water and soil gas, sorption, and the temperature of the water (Larson and Weber, 1994).

Volatilization is characterized by the Henry-law constant of the dissolved contaminant of interest. The Henry-law constant is expressed as the concentration of a species in the gaseous phase divided by the concentration of the species in the aqueous phase when these two phases are in equilibrium with respect to the species of interest

(Lyman et al., 1990). Thus, the Henry-law constant of a chemical determines the tendency of a contaminant to volatize from groundwater into the soil gas. Therefore, the greater Henry-law constant, the greater the tendency to volatilize from the aqueous phase. Henry's law constant can be computed from the ratio of the concentration of the compound in the gas phase (C_g), to the concentration of the compound in the aqueous phase (C_l) expressed in the same units (e.g., moles per liter or moles cubic centimeter), that is,

$$H = \frac{C_g}{C_l}. \qquad (1.2)$$

This constant is temperature-dependent, which increases with temperature.

1.4.2.1. Volatilization of carbon tetrachloride

Carbon tetrachloride has high vapor pressure. As a result, CCl_4 may readily vaporize into atmosphere when present in shallow soil and surface water. Additionally, CCl_4 dissolved in groundwater may have a propensity to vaporize and migrate through unsaturated soil eventually releasing to the atmosphere. The vapor phase migrates by diffusion and sinks by density-driven advection.

In the vadose zone (unsaturated), volatilization is the dominant process for removal of DNAPL. Other processes may enhance DNAPL degradation in the unsaturated zone relative to the saturated zone such as biodegradation through the ready availability of oxygen, and volatilization (Rivett, 2004). Biodegradation and volatilization act as a combined mechanism for the mass removal of volatile and semi volatile organic compounds from the unsaturated zone. If the groundwater plume is at or near the water table, the volatilization of the chemicals of concern to the air phase from groundwater becomes significant. If, however, the groundwater plume is at some depth below the water table, the migration of the chemicals to the water table and to the soil gas phase above the water table is less significant, and diffusion and dispersion become the predominating mechanisms. Diffusion in water is typically four orders of magnitude slower than in a gas phase (Davis et al. 2004).

Because the vapor pressure of many DNAPL compounds is relatively high, the lifespan of residual DNAPL in the unsaturated zone can be much less than the lifespan of residual DNAPL below the water table. The vaporization process can deplete residual chlorinated solvent DNAPLs within 5-10 years in relatively warm and dry climates (Kueper, 2003).

1.4.3. Sorption

Sorption is the process whereby dissolved contaminants partitions from the groundwater and adheres to the particles comprising the aquifer matrix. The attraction occurring between the outer surface of a solid particle and a contaminant is called adsorption, while the uptake of the contaminant into the physical structure of the solid is absorption. The sorption process is often reversible and, in some cases, the solute is permanently retained by the medium. In the groundwater, the sorbing species is called the sorbate, and the solid media, usually soil, to which the sorbate is attracted is known as the sorbent.

The sorption amount dependents on aquifer matrix properties (organic carbon and clay mineral conteny, bulk density, specific surface area, and porosity) and contaminant properties (solubility, hydrophobicity), (Chiou et al., 1983; Alley, 1993; Ferrante, 1996).

In bench experiments, it is possible to predict the amount of sorption expected for a certain solute, if it interacts with a specific aquifer material under equilibrium conditions. With these experiments, it is possible to visualize the solute distribution between solid and aqueous phase by plotting the solute concentration on solids versus the solute concentration in the aqueous phase at a constant temperature. These sorption isotherms generally exhibit one of three characteristic shapes, depending on the sorption mechanism. The three most important types of sorption isotherms are known as Langmuir isotherms, Freundlichs isotherm, and linear isotherms, which is a special case of the Freundlich isotherms.

Sorption of contaminants is generally described by their distribution coefficient (K_d), which is defined as the ratio of the sorbed contaminant concentration to the dissolved contaminant concentration at equilibrium, (Alley, 1993).

The extent of the sorption process is directly correlated with the octanol-water partition coefficient K_{ow} [-] of the solute and the percentage of organic carbon in the sediment f_{oc} [-]. The distribution coefficient for a specific solute/aquifer material system can, therefore, be expressed as (Karickhoff et al., 1979):

$$K_d = K_{oc} f_{oc}. \tag{1.3}$$

A K_{oc} value is a measure of the tendency of an organic compound to be adsorbed by soil. The higher the K_{oc}, the higher its potential to be adsorbed and the lower its potential to migrate.

As mentioned earlier, sorption slows the migration of a solute compared to the bulk groundwater movement. When the velocity of the bulk groundwater is greater than the average velocity of the solute, the solute is said to be retarded. This effect is described by the retardation factor R [-], defined as (Fetter, 1993):

$$R = \frac{v_x}{v_c} \tag{1.4}$$

where,

R: coefficient of retardation, [-];

v_x: advective groundwater velocity, [$L\ T^{-1}$];

v_c: retarded contaminant transport velocity, [$L\ T^{-1}$].

If no sorption occurs, i.e. K_d equals 0, the retardation factor, R, equals to 1. Typically R is not estimated from Eq.(1.4). Various methods can be used to estimate R. These methods require information about the soil bulk density, effective porosity, fraction of organic carbon in the aquifer, and the organic carbon-partitioning coefficient of the constituent. The coefficient of retardation for linear sorption is determined from the distribution coefficient using the relationship, (Freeze and Cherry, 1979):

$$R = 1 + \frac{r_b K_d}{w}. \tag{1.5}$$

where,

ρ_b: bulk density of aquifer, [$M\ L^{-3}$];

ω: effective porosity, [-].

1.4.3.1. Sorption of carbon tetrachloride

Many researchers have developed methods for estimating K_{oc} values based on measurable properties such as the octanol/water partition coefficients, (K_{ow}), four of the most common correlation are given in the following equations (Lyman et al. 1990):

$$log(K_{oc}) = 3.64 - 0.55 \times log(S) \tag{1.6}$$

$$K_{oc} = 0.63 \times K_{ow} \tag{1.7}$$

$$log(K_{oc}) = 5.3 - 0.54 \times log(W \times 10^9) \tag{1.8}$$

$$log(K_{oc}) = 4.277 - 0.557 \times log(S_m) \quad (1.9)$$

where,

S: is the water solubility of the organic compound, [ML^{-1}];

S_m: is the molar water solubility of the organic compound, [$\mu mol\ L^{-1}$];

W: is the water solubility in mole fraction (mole-compound/mole-water).

Equations (1.6) and (1.9) are likely to provide the most reliable predictions for K_{oc}. The parameters *S*, S_m, and *W* for carbon tetrachloride are 800 mg/l, 5200 μmol/l, and 9.4×10^{-5} mol/mol, respectively. The estimated value of K_{oc} for CCl_4 from equations (1.6) and (1.9) are 110.48 and 161.11 (μg/g-oc)/(μg/mL), respectively. Experimentally determined K_{oc} values for sorption of carbon tetrachloride on soil with organic carbon contents of 1.49 and 0.66% are 143.6 and 48.89 (log K_{oc} = 2.16 and 1.69), respectively (Walton et al., 1992).

The retardation factor of carbon tetrachloride in breakthrough sampling in groundwater ranged from 1.4 to 1.7, indicates that adsorption is a relatively minor fate process (Mackay et al., 1983). Retardation factors for carbon tetrachloride measured in a flow-through system studying sorption of organics to aquifer materials with very low organic carbon (0.07-0.025 %) range from 1.10 to 1.46 (Larsen et al. 1992).

The main sorbing phase for organic solutes is the rock phase that may have organic detritus, e.g. humic material, deposited at the time of rock deposition. This organic material is referred to as the function of organic carbon (f_{oc}) within the geologic or soil matrix. Although f_{oc} values may be about 1% or so in organic-rich soil horizons, many aquifers comprise geologic strata with low values. A value of f_{oc} =0.02 % is recorded for the Borden glaciolacustrine sands in Canada (Rivett and Allen-King, 2003). Truex et al. (2001) estimated the fate of carbon tetrachloride in the Hanford aquifer using stochastic parameters obtained by Monte Carlo methods. The f_{oc} value used in calculation was 0.002. In Alsatian aquifer, an estimated fractional organic carbon content of the aquifer (f_{oc}) is 0.001 (Schafer, 2001). The estimated K_{oc} can be used to calculate K_d if f_{oc} is measured for the specific aquifer by equation (1.3).

1.4.4. Degradation

Degradation mechanisms including biodegradation and abiotic degradation mechanism are considered as destructive processes.

1.4.4.1. Abiotic degradation

Abiotic degradation mechanisms can affect the fate and transport of chlorinated solvents in groundwater. Abiotic reactions have been found to be of fairly limited importance in groundwater relative to biodegradation. Common groups of abiotic reactions include hydrolysis, dehydrohalogenation, and reduction reactions including hydrogenolysis and reductive elimination. Hydrolysis is a chemical substitution reaction in which an organic molecule reacts with water or a component ion of water. The byproducts of hydrolysis are alcohols and alkenes (Knox et al. 1993). Because these byproducts biodegrade easily, hydrolysis is difficult to measure.

Abiotic degradation of carbon tetrachloride

In general, the rates of hydrolysis are often quite slow within the range of normal groundwater temperatures, with half-lives of days to centuries (Vogel, 1994). Jeffers et al. (1996) found that the rate of hydrolysis for dilute solutions of carbon tetrachloride was first-order and estimated half-life around 40 years at 25°C. The degradation of carbon tetrachloride by hydrolysis is slow. Natural hydrolysis of CCl_4 may lead to the formation of CO_2 and HCl (Jeffers et al. 1989 and 1996).

Truex et al. (2001) estimated the first-order abiotic transformation rate of carbon tetrachloride in Hanford aquifer and reported to be 4.6×10^{-5} day^{-1} to 2.7×10^{-7} day^{-1}. The half-life of CCl_4 estimated in the Hanford aquifer was between 36 and 290 years at 19°C.

1.4.4.2. Biodegradation

Biodegradation refers to a series of biochemical reactions mediated by microorganisms that act to break down organic compounds into other substances (Suarez et al., 1999). Typically, molecules are degraded to molecules of a simpler structure that often have lower toxicity. Biodegradation is dependent on the groundwater geochemistry, the microbial population and the contaminant properties.

Biodegradation can occur in the presence or absence of dissolved oxygen or under aerobic and anaerobic conditions.

Chlorinated solvents can biodegrade through three different pathways, including:

- Direct oxidation, whereby the chlorinated compound is directly used as a growth substrate (electron donor/food source) and broken down to inorganic molecules such as carbon dioxide, water, and chloride.
- Chlorinated solvents act as electron acceptors in an anaerobic process called reductive dechlorination, whereby the chlorinated compound is converted to another chemical by replacing chlorine atoms with hydrogen atoms.
- Co-metabolism, whereby the chlorinated compound is converted to another chemical while microorganisms use other carbon compounds for their growth substrate (food source).

The most important process for biodegradation of chlorinated solvents is reductive dechlorination. Because chlorinated solvents are utilized as electron acceptors during reductive dechlorination, an appropriate carbon source is required for microbial growth to occur. Reductive dechlorination has been demonstrated under nitrate-and sulfate-reducing conditions, but the highest rates of biodegradation occur during methanogenic conditions.

The generalized process of biodegradation of chlorinated solvents begins in the saturated subsurface where native/anthropogenic carbon is utilized as an electron donor, and dissolved oxygen is utilized first for the prime electron acceptor. This degradation process is referred to as aerobic. Anaerobic degradation occurs when oxygen has been depleted and other electron acceptors such as nitrate, sulfate, carbon dioxide, iron or manganese facilitate degradation.

Biodegradation of carbon tetrachloride

The conditions that favor biodegradation of CCl_4 are predominantly anarobic and require the presence of biodegradable organic carbon (Bouwer and McCarty 1983a; Cobb and Bouwer 1991). The following sections discuss biodegradation of carbon tetrachloride under both aerobic and anarobic conditions:

Aerobic

Some highly chlorinated solvents, including carbon tetrachloride and tetrachloroethylene, are not known to be degraded under aerobic conditions,

(McCarty and Semprini, 1994). Many studies showed that carbon tetrachloride is resistant to aerobic biodegradation, (Cochran et al., 1988; Oldenhuis et al., 1989 and Vannelli et al., 1990).

Anaerobic

Carbon tetrachloride is degraded easily in anaerobic biodegradation condition via reductive dechlorination rather than through oxidation reactions (Rifai et al. 1995; Nyer and Duffin, 1997). In reductive dechlorination, chlorine atoms are sequentially removed from the molecule and replaced with hydrogen, producing a series of intermediate products until complete dechlorination is achieved to produce to chloroform (CF), dichloromethane (DCM), chloromethane (CM) and ultimately methane (see Figure 1.4). Carbon tetrachloride biological destruction, and its degradation products, has been observed under denitrifying, sulfate-reducting, acetogenic, fermentative, and methanogenic conditions by a varity of organisms (Bouwer, 1994 and Picardal et al., 1995).

The denitrification/cometabolism degradation of carbon tetrachloride results in little to no production of chloroform. However, the mechanisms of this degradation process are not as well understood as reductive dechlorination and contain numerous limiting factors. Basically, carbon tetrachloride is cometabolized to eventually produces carbon dioxide and possibly formate (Lasatoskie, 1999). The degradation pathway of carbon tetrachloride is shown in Figure 1.4.

Many studies have shown biodegradation of carbon tetrachloride under anaerobic conditions. Bouwer and McCarty (1983a) showed that under methanogenic conditions, carbon tetrachloride was found to be degraded to below the detection limit (< 0.1 μg/l) within 16 days and carbon dioxide was the only identified degradation product. In a continuous-flow column study, the authors found that 99% of CCl_4 was degraded in the column and carbon dioxide being the major degradation product. Bouwer and McCarty (1983b) did a similar study but under denitrifying conditions. They found that carbon tetrachloride degraded rapidly and chloroform and carbon dioxide were the identified degradation products. The biodegradation of carbon tetrachloride using aquifer material has been studied by Parsons et al., 1985, showed the occurrence of reductive dehalogenation of CCl_4 to chloroform. Egli et al (1987) observed degradation of dechlorinated carbon tetrachloride to trichloromethane and dichloromethane within 6 days.

Truex et al. (2001) found that there is no biotic degradation of carbon tetrachloride at Hanford aquifer because this is an anaerobic process that is inhibited by the dissolved oxygen present in Hanford aquifer. Furthermore, Hanford aquifer has very low levels of the organic carbon needed to support biotic transformation of CCl_4.

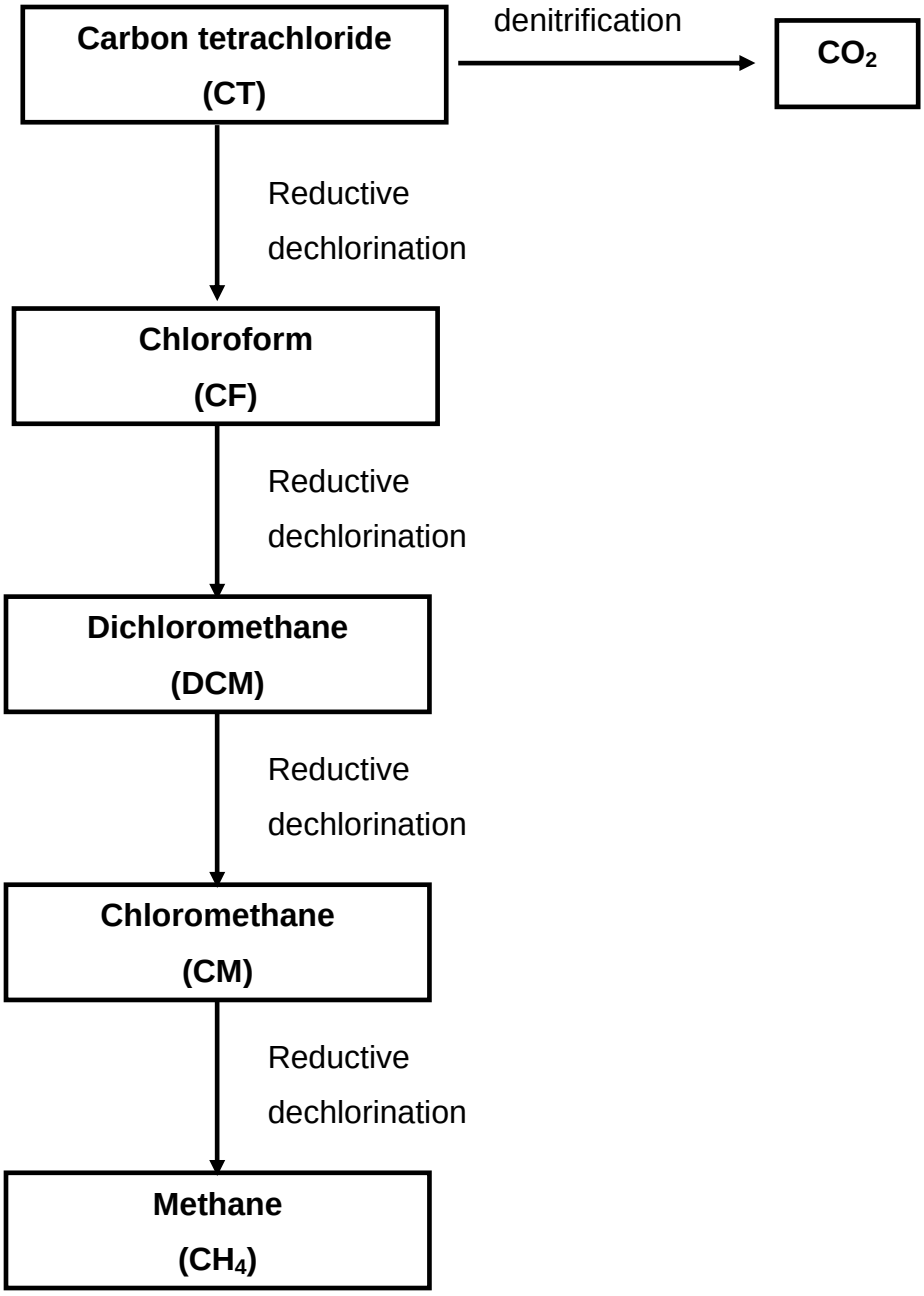

Figure 1.4. Anaerobic degradation pathway of carbon tetrachloride.

1.4.4.3. Biodegradation rate constant

Microbial and chemical degradation of an organic substance in a soil are generally grouped and described by a first order degradation law:

$$C = C_0 e^{-\lambda t} \tag{1.10}$$

where,

C: is the biodegraded concentration of the chemical, [ML^{-3}];

C_0: is the initial solute concentration of the chemical, [ML^{-3}];

λ: is the first order degradation constant, [T^{-1}].

Degradation rate is proportional to the concentration. The first-order biodegradation rate constant (λ) can be estimated from laboratory microcosm data by evaluating the slope of the best-fit line on a plot of concentration versus time using a semi-logarithmic scale for concentrations. Biodegradation rate constant (λ) is used in solute transport models to characterize the effect of biodegradation on contaminant migration, (Newell et al, 2002).

The half-life, $t_{1/2}$ [T], of a chemical is defined as the time needed to degrade half of its initial concentration. It is defined by:

$$t_{1/2} = \frac{\ln 2}{\lambda} \tag{1.11}$$

This half-life value is used to calculate the biodegradation rate constant. Except for first-order reaction, the half-life is not constant but changes depending upon the extent to which the reaction has occurred. For this reason, half-life is, generally, used to describe only first-order reactions.

Suarez et al. (1999) used 138 studies to estimate biodegradation coefficients for chlorinated compounds. The kinetic expressions used to estimate the degradation rate include Monod kinetics, and first-order reaction. More than 40 studies reported zero-order rates; a mean value of carbon tetrachloride for anaerobic rate was 0.04 mg/L-day. In the first-order rate, the mean value for carbon tetrachloride equals to 0.11 day^{-1}. Overall, first-order rate coefficient of carbon tetrachloride is between 0.004 and 0.49 day^{-1}. Doong et al. (1996) studied the influence of electron donors and microbial concentration on the rate of dechlorination of carbon tetrachloride under anaerobic conditions, the pseudo-first-order degradation rate constant ranged from 0.0057 day^{-1} to 0.135 day^{-1}.

1.5. Summary

The truck tanker accident in 1970 has spread some 4000 l of carbon tetrachloride in the south of Strasbourg. Because of vaporization and other degradation mechanisms, an unknown amount of CCl_4 has leaked into the subsurface. In 1992, about twenty years after the accident significant concentrations of the chemical have been located at different wells in the Alsatian aquifer.

We have briefly provided some of the physiochemical properties of CCl_4 and its expected impact on the environment and local community. The data provided here will be used in the following chapters to build our numerical modeling of the problem and the associated assumptions and simplifications, and to set the tuning and calibration parameters.

CHAPTER 2

CHAPTER 2
BASIC EQUATIONS OF FLOW AND TRANSPORT IN POROUS MEDIA

Before discussing the appropriate governing model for the transport of CCl_4 in the aquifer, we briefly present, in this chapter, the basic definitions of the porous-medium properties and the governing equations of single-phase flow and transport of solute in saturated porous media. The water flow is described by the Darcy law and the continuity equation that governs the volumetric balance equations. The solute transport is described by a convection-diffusion-dispersion equation. We also introduce the numerical model, TRACES, which is used to approximate the flow and transport equations.

2.1. Properties of saturated porous media

A porous medium consists of a solid matrix with interconnected void spaces. The void spaces can be completely or partly filled with water and/or other fluids like oil or gas. The pores are the spaces that are not filled by solid material. In this thesis, only water saturated porous media are considered. The saturated zone is, therefore, formed of porous material whose pores are filled with water. The main parameters that characterize a porous medium are the porosity and permeability.

2.1.1. Porosity

The presence of void space distributed within the solid matrix is characterized by the porosity of the medium. The porosity is a dimensionless parameter expressed by the volume of void spaces per unit volume of the aquifer material. Since the isolated or disconnected pores do not account for the flow, the concept of effective porosity is introduced, which is the ratio of volume of the interconnected pores to the total volume of the soil or the rock. In granular porous media, such as the alluvial aquifer, the effective porosity is typically almost equal to the total or bulk porosity. The porosity of a sand medium can be strongly affected by the packing and the grain size distribution.

2.1.2. Permeability

The *Permeability* is a measure of the medium ability to transmit a fluid flow under the influence of a driving pressure. This parameter depends on the size, shape and interconnectness of pores spaces. Finer-grained material exhibits low permeability, while coarser-grained material generally exhibits higher permeability. The *intrinsic permeability* is expressed, as follows:

$$\boldsymbol{k} = \frac{\mu}{\rho g}\frac{Q}{A}\frac{1}{\left(\Delta p/\Delta s\right)}, \tag{2.1}$$

where,

Q: the volumetric flow rate, [L^3T^{-1}];

μ: the dynamic viscosity of the fluid, [$ML^{-1}T^{-1}$];

A: the cross–sectional area of the flowing fluid, [L^2];

$\Delta p/\Delta s$: the applied head difference across the length, [-].

The permeability is a function of the medium. For a medium saturated with water, it is customary to define the hydraulic conductivity. Unlike the permeability, the hydraulic conductivity takes into account the particular fluid that is present in the medium. In an isotropic medium, the hydraulic conductivity is defined as:

$$K = \frac{\boldsymbol{k} r\, g}{m} \tag{2.2}$$

where,

K: is the hydraulic conductivity, [LT^{-1}];

$\boldsymbol{k}$: is the intrinsic permeability of the medium, [L^2];

ρ : is the fluid density, [ML^{-3}];

g: is the acceleration of gravity, [LT^{-2}];

μ: is the fluid viscosity, [$ML^{-1}T^{-1}$].

It is clear from equation (2.2) that K incorporates the medium permeability $\boldsymbol{k}$, and the fluid properties ρ and μ.

Many geological formations are anisotropic where the permeability in the direction of the geological layers is greater than in the perpendicular direction. Moreover, in heterogeneous media, the permeability varies in space. The permeability in natural soils may vary from 10^{-8} m^2 for very conducting to 10^{-16} m^2 for poorly conducting aquifers (Bear, 1988). The permeability depends on the microscale geometry of the medium, i.e., the grain sizes and the interconnectedness and the orientation of pores. Several empirical and theoretical relationships relate the permeability to the porosity, the effective grain diameter, and other medium parameters.

2.2. Groundwater flow equations

In order to model groundwater flow in complicated large scale media, the governing equations are solved numerically and given by the Darcy law and the conservation equations.

2.2.1. Darcy's law

The fundamental law of fluid flow in a porous medium is the Darcy law. The basic concept is that the groundwater flows from levels of higher energy to the levels of lower energy. This energy is essentially the results of the height and the pressure. The Darcy law in the porous media expresses the filtration velocity in a steady state or transient state as a function of the pressure gradient and the gravity. The Darcy's law is written by the general formula (Bear, 1979), as follows:

$$q = -\frac{\mathbf{k}}{\mu}\left(\nabla p + \rho g \nabla z\right), \tag{2.3}$$

where,

q: is the Darcy velocity or specific discharge, [LT^{-1}];

μ: is the dynamic fluid viscosity, [$ML^{-1}T^{-1}$];

p: is the fluid pressure, [$ML^{-1}T^{-2}$];

z: is the elevation above some arbitrary datum (is the vertical coordinate), [L].

If the density is assumed to be constant, the Darcy law (2.3) can then be simplified as:

$$q = -\frac{\mathbf{k}\rho g}{\mu}\nabla\left(\frac{p}{\rho g} + z\right) = -K\nabla h, \tag{2.4}$$

where,

$h = \frac{p}{\rho g} + z$ represents the groundwater head (the piezometeric head), [L];

$K = \frac{\mathbf{k}\rho g}{\mu}$ is the hydraulic conductivity coefficient or the permeability, [LT^{-1}].

Remark: q is not the true velocity, as it assumes flow through an open pipe and does not take into account the fact that water is only able to flow through the pores between solid grains. To find the actual groundwater velocity (average velocity), the Darcy velocity is divided by effective porosity w:

$$u = \frac{q}{w}$$

In an isotropic medium, the hydraulic conductivity K, or similarly the intrinsic permeability **k** is a scalar. However, if the porous medium in three-dimensional space is anisotropic, the hydraulic conductivity is defined as a symmetric tensor of the form:

$$K = \begin{pmatrix} K_{xx} & K_{xy} & K_{xz} \\ K_{xy} & K_{yy} & K_{yz} \\ K_{xz} & K_{yz} & K_{zz} \end{pmatrix}$$

The hydraulic conductivity tensor can be diagonalized introducing three mutually orthogonal axes called *principal directions* of anisotropy. In the following, we suppose

that the principal axes are aligned with the *x, y, z* directions. The tensor *K* is therefore diagonal, that is:

$$K = \begin{pmatrix} K_{xx} & 0 & 0 \\ 0 & K_{yy} & 0 \\ 0 & 0 & K_{zz} \end{pmatrix}$$

In practice, two permeabilities are distinguished: the vertical permeability K_{zz} and the horizontal permeability $K_{xx}=K_{yy}$ (de Marsily 1981 and Chavent et al. 1985).

2.2.2. The continuity equation

The continuity equation is based on the principle of the conservation of mass of water. In a control volume, the mass flux due to the sources and sinks is equal to the temporal change of mass and the mass flux across the volume boundaries (Bear, 1979 and Chavent et al. 1985):

$$\frac{\partial(\omega\rho)}{\partial t} + \nabla\cdot(\rho q) = \rho f \tag{2.5}$$

where, *f* represents the sink/source term for the fluid, [T^{-1}].

The porosity is generally slightly pressure-dependent (Kinzelbach, 1986). However, this aspect is neglected in this work, i.e., the matrix is considered incompressible. The density ρ depends only on the pressure *p* at a constant temperature. One can then write:

$$\frac{\partial(\omega\rho)}{\partial t} = \frac{\partial(\omega\rho)}{\partial p}\frac{\partial p}{\partial t} = \frac{s}{g}\frac{\partial p}{\partial t}, \tag{2.6}$$

where, $s = g\dfrac{\partial(\omega\rho)}{\partial p}$, [$L^{-1}$], is the specific storage coefficient which gives the mass of fluid added to storage (or released from it) in a unit volume of porous medium per unit rise (or decline) of the pressure head $p/(\rho g)$

By substituting Eq. (2.6) into Eq. (2.5), the continuity equation is obtained in terms of the pressure. If the spatial variation of density is negligible, the continuity equation becomes:

$$\left(\frac{s}{\rho g}\right)\frac{\partial p}{\partial t}+\nabla\cdot q=f, \tag{2.7}$$

The relation between the hydraulic head and the pressure is given by (Bear 1979 and Chavent et al. 1985):

$$p=\rho g\left(h-z\right)$$

Then, one can write:

$$\frac{\partial p}{\partial t}=g\left(h-z\right)\frac{\partial \rho}{\partial t}+\rho g\frac{\partial h}{\partial t}$$

By using(2.6), we obtain:

$$\frac{\partial p}{\partial t}=\left(\left(h-z\right)s/\omega\right)\frac{\partial p}{\partial t}+\rho g\frac{\partial h}{\partial t}$$

It follows that,

$$\frac{\partial p}{\partial t}=\left(\frac{1}{1-\left(h-z\right)s/\omega}\right)\rho g\frac{\partial h}{\partial t} \tag{2.8}$$

In particle, the quantity $\left(\left(h-z\right)s/\omega\right)$ is negligible with respect to 1 (Chavent et al. 1985, and Banton & Bangoy 1997). Then:

$$\frac{\partial p}{\partial t}\approx\rho g\frac{\partial h}{\partial t} \tag{2.9}$$

By replacing Eq. (2.9) in Eq. (2.7), the mass balance equation of an incompressible fluid in the non-deformable porous medium is written in the general form:

$$s\frac{\partial h}{\partial t}+\nabla\cdot\left(K\nabla h\right)=f. \tag{2.10}$$

In steady-state, the piezometric head is constant over time. Equation (2.10) reduces to the following form:

$$\nabla\cdot q=f. \tag{2.11}$$

2.2.3. Initial and boundary conditions

The transitory flow problem described by the continuity equation and Darcy's law (2.4) requires knowledge of the initial and boundary conditions. Initial conditions

provide the necessary set of primary variables in the computational domain at the beginning of the simulation. Additionally boundary conditions (BC) have to be supplied at the margins of the model domain. These boundary conditions represent the interaction between the domain and the surrounding environment.

Various types of boundary conditions are the following:

- Dirichlet-BC: has fixed value of the head at the boundary of the domain.

  $$h(\mathbf{x},t) = h^D(\mathbf{x},t)$$

  where h^D is a known function.

  In the steady state, this type of boundary conditions is necessary to guarantee the uniqueness of the solution. The conditions of prescribed head value can be, for example, the contact of the aquifer with a river, rivers/lakes, etc.

- Neumann-BC: describes the flux of a quantity perpendicular to the boundary of the domain. It is expressed by:

  $$q \cdot n = -K \frac{\partial h}{\partial n}(\mathbf{x},t) = q^N(\mathbf{x},t),$$

  where, n is the outward normal vector on the boundary and q^N is a known function.

  A condition for prescribed flux can be the impermeable boundaries where the flux is zero, inflow or outflow through the boundaries.

- Cauchy or Fourier-BC: is a combination of Dirichlet and Neumann boundary conditions. The flow across the boundary is calculated from a given value of the head, such that:

  $$-K \frac{\partial h}{\partial n}(\mathbf{x},t) = g^F(\mathbf{x},t)h + f^F(\mathbf{x},t),$$

  where f^F and g^F are known functions.

  An example of this case is the interactions of an aquifer with a river.

2.3. Transport of solute in the porous medium

Water, in its movement, can carry materials in dissolved form. The transport of such pollutants is a process which takes into account several physical mechanisms such as convection, hydrodynamic dispersion, molecular diffusion, and chemicals mechanisms such as adsorption, radioactive decay/filiations, and precipitation/dissolution. The fluid-medium interaction may fasten or reduce the spreading of the pollutant in the porous medium.

2.3.1. Convection

The convection is the movement of the pollutant dissolved in the groundwater in the direction of the flow. The convection is derived by the velocity of the groundwater. Thus, an increase in groundwater velocity will result in farther travel of the contaminant.

The convection is, generally, the dominant mass transport process in groundwater flow system (Domenico and Schwartz, 1990). The migration of a contaminant owing to convection is significantly influenced by the aquifer hydraulic conductivity, effective porosity, and hydraulic gradient (Wiedemeier et al. 1999).

In a uniform porous media, water will travel vertically downward until it hits the water table and then move in the down gradient direction of the aquifer. Fractures may create preferential flow paths that redirect groundwater flow; fractures of even a few millimeters across may govern groundwater flow (Wolfe et al., 1997).

The convection equation is given by:

$$\frac{\partial C}{\partial t} = -\nabla \cdot (Cu), \tag{2.12}$$

where,

C: is the concentration of solute, [ML^{-3}];

u: is the actual groundwater velocity, [LT^{-1}].

2.3.2. Dispersion and diffusion

These mechanisms may lead the contaminant to spread in directions different from the water flow paths. The molecular diffusion is due to concentration gradients within the liquid phase. This mechanism is independent of the flow velocity. It produces a flux of particles from region of high contaminant concentration to regions of low concentration. The mechanical dispersion is a phenomenon of spreading caused by fluctuations in the velocity field and heterogeneities at the microscopic scale. Reactive and non-reactive solutes may spread due to dispersion both along and perpendicular to the groundwater flow. The dispersion increases in heterogeneous material due to non-uniform groundwater flow paths.

The equation of dispersion-diffusion is given by:

$$\frac{\partial C}{\partial t} = \nabla \cdot \left(D \cdot \nabla C \right), \tag{2.13}$$

where D is the dispersion-diffusion tensor which represents the contribution of the mechanical dispersion and of molecular diffusion in porous media. This tensor, in the three-dimensional space, takes the form:

$$D = D_c + D_m$$

where,

D_c: is the mechanical dispersion tensor (Bear, 1979):

$$D_c = \|u\| \left(\alpha_l E(u) + \alpha_t \left(I - E(u) \right) \right)$$

with,

$$E_{i,j}(u) = \frac{u_i u_j}{\|u\|^2}, \quad i, j = 1,...3;$$

D_m: is the diagonal tensor of the molecular diffusion in the porous medium, [L^2T^{-1}];

α_l: is the longitudinal dispersivity, [L];

α_t:is the transversal dispersivity, [L].

Unlike the dispersion, the diffusion can occur both in the absence or presence of convective flow. It is generally less significant than dispersion in most groundwater flow problems.

The three mechanisms mentioned above (convection, dispersion, and diffusion) cause the contaminant to spread in the direction of flow both longitudinally and transversally. The combined processes of advection and dispersion result in a reduced concentration of the dissolved solute (dilution) as well as plume spreading. Dispersion generally causes contaminants to migrate 10 to 20 percent further than migration created by advection alone. The processes of advection, dispersion, and diffusion control the movement of the contaminant (Clement et al. 2004).

2.3.3. The equation convection-diffusion-dispersion

In the case of conservative and non-reactive transport, the integration processes of convection, molecular diffusion and mechanical dispersion are given by the following equation:

$$\frac{\partial C}{\partial t} = -\nabla \cdot (Cu) + \nabla \cdot (D \cdot \nabla C), \tag{2.14}$$

In the presence of an instantaneous and linear adsorption, the relation between the solute concentration C and the sorbed concentration in the solid C_s, is given by Eq. (2.15). The total mass of solute per unity of volume can be written as:

$$\omega C + \rho_s (1-\omega) C_s \tag{2.15}$$

where ρ_s represents the density of solid, [ML^{-3}].

Assuming instantaneous linear adsorption, the retardation factor R can be defined by:

$$\omega \frac{\partial C}{\partial t} + \rho_s (1-\omega) \frac{\partial C_s}{\partial t} = \omega \left(1 + \rho_s \frac{(1-\omega)}{\omega} K_d \right) \frac{\partial C}{\partial t}$$
$$= \omega R \frac{\partial C}{\partial t}$$

where,

$$R = \left(1 + \rho_s \frac{(1-\omega)}{\omega} K_d \right).$$

By taking into account the spatial immobility of sorbed solute due to the convection or to the dispersion, the equation of transport becomes:

$$R \frac{\partial C}{\partial t} = \nabla \cdot (D \cdot \nabla C) - \nabla \cdot (Cu) \tag{2.16}$$

With, $R \geq 1$, this term decreases the transport velocity of the solute with respect to the velocity of the groundwater.

In the case of a degradation mechanism of first order (decrease radioactive) and in the present of source/sink function, the equation of transport becomes:

$$R\left(\frac{\partial C}{\partial t} + \lambda C\right) = \nabla \cdot \left(D \cdot \nabla C - Cu\right) + f_c \qquad (2.17)$$

where,

λ: is the degradation coefficient, [T^{-1}];

f_c: is the sink/source term which describing the outlet/inlet in the domain, [$ML^{-3}T^{-1}$].

In addition to the initial conditions given for *C* at t=0, the boundary conditions, related to the transport problem, can be:

- Dirichlet type: prescribed concentration: $C(\mathbf{x},t) = C^D(\mathbf{x},t)$,
- Neumann type: prescribed head value: $-D_c \frac{\partial C}{\partial n}(\mathbf{x},t) = q^N(\mathbf{x},t)$,
- Fourier conditions: a combination of head and concentration;

2.4. Numerical solution of the flow and transport problems

Several types of numerical methods can be used to solve the groundwater flow and solute transport equations. Numerical simulators that are based on conventional finite difference (FD) of finite volume (FV) methods may not be ideal for our purpose.

The transport problem is dominated by convection. The accuracy of the predicted velocity field is thus crucial. Conventional methods that intend to approximate the velocity by deriving the pressure head in a post-processing step may not be accurate in heterogeneous media. It is also well know that first order approximation method have poor convergence near chocks or sharp fronts of convection dominated problems. Fine girddings are thus required to reduce the numerical diffusion. We have used the numerical model TRACES, that combines the mixed hybrid finite element (MHFE) and discontinuous Galerkin (DG) methods to solve the hydrodynamic state and mass transfer problems.

The MHFE method, which is based on the lowest order Raviart-Thomas space (Raviart and Thomas, 1977), is used to solve the flow problem. With the MHFE, the pressure head and the velocity field are approximated individually with the same order of convergence (Thomas, 1977). The original mixed finite element method leads to a symmetric but indefinite linear system with the enter-element fluxes and cell average pressures as primary unknowns (Brezzi et al., 1991, Chavent and Roberts, 1991). This is a major drawback because the number of unknowns, which equals to the number of faces plus the number of cells, is relatively large. Besides, solvers like Conjugate Gradient (CG) or Choleski decomposition cannot be implemented efficiently. To overcome this drawback, a hybridization technique is implemented by adding new degrees of freedom that represent the pressure traces at the grid boundaries (Brezzi et al., 1991, Chavent and Roberts, 1991). With the MHFE method, the primary unknowns are the traces of the pressure and the linear system is symmetric and positive definite. It is known that the MHFE method is superior to the conventional finite element and finite volume methods in heterogeneous media (Mosé et al. 1994, Durlofsky, 1994).

A splitting-operator technique is used to solve the convection-diffusion equation. The diffusion operator is solved by the MHFE method and the convection operator by the DG method. This method was first introduced by Siegel et al. (1997) and then extended for multicomponent miscible flow of radioactive elements by Hoteit et al. (2004). The DG method is stabilized with a multidimensional slope limiter introduced by Chavent and Jaffré, 1986. A second order Runge-Kutta scheme is used to discretize the time operator. The combined DG and MHFE method conserves mass locally at the element level and avoids spurious oscillations even for full range of cell peclet numbers without adding excessive numerical diffusion (Siegel et al. 1997).

2.4.1. Numerical model

The numerical model used in this work is TRACES (Hoteit et al., 2003), as previously mentioned. As documented by Hoteit et al., 2003, TRACES (Transport of Radio ACtive Elements in the Subsurface) is a computer program for the simulation of flow and reactive transport in saturated porous media. It is written in FORTRAN 95 and is portable to different platforms. TRACES handles transient and steady state

computations in 2D and 3D heterogeneous domains. It is based on mixed and discontinuous finite element methods. The code is flexible in describing complicated geometries by using triangles or quadrangles in 2D, and tetrahedrons, prisms or hexahedrons in 3D. These numerical methods can also handle parameter contrasts between adjacent elements. Boundary conditions and almost all parameter values can vary in space. A material property index is assigned to each grid element. Boundary conditions, source terms, fluid and porous matrix properties can change with time, based on a user-specified tabular function. Numerous types of boundary conditions can be used, including conditions depending on the sign of water fluxes.
The following transport processes are supported in TRACES: water flow with anisotropy (full tensor of permeability), convection, dispersion, diffusion, instantaneous reversible adsorption (based on linear, Freundlich, Langmuir, user-specified tabular function isotherms), precipitation/dissolution and radioactive generation/degradation (radionucleides). Concerning radionucleides migration, TRACES can handle all kind of decay chains.

2.5. Summary

We have reviewed the governing equations that describe flow and transport in porous media. A brief description of the numerical model is provided. TRACES is used in our simulation study. TRACES uses the mixed hybrid finite element and discontinuous Galerkin methods. These methods are superior to the conventional FD and FV methods. The conventional methods, which have first order approximations, are expected to produce significant false spreading of fronts (numerical diffusion) and are generally inflexibility to describe complicated geometries with high contrast in permeability. Furthermore, the conventional FD and FV methods cannot properly handle full tensor of dispersion/diffusion. In the following chapter, the used equations and the main assumptions and simplifications in our model are discussed.

CHAPTER 3

CHAPTER 3
THE CCL_4 MODELING POLLUTION IN THE ALSATIAN AQUIFER

The model concept and its design included the numerical simulator (TRACES), the discretization of the simulation domain, and boundary conditions are presented in this chapter. The recharge of the aquifer and surface-water/groundwater interactions are introduced. We give a brief description of the observation wells that installed in the study area. Then the location of the contamination source and dimensions are defined. We summarize the definition of temporal moments method, their physical meaning and their general equations. The sections that follow show the relation between source behavior and parameter uncertainty. Some of the methods for solving the problem of the parameter uncertainty and some of the studies on parameter uncertainty are reviewed. We also introduce the uncertain parameter values which is used to estimate the source behavior. These included porosity, dispersivity coefficient, and hydraulic conductivity.

3.1. Conceptual model

The purpose of a conceptual model is to organize field data and to consider how these data are translated into a physical or mathematical model. It is, therefore, one of the first steps in the modeling procedure. The construction of a conceptual model includes the definition of the basin boundaries, aquifers and non-aquifers, recharge and discharge sources and the hydrochemical pattern. When natural phenomena are

represented, a number of simplifications and assumptions have to be made (Anderson and Woessner, 1992).

In order to define the conceptual model, a number of simplifying assumptions were based on field observations, and literature review. The aquifer is represented by a three dimensional domain.

The study site has complex heterogeneous and anisotropic hydrogeological conditions. In the groundwater system, carbon tetrachloride and its toxic constituents have actions of convection, dispersion, and diffusion. Volatilization of the CCl_4 at the site (saturated zone) is insignificant. The sorption of CCl_4 can be neglected due to its low distribution coefficient and low organic matter content, as discussed in Chapter 1.

The domain is highly heterogeneous due to the sedimentation effect, which provides anisotropic flow properties. The behavior of the pollutant plume is strongly influenced by the contrast of permeability within the alluvial aquifer. The 3D model consists of layers of variable thickness and zones division of different hydrodynamic properties (hydraulic conductivity, porosity).

3.2. Model design

The design of the model included the selection of numerical simulator, spatial discretization of the aquifer, and the assignment of model parameters. The model is set to agree as much as possible with the conceptual model of flow and transport in the aquifer.

3.2.1. Numerical model

The flow and transport modeling was carried out using TRACES, which was developed by Hoteit et al., 2003 at IMFS. TRACES combines the mixed-hybrid finite element (MHFE) and discontinuous Galerkin (DG) methods to solve the hydrodynamic state and mass transfer problems.

3.2.2. Model discretization

In order to solve the partial differential equation by a numerical model, a grid is superimposed over the area. A suitable spatial mesh is an important aspect of the model. The spatial scale of the grid is an important feature affecting the results of the model simulation. The size of the cells determines the ability of the model to describe variations, as well as, influence the amount of data needed as input to the model. A fine grid gives more details to the model but requires more input data.

The planar area of the simulation domain is 20x6 km^2 with a depth of about 110 m (see Figure 3.1). The simulation domain is discretized into a non uniform mesh with 25388 nodes and 45460 irregular prismatic elements (see Figure 3.2). The domain is divided into 10 successive layers according to the estimated geometry of the cross sections (the landfill site was divided into 8 zones by soil type). The layers have different depths (numbered from bottom to top) between 5 and 15 m. The source term is located around eight mesh elements.

3.2.3. Modeling the boundary conditions

The boundary conditions are crucial for the simulation, as they control the direction of flow. Several studies were preformed at IMFS to numerically model the subsurface water flow and contaminant migration in the Alsatian aquifer (Hamond (1995); Beyou, (1999)). Hamond, (1995) estimated the hydraulic head and water-flow velocity in the area between Kogenheim and Strasbourg by using a 2D steady-state model. A sketch of the domain is shown in Figure 3.1. The accuracy of their model was validated using the average values of measured head data during the period between 1970 and 1994. They also analyzed the flow trajectories and the travel times of water particles between Benfeld and Strasbourg. The model was calibrated with 34 points of measurement head, where the maximum difference between the measured and predicted piezometers was less than 10 cm for 31 points and 16 cm for the 3 other measurements.

The measurements in the aquifer showed that the contaminated zone is located approximately in the groundwater between Benfeld and Erstein, South-West/North-East. The contaminated zone is confined within a rectangle domain of 6 km width and 20 km length. The contaminated domain is located between Huttenheim upstream of

Benfeld and Illkirch downstream of Erstein (see Figure 3.1). The flow and contaminant transport problem are solved in the contaminated aquifer which is described by a 3D computational domain. To be able to solve the water flow problem, the boundary conditions that involve the hydraulic head and water flow rates at the vertical boundaries of the 3D domain should be predetermined. To define those boundary conditions, the hydraulic head and velocity field are computed in a 2D far field that encloses the Alsatian aquifer and a couple of kilometers of the surrounding aquifer. A planer cross-section of the far field and the Alsatian aquifer are sketched in Figure 3.1. The Alsatian aquifer is represented by the dashed rectangular zone (reduced domain) in Figure 3.1. The computed hydraulic head from the 2D far field at the boundaries of the reduced zone is used as boundary conditions for the flow and transport equations in the 3D domain. Water flow is essentially horizontal in the aquifer, therefore, we assumed that the hydraulic heads is constant along the depth of the aquifer at the vertical boundaries of the 3D domain.

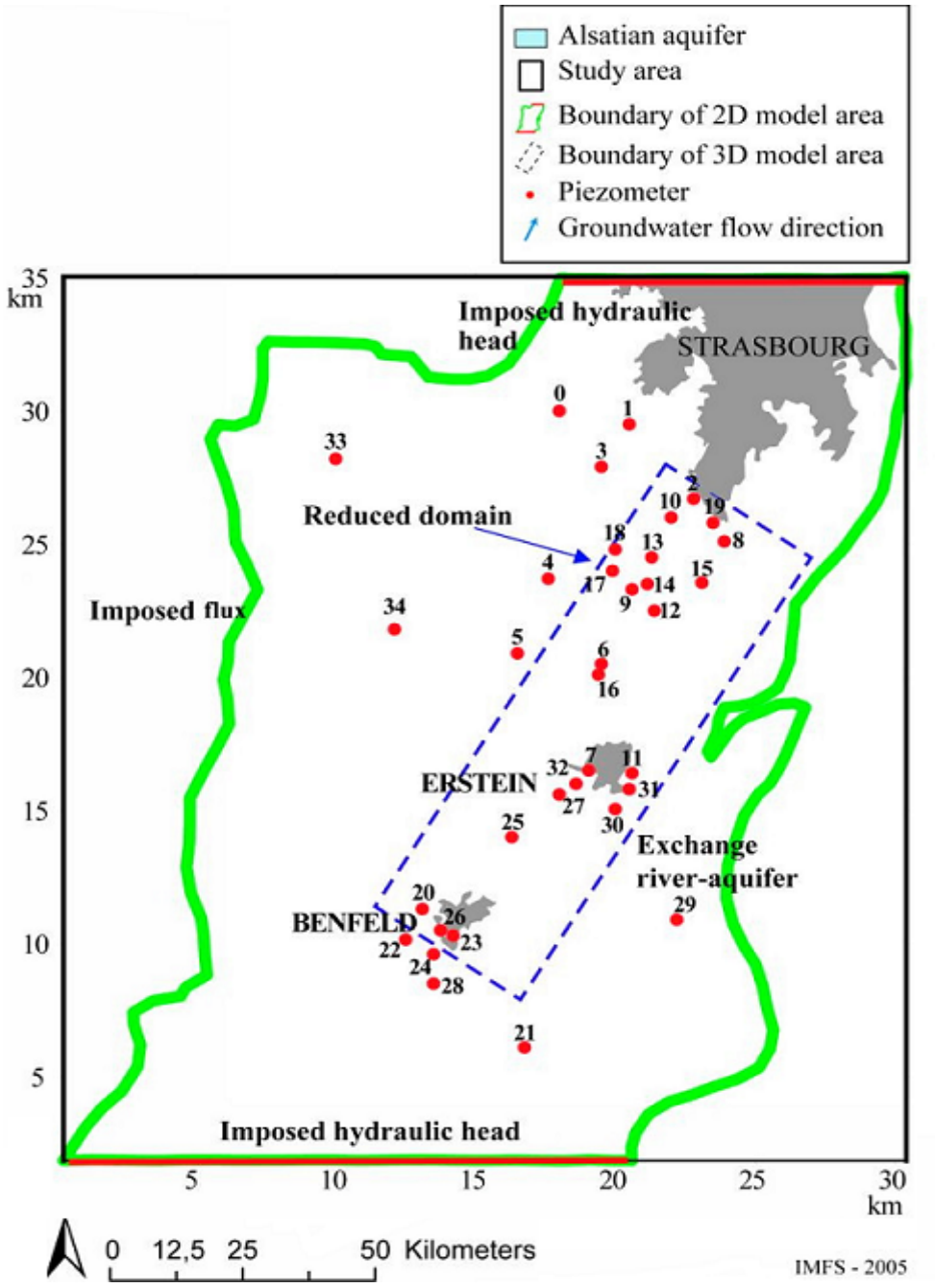

Figure 3.1. Computational far field and near field with the corresponding boundary conditions.

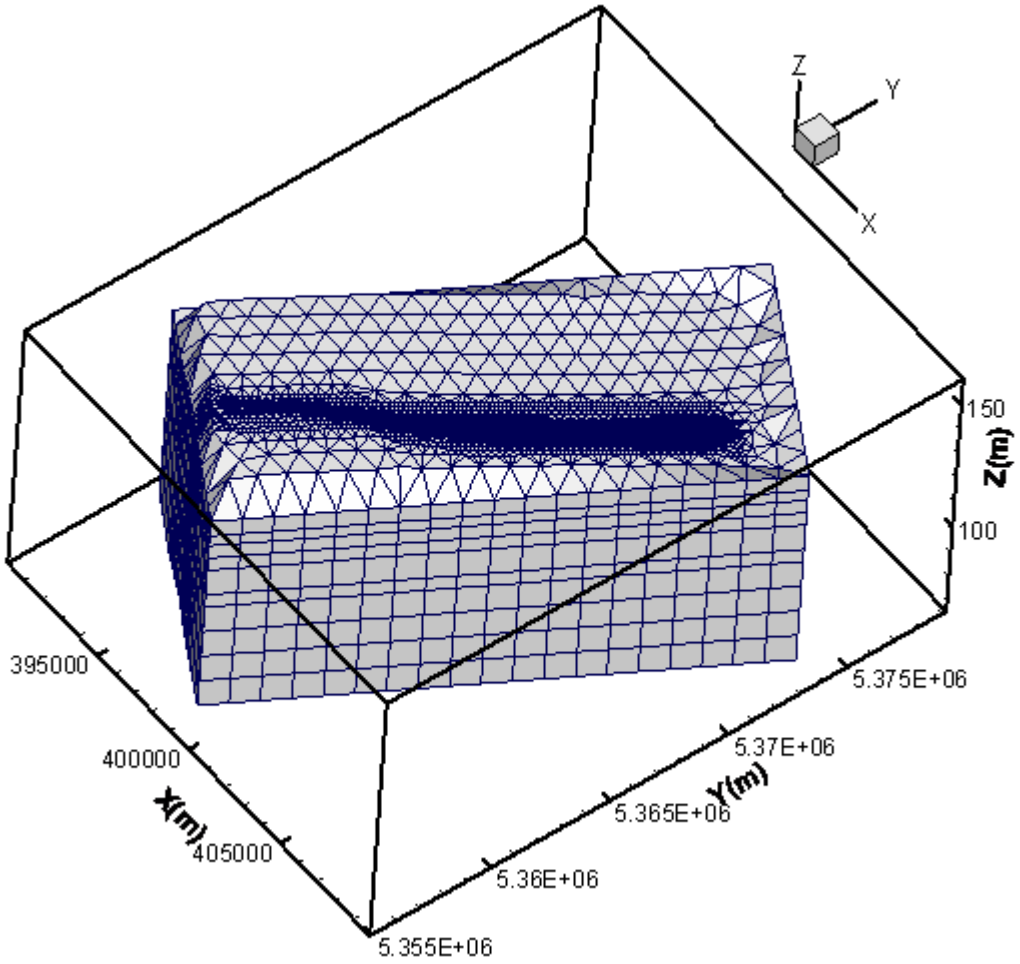

Figure 3.2. Computational mesh of the 3D domain.

3.3. Recharge

Recharge to an unconfined aquifer generally results from vertical percolation of precipitation through the unsaturated vadose zone to the surface of the water table. Infiltration of rainwater is a major source of recharge of the aquifer. A study of the mean precipitation in the study area that was carried out by CEREG under PIREN-Eau/Alsace program showed that approximately 620 ML/yr of water recharges the groundwater at the center of the Alsatian aquifer and that 680-740 ML/yr recharges the north-eastern margin of the aquifer. They generated a map of mean rainfall using five rainfall gauging stations. The groundwater recharge can be estimated to 5-10%

of the precipitation. Recharge of the aquifer is assumed as an average recharge and the fluctuations in time are not known precisely.

3.4. Aquifer-rivers interactions

Surface water-groundwater interactions need to be quantified in two ways in the context of groundwater resource estimates:

- Discharge of groundwater to surface water when the groundwater level is higher than the river stage.
- Recharge of groundwater by surface water when the elevation of river stage is higher than groundwater level.

The interactions are therefore, controlled by stream flow water table, configuration and geology (Lerner, 2003).

The river-aquifer interactions are described by the following equations:

$$Q_{riv} = l\,(h_s - h_R) \qquad si\ h \geq h_R$$

$$Q_{riv} = l\,(h_s - h) \qquad si\ h < h_R$$

where,

Q_{riv}: is the discharge exchange between aquifer and river, [M^3/L];

λ: is the exchange coefficient, [L^2T^{-1}]. It depends on the hydraulic conductivity of riverbed [L/T], the thickness of the river bed [L], and the width and length of the river along which seepage occurs [L].

h_s: is the head in the river, [L];

h_R: is the elevation of the river bed, [L];

h: hydraulic head in the aquifer, [L].

The complex hydrographic network includes many rivers in the study area: the Rhine, the Ill, the Bruche, the Ehn, the Andlau and the Scheer as well as, the Zembs and the forks of phreatic of the Rhine zone (see Figure 3.3).

The interaction between the rivers and the aquifer at the Alsace region has been studied by the SEMA/DIREN. The exchange coefficient of the Rhine has been estimated to about 10^{-6} m/s by taking into account the discharge of the contra-cannel.

The canalization of the Rhine in Alsace was established to maintain a constant water level of the river and for agriculture purpose. The presence of drainage of the contra-cannel complicates the description of the exchange aquifer-rivers as this reduces the water level of the Rhine. Therefore, a reduced value is used for the exchange coefficient and for the discharge evacuated by drainage.

The surface-water/groundwater interactions are modeled in the 2D far field that encloses the Alsatian aquifer and the Rhine River (see Figure 3.1).

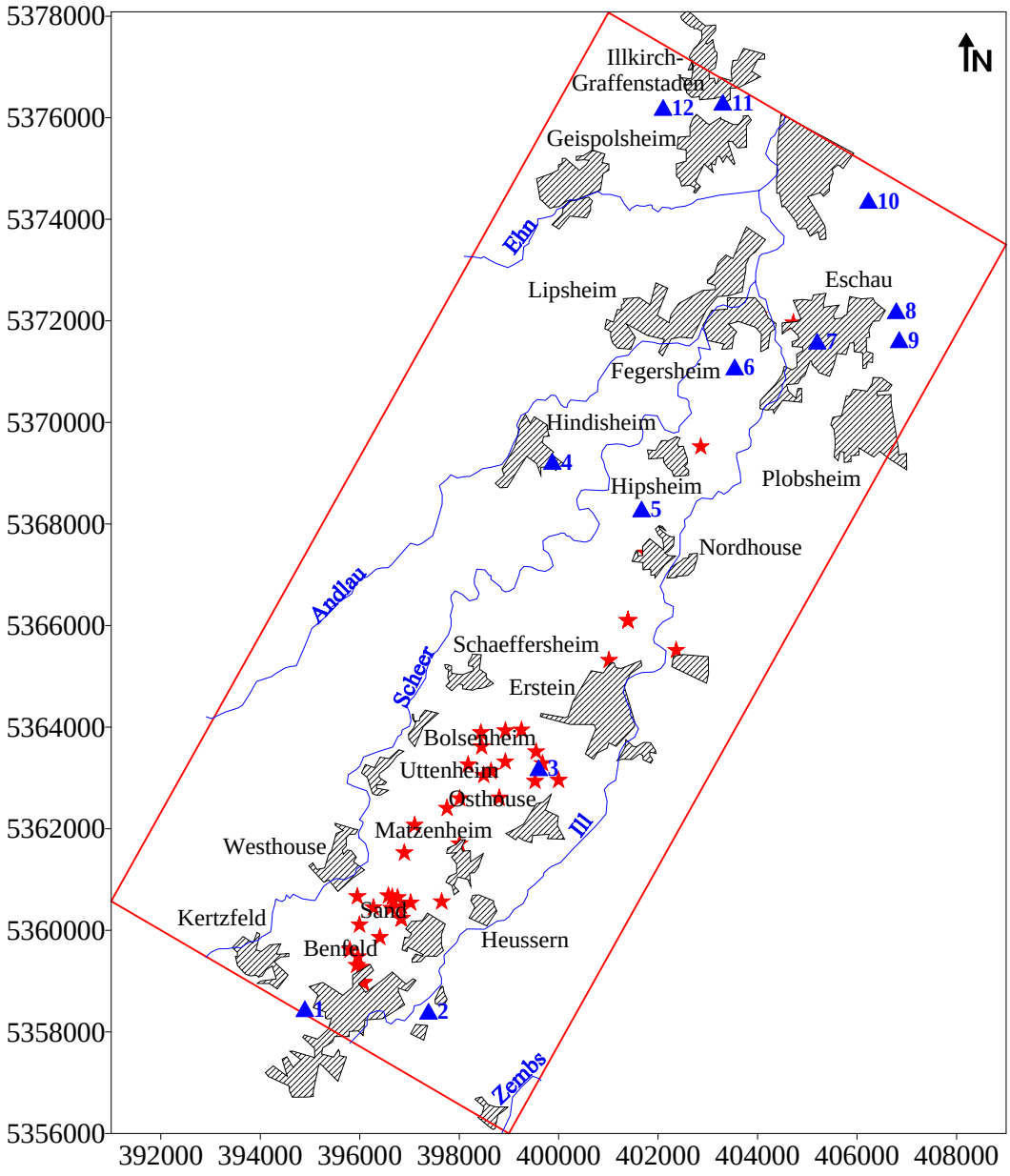

Figure 3.3. Location of observation (stars) and pumping wells (triangles).

3.5. Field wells

The groundwater in the region is mainly used for domestic and livestock water supplies. Three wells are constructed to supply the city of Erstein in drinking water: the Château d'eau, the Postal, and the Negerdorf wells. These wells are located in

the south of Erstein. The old well Château d'eau, which was drilled in 1922, collected water at a depth between 12 and 26 m. This well was only used in necessary situations. The Postal well was used to supply water to the city. It was constructed in 1972 and collected water at a depth between 26 and 59 m. In 1991, the Negerdorf well (Figure 3.6) was constructed to replace the Postal well. It consists of three pumps with a pumping rate of 300 m^3/h each (BRGM, 1992). The Negerdorf well (No. 308-1-077), is located downstream of the pollution source and collects water at a depth between 49 and 79 m. The analysis of the samples collected from the Negerdorf well is very important since it is representative of what is happening for all the piezometers and pumping wells (fluctuation in the concentrations), see Figure 3.4.

The aquifer structure between Benfeld and Erstein could be visualized clearly due to geological profiles carried out during the installation of 34 wells and piezometers. These data have been obtained from the BRGM database. There are also 12 pumping wells for home and industrial usage, see Figure 3.3. Groundwater monitoring network was installed to monitor water quality. Water sampling is carried out from about forty shallow piezometers, (IMFS-BURGEAP, 1999).

In 1996, three piezometers were installed with a multi-level sampler that take samples from many small discrete zones in the aquifer to provide accurate vertical contaminant concentration profiles. Depth profiles are often considered necessary aspect of groundwater-quality monitoring because contaminant concentrations can vary significantly in the vertical direction and, in some situations, the entire zone of contamination may occupy only a small part of the total aquifer thickness.

These multi-level piezometers were located in Benfeld, Erstein, and Sand (EAT Environment, 1997), respectively, see Figure 3.6. Several individual screens are used to sample groundwater at specific depths. These multi-level piezometers are defined as follows, (Repot of Alsace Region, 1997):

- The piezometer PZ1 (No. 308-1-155; Figure 3.6) is located in Benfeld city. The multi-level well reaches about 85 m in depth with 8 multi-level samplings, which are: 1.76-6.76 m, 7.76-12.76 m, 16.26-21.26 m, 28.26-33.26 m, 40.26-45.26 m, 52.26-57.26 m, 64.26-69.26 m, and 79.76-84.76 m below the surface.

- The piezometer PZ2 (No. 308-1-156; Figure 3.6) is located in Sand. The multi-level well reaches about 80 m in depth with 7 multi-level samplings, which are: 2.91-7.91 m, 14.91-19.91 m, 26.91-31.91 m, 38.91-43.91 m, 50.91-55.91 m, 62.91-67.91 m, and 74.91-79.91 m below the surface.
- The piezometer PZ3 (No. 272-6-276; Figure 3.6) is located between Erstein and Nordhouse city. The multi-level well reaches about 78 m in depth with 8 multi-level samplings, which are: 1.71-6.71 m, 10.21-15.21 m, 22.21-27.21 m, 34.21-39.21 m, 42.71-47.71 m, 52.21-57.21 m, 64.21-69.21 m, and 72.71-77.71 m below the surface.

An industrial piezometer PZ4 (No. 308-1-143, Socomec; Figure 3.6), which is 15 m deep, is located in Benfeld near piezometer PZ1. This is the nearest piezometer to the accident location. It has been monitored for several years. The observed concentration of CCl_4 showed fluctuation in the concentrations, as shown in Figure 3.5.

At the source zone (Benfeld), an additional well and surface water samplings were installed in 2004 to monitor the concentration of CCl_4 at the source area. These new measured concentrations were integrated in the study carried out by VILLIGER-Sytemtechnik, (2004). From the new and old concentration of CCl_4 near the accident area (Benfeld), VILLIGER-Sytemtechnik expected two source zones, as sketched in Figure 3.7.

Concentration data of carbon tetrachloride from these pervious piezometers had been collected spasmodically between 1992 and 2004. However, only 16 piezometers were used for calibrating the developed model and simulations were performed for the period from 1970 to 2024 (BRGM, 1993).

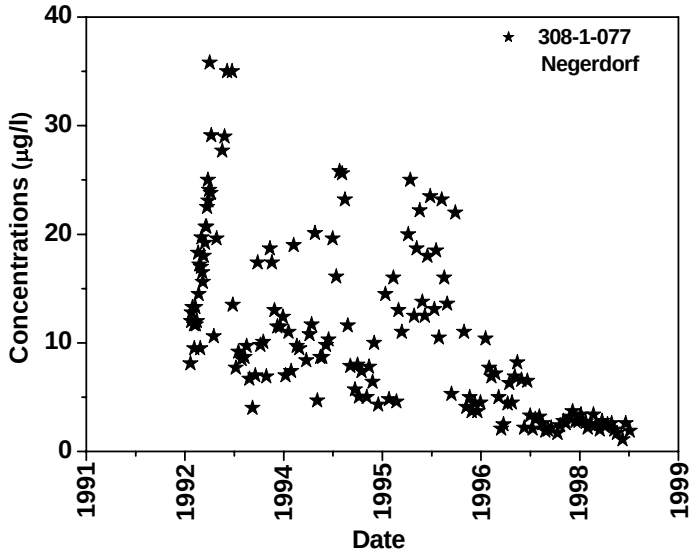

Figure 3.4. Distribution of CCl_4 concentration at Negerdorf piezometer.

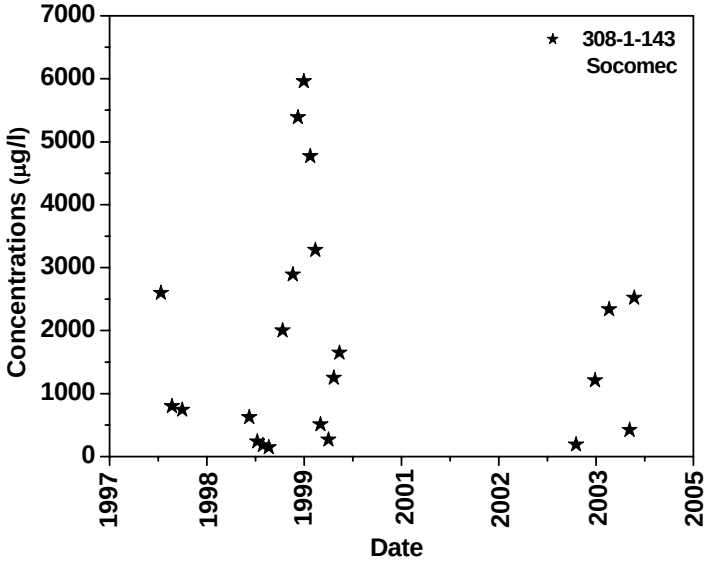

Figure 3.5. Distribution of CCl_4 concentration at Socomec piezometer.

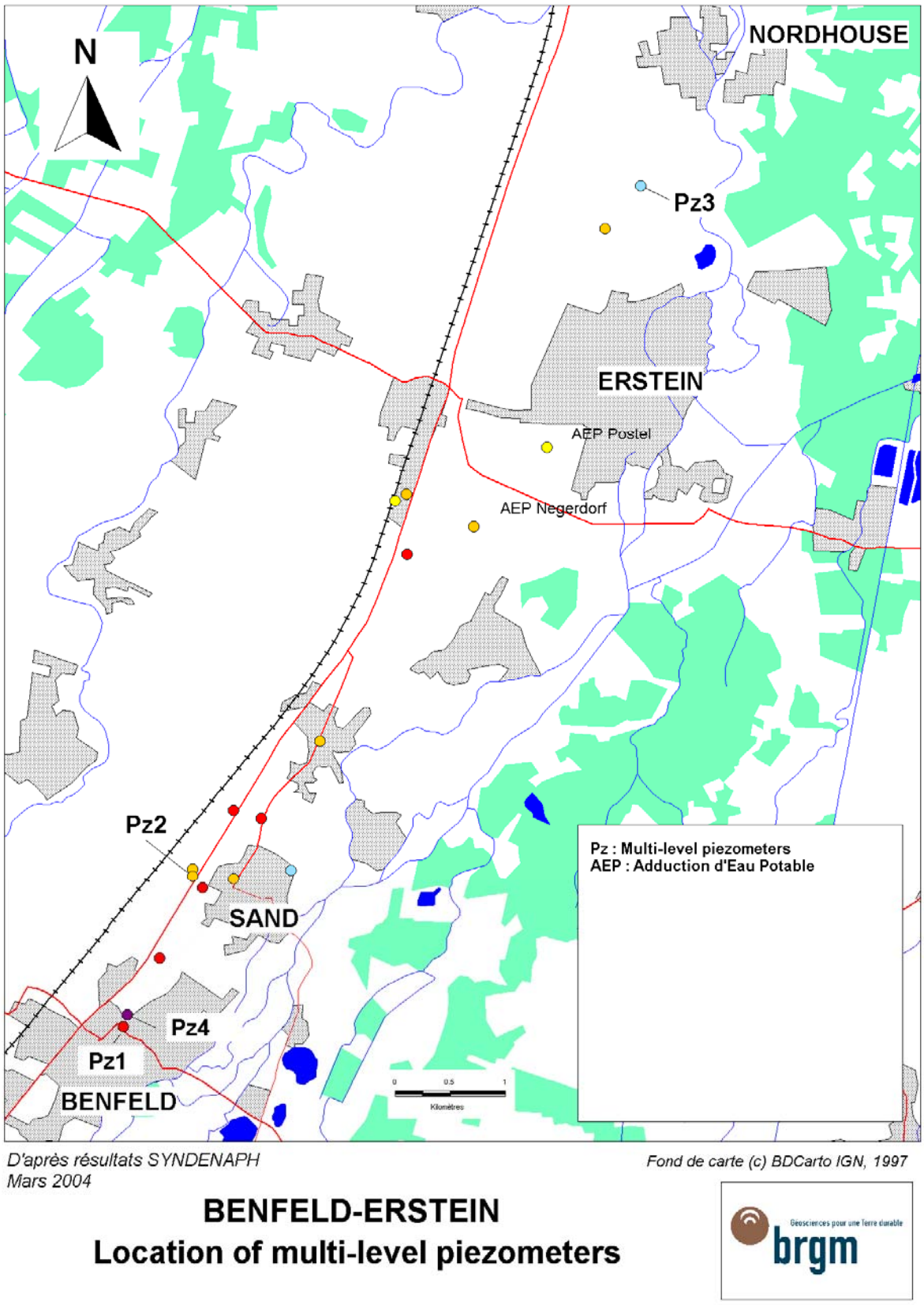

Figure 3.6. Location of multi-level piezometers and water supply wells.

3.6. Source zone

The location of the contamination source and depth of the contaminant source are not known or uncertain. One of the main motivations of this work is to understand the behavior of the contaminant source at different depths and eventually to predict its migration in the aquifer. Numerous water samples within the area near the location of the accident were taken and analyzed as shown in Figure 3.8.
A three dimensional model is used to study the behavior of the contaminant source at different depths. In order to estimate the source pollution behavior, we must define the source location and depth of the contaminant source:

3.6.1. Location of the contaminant source

To specify the location of the contaminant source, we used the measured concentration of carbon tetrachloride collected in 2004 by VILLIGER-Sytemtechnik (see Figure 3.7).and the mesh of the 3D domain. In Figure 3.7, we can see the location of the source zones were given by VILLIGER-Sytemtechnik study. In our study, we used the mesh of the 3D domain, and we considered the source location in two mesh elements, for the following reasons:
First, in these two mesh elements we found the highest concentrations of CCl_4. second, the accident have been happened in the location of one of these two mesh elements, in addition, the measurements were obtained from the multi level piezometer (308-1-156) showed high concentrations, however, since the flow direction is north east as we see in Figure 3.7, then it is most probably that the contaminant passed through these mesh elements.

3.6.2. Depth of the contaminant source

In porous media for DNAPL, the pollution depth and area of the infiltration can be approximated by:

$$V_{HC} = S_r \theta_T V \tag{3.1}$$

where,

V_{HC}: the volume of the pollutant, [M^3];

S_r: the residual saturation, [-];

θ_T: the porosity of the medium, [-];

V: the volume of the contaminated aquifer, [M^3].

Based on a note of the SGAL in 1971, the volume of the infiltrated CCl_4 (V_{HC}) is about 4 m^3. The parameters S_r, and θ_T are approximately 2-5% and 15-35%, respectively. Therefore, the volume of the contaminated aquifer is about 230 m^3 to 1300 m^3.

To define the depth of the contaminant source, we based our analysis on the results taken in 1997 from a multi-level piezometer (308-1-155) at Benfeld (EAT, 1997). These results showed that the concentration of CCl_4 is small under 35 m depth. So the source is considered the first four layers in our numerical model (each layer has two mesh elements); the thicknesses of the layers are 16, 4, 5, and 5 m from top to the bottom, respectively. If we assume that the pollution depth is 35 m then the surface of infiltration is 7 to 37 m^2.

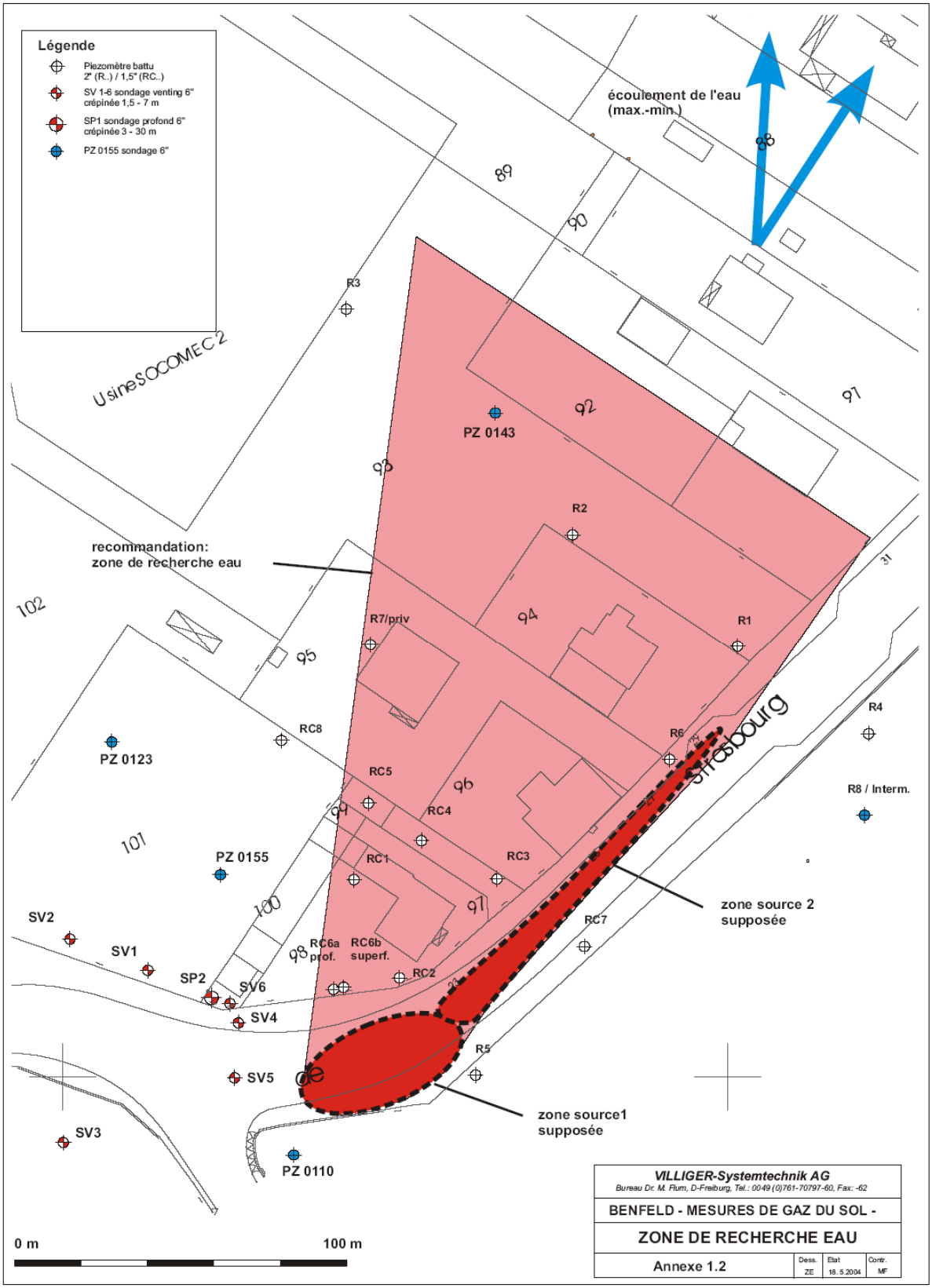

Figure 3.7. Location of the source zones, VILLGER-Systemtechnik report, 2004.

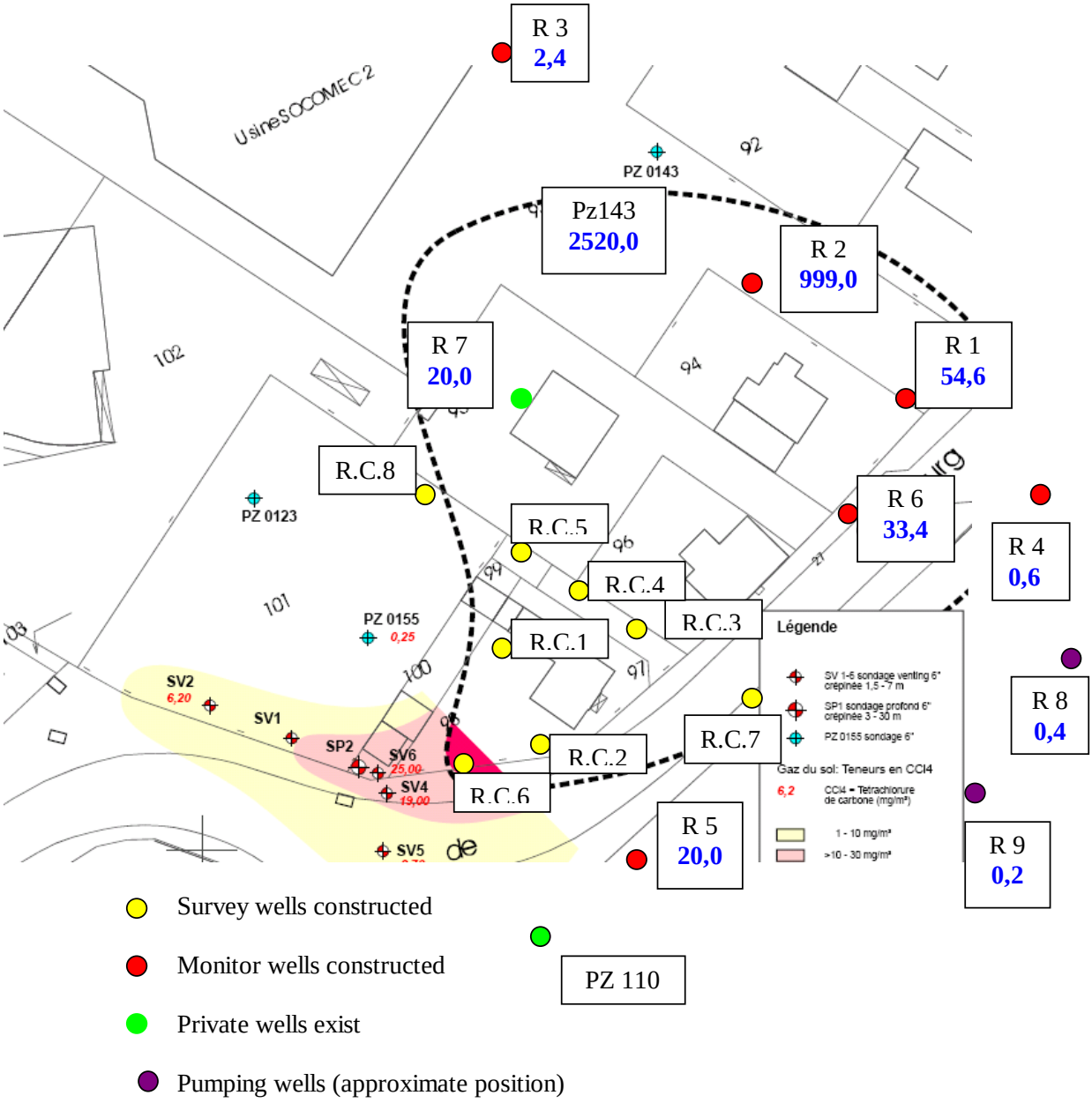

Figure 3.8. Observed concentrations of CCl_4 collected on 18/05/2004, VILLGER-Systemtechnik report, 2004.

3.7. Estimation of the travel time by temporal moments method

One of the main difficulties we faced in this study is the unknown source term that describes the amount of soluble CCl_4 in the groundwater. In order to determine the behavior of the source term that is a function of depth and time, we used the so-called, temporal moments.

3.7.1. Temporal moments

The concept of moments both in space and time, is not new. It is used in statistics, mechanics, and many other engineering disciplines. Harvey and Gorelick (1995) and Cirpka and Kitanidis (2000) discussed the physical meaning of temporal moments in the context of characterizing flow and transport in heterogeneous aquifers.

The method of temporal moments is an efficient way for analyzing breakthrough curves (BTC_S) without any assumption about the transport process. Nevertheless, moments can be used to calculate particular model parameters, (Dagan and Nguyen, 1989).

The definition of the *k-th* temporal moment m_k [MT^kL^{-3}] of a local breakthrough curve at location x is (Kucera, 1965; Valocchi, 1985):

$$m_k = \int_0^{\infty} t^k c(x,t)dt, \tag{3.2}$$

where c (x, t) is the local concentration measured over time at location x.

Thus the zeroth moment, m_0, becomes

$$m_0 = \int_0^{\infty} C(x,t)\cdot dt \tag{3.3}$$

The normalized *k-th* moment is obtained from:

$$\mu_k = \frac{m_k}{m_0} = \frac{\int_0^{\infty} t^k c(x,t)\,dt}{\int_0^{\infty} c(x,t)\,dt} \tag{3.4}$$

The first normalized moment, μ_1, also called the mean breakthrough time, is given as:

$$\mu_1 = \frac{m_1}{m_0} = \frac{\int_0^{\infty} tc(x,t)\,dt}{\int_0^{\infty} c(x,t)\,dt} \tag{3.5}$$

General moments are given by:

$$m_k = \frac{1}{m_0} \int_0^{\infty} (t - m_1)^k\, c(x,t)\,dt. \tag{3.6}$$

The physical meaning of the temporal moments is:

The zeroth temporal moment: is the area under the breakthrough curve. It denotes the total mass that passes by the location of observation.

The first temporal moment: corresponds to the center of gravity of the area under the curve. For breakthrough curve, if normalized by zeroth moment, it quantifies the mean arrival time of the solute under investigation.

The second temporal moment: normalized by the zeroth moment corresponds to the moment of inertia in mechanics. In statistics, it is the variance of a probability density function. For local breakthrough curves, it quantifies the spread or diffuseness of the breakthrough around the mean arrival time.

The Normalized Second Central Moment corresponds to the relative spread of a breakthrough curve.

3.7.2. Implementation of the temporal moments method

As previously motioned, the source function describes the dissolution of CCl_4 in the groundwater at the accident location is an unknown. We have found that the source function has a significant effect on the concentration distribution in the contaminated area in the aquifer, as expected. In order to estimate the source function, travel time between the source and the observation points is needed. The method we used to determine the travel time is based on the temporal moments.

The travel times for CCl_4 between the source location and the wells were calculated from a tracer response curve resulting from the imposition of an idealized instantaneous tracer pulse at the source location. Analysis of the simulation results (response curves) was confined to the first temporal moment of the model output.

The area under the breakthrough curve (the zeroth moment) was calculated for each location using the trapezoidal rule, by using equation (3.5). The mean travel time (the first moment) for each location was calculated from:

:

$$t_c = \frac{\int_0^{\infty} C_{cal}(t) \cdot t \cdot dt}{\int_0^{\infty} C_{cal}(t) \cdot dt} \tag{3.7}$$

3.8. Source estimation associated with parameter uncertainty

The estimation of the source term in the aquifer is influenced by the formation and fluid properties such as porosity, hydraulic conductivity and dispersivity coefficients. In order to estimate the unknown sources of groundwater pollution, aquifer parameters should be accurate and more representative of the real situation in the field. Unfortunately, aquifers in general are heterogeneous, and data on aquifer properties are expensive and borne to error. Therefore the aquifer parameters are subject to uncertainty. If one does not rigorously quantify the uncertainty of model parameters, the unquantified of model output renders the models useless. Therefore, studies usually focus on evaluating the propagation of input uncertainty through the flow and transport models to quantify its effect on output uncertainty.

The increasing awareness of the uncertain nature of porous media has led to significant research efforts towards a better understanding of flow and transport processes in subsurface. The main approaches include stochastic and fuzzy-set-based methods (Gelhar, 1993; Bardossy and Duckstein, 1995; Hoogeweg, 1999; Chen, 2000; Blair et al., 2001). The stochastic method is frequently used for evaluating uncertainties in groundwater flow and transport processes (Christakos et al., 1998; Zhu and Sykes, 2000 a, b). It attempted to characterize parameter uncertainties through statistical methods and could be classified as analytical or numerical (Freeze et al., 1990). The analytical methods included random parameters as coefficients in partial differential equations. Then the stochastic differential equations could be solved, generally using spectral methods to analyze perturbed

forms of equations (Graham and Mclaughlin, 1991; Connell, 1995; Vanderborght et al., 1998; Kaluarachchi et al., 2000). The numerical methods involved solving the governing equation using finite element or finite difference approaches based on probability distributions of the input parameters (Abdin et al., 1996; Davis and Keller, 1997; Naff et al., 1998a, b; Hu and Huang, 2002; Hu et al., 2002), where the most popular approach so far was the Monte Carlo simulation (Lahkim and Garcia, 1999). Another major approach for uncertainty analysis is through fuzzy set theory, which is suitable for situation when probabilistic information is not available. This approach described uncertain parameter based on a non-probabilistic framework. It can handle uncertainties in a direct way without generating a large number of realization (Bardossy and Disse, 1993; Schulz et al. 1999; Chen, 2000).

A lot of research is devoted to studies on parameter uncertainty, especially the hydraulic conductivity. Some related studies in this field are reviewed as follows.

Levy and Ludy (2000) used a Gauss-Hermite quadrature approach to quantify the uncertainty of the delineation of one-and five-year wellhead protection area (WHPA) for two municipal wells in a buried-valley glacial-outwash aquifer (not including spatial correlation). A shallow, unconfined flow system was modelled with MODFLOW, where six modelling parameters were used for the uncertainty analysis. The horizontal hydraulic conductivity of the outwash deposits, vertical-to-horizontal hydraulic conductivity of the silty-sand, recharge, river conductance and effective porosity of the outwash deposits. The prior estimates of each parameter were derived from field data, literature data, other modelling studies and subjective hydrogeological understanding and then modified based on the study's MODFLOW simulations. The flow model was used to explore the ranges of possible parameter values that still produced acceptable calibration results given the possible ranges of all other model parameters included in the uncertainty analysis.

Copty and Findikakis (2000) estimated the uncertainty quantitatively in the evaluation of groundwater remediation schemes due to natural heterogeneity represented by the hydraulic conductivity. The hydraulic conductivity was defined as a random spatial variable whose statistical structure was inferred from available hydraulic conductivity data. Multiple realisations of the hydraulic conductivity field were generated by Monte Carlo simulations. The probability that each of the realisations may represent the actual hydraulic conductivity field was estimated by simulating the historical spread of a groundwater plume and compared with measured concentrations.

Abbaspour et al. (1998) present a model of uncertainty analysis to account for the special characteristics of environmental data: spatial and/or temporal autocorrelation, natural heterogeneity, measurement errors, small sample size, and simultaneous existence of different types and qualities of data. They treated hydraulic conductivity, porosity and longitudinal dispersivity as random variables in order to model a chloride plume from a landfill. The prior uncertainties of these variables were subjectively estimated. The uncertainties are propagated to a goal function, which defines the best alternative. A data worth model was used for the reduction of uncertainty in the model.

As mention above, model uncertainty arising from parameters can be analyzed using several techniques. In the present work, parameter uncertainties and the source estimation were analyzed through trial and error technique and Monte Carlo method.

1) **Trial and error:** The method of trial and error initially involves selecting values for the unknown parameters and then solve the direct problem. The parameters are then manually adjusted by using the comparison between the observed and approximated concentrations. Comparisons can be done by using mathematical measures such as the mean value and standard deviation. If the match is unsatisfactory, a second estimation is done for the unknown parameters and so on until a satisfactory match is reached. When many parameters are sought, the method of trail and error can be time consuming and inefficient. Despite the fact that this method is generally slow for refinement of unknown parameter values, it does enable the modeler to asses some of the assumptions made about the model being calibrated.

2) **Monte Carlo methods** are one of the most widely used methods for uncertainty analysis, with diverse applications. This method consisted of iterative individual sampling to produce multiple simulation realizations, and analysis of the realizations to present the final outputs. The outputs realization was usually presented in the form of a probability distribution or a cumulative frequency distribution (James and Oldenburg, 1997; USEPA, 1997).

3.9. Parameter uncertainty

Parameter uncertainty assess the impact of fluid and medium properties on the ultimate results of the model. Parameter uncertainty associated with parameter variations and heterogeneity within the aquifer, measurement errors, and lack of measurements. The uncertain parameters here include porosity, dispersivity coefficient, and hydraulic conductivity.

3.9.1. Porosity

The Rhine aquifer consists essentially of sands and gravels. The estimated porosity varies slightly between 10% and 20% (Hamond, 1995; Beyou, 1999). The values of the porosity were estimated through trial and error within the provided range to improve our match.

3.9.2. Hydraulic conductivity

The morphology of the Alsatian aquifer is highly influenced by the alluvial deposits and deformations of the alluvial plain of the Rhine and its tributaries (end of the Tertiary, Quaternary period). The formation is made up of fluvial sedimentation (coarse deposits of channels, fine deposits of floodplains), which results from the floods of the Vosgen streams at the Rhine Graben margins. The alluvial deposits consist of a mixture of sands, pebbles and gravels locally divided by clay layers of varying extension and thickness.

The sediments in the upper Rhine Valley consist mainly of Tertiary marls covered by Pliocene and Quaternary alluvial carbonate-rich. This strata represents the reservoir host rocks of the shallow groundwater (Simler, 1979) and consists mineralogically of mainly carbonates as well as crystalline gravels. The area consists of highly permeable alluvial deposits.

The interpretation of the geological profiles was used to identify seven lithological units that depend on the percentage of sands, the proportion of pebbles and gravels or their argillaceous characteristic. By considering the entire thickness of the aquifer,

from the non-saturated zone to the impermeable marly substratum which is about 80 m, the following categories can be classified:

- Loess, loam, clay
- Compacted clay
- Sandy clay or clayey sand
- Fine sand to very fine (sand content > 70%)
- Sandy alluvial (sand content between 50% and 70%, with 20% to 40% of pebbles or gravels)
- Medium alluvial (sand content between 30% and 50% (coarse sand), medium gravels and pebbles)
- Coarse alluvial (sand content < 20%, with medium to coarse gravels and pebbles (80% to 100%)).

The discrimination of the seven alluvial classes agrees fairly well with the assumed hydraulic conductivities in the different layers. From lithological profiles, thirty cross-sections have been carried out according to this classification.
The proposed cross sections describe the aquifer structure with some uncertainty in the extension of the sedimentary bodies.
The model area is divided into a number of zones such that a maximum and a minimum hydraulic conductivity coefficients are assigned to each zone.
In Table 3.1, we present the categories of the hydraulic conductivity and their compatibility with the lithology of the aquifer formation between Benfeld and Erstein.

Table 3.1. The categories of permeabilities considered in the model

Lithology	Hydraulic conductivity (m/s)
Marly substratum Clay, Sandy clay, clayey sand	10^{-8} to $2.5.10^{-6}$
Loess	$2.5.10^{-6}$ to $2.5.10^{-5}$
Fine sand to very fine (sand content > 70%)	$2.5.10^{-5}$ to 1.10^{-4}
Sandy alluvial (50%< sand content>70%)	1.10^{-4} to $5.5.10^{-4}$
Medium alluvial containing clay lens or high content of sand	$5.5.10^{-4}$ to $1.5.10^{-3}$
Medium alluvial (30% < sand content>50%)	$1.5.10^{-3}$ to $3.5.10^{-3}$
Coarse alluvial containing sandy lens or clayey	$3.5.10^{-3}$ to 1.10^{-2}
Coarse alluvial (sand content <=20%)	1.10^{-2} to 2.10^{-2}

In this work, Monte-Carlo method is used to estimate the hydraulic conductivity for each grid block in the domain.

3.9.3. Dispersivity

Dispersivity represents the spreading of the contaminant over a given length of flow. Early studies led to the belief that a single value of the dispersivity parameter (α) for an entire medium is sufficient to characterize the spreading processes of tracer solutes in porous medium (Bear, 1972). However, numerous studies have shown that dispersivity measured in the laboratory often fails to give adequate description of transport behavior in field scale. Dispersivities estimated from field observations are often much larger than those measured in the laboratory for the same type of porous material (Pickens and Grisak, 1981). Numerous studies suggest that dispersivity depends on the mean travel distance and the scale of the observations (Peaudecerf and Sauty, 1978; Sudicky and Cherry, 1979; Pickens and Grisak, 1981a). The scale

dependency of the dispersion adds complexity in characterizing solute transport in the field.

Gelhar et al. (1992) presented a review of dispersivity observations from 59 different field sites and found that longitudinal dispersivities ranged from 10^{-2} to 10^{4} m for scales of observation from 10^{-1} to 10^{5} m. At a given scale, the longitudinal dispersivity values were found to range over 2 to 3 orders of magnitude (Gelhar et al, 1992). Overall, the data indicated a trend of a systematic increase of the longitudinal dispersivity with observation scale.

In addition to estimating longitudinal dispersivity, it may be necessary to estimate the transverse and vertical dispersivities (α_T and α_z respectively) for a given site. Several empirical relationships between longitudinal dispersivity and transverse and vertical dispersivities have been described. Commonly, α_T is estimated as 0.1 α_l (Gelhar et al., 1992), or as 0.33 α_l (ASTM, 1995; US EPA, 1986). Vertical dispersivity (α_z) may be estimated as 0.05 α_l (ASTM, 1995), or as 0.025 α_l to 0.1 α_l (US EPA, 1986). Generally, longitudinal dispersivities are assigned much larger values than vertical dispersivity (Domenico and Schwartz, 1998).

In this work, an initial longitudinal and transverse dispersivities have been considered based on prior information from similar geological formations (Gelhar et al., 1992). The dispersivity coefficient is estimated by trial and error using the range of selected values until the modeled and observed contaminant distribution patterns match. The details are provided in the next chapter.

3.10. Summary

In this Chapter, we assigned the workflow and the pathlines that we followed to model the Alsatian contamination problem. A significant amount of data have been gathered from various sources. The main difficulties in modeling the problem are:

1. Unknown contamination zone and boundary condition.
2. Unknown amount of leaked CCl_4 that has been dissolved in water.
3. High uncertainty in the properties of the aquifer formation and the chemical.

The above difficulties are addresses as follows:

1. Based on the observed concentrations in different wells, the borders of the contaminated zone are identified between Huttenheim and Illkirch. The contaminated zone is enclosed within a 3D domain of 6 km width, 20 km length, and about 110 m depth. A 2D domain that contains the contaminated zone, which has nearly the dimensions 30 km x 35 km, is used to estimate the heads and the flow rates at the boundaries of the 3D domain.

2. Measured data are used to identify the location of the contaminated source that is supposed to feed the aquifer from continuous dissolution of CCl_4. The source is about 30 m deep that corresponds to 4 different layers of the 3D mesh. The travel time of contaminants between the source and wells is estimated by using the temporal moments.

3. A significant amount of data have been gathered from various sources. These data were useful to set upper and lower physical limits of properties like the porosity, hydraulic conductivity, and dispersivity. The temporal moments method, trial and error, and Monte-Carlo are used to estimate the source behavior.

CHAPTER 4

CHAPTER 4
APPLICATIONS AND RESULTS

4.1. Estimation of the source term

The ultimate objective of this work is to provide a reliable prediction of the contaminate migration in the aquifer located between Benfeld and Erstein. In this chapter, we review the previous studies on identification of unknown pollution sources. Suitable measurements from available monitoring networks are selected. This chapter includes two main parts. The first part presents the methodology that was adopted to achieve the objective of the study. That included the determination of the source behavior at the accident location. While the second part presents the uncertainty on the source behavior, by assuming various source scenarios. The uncertainty on the source behavior was preformed by assuming different parameter values. These include porosity, dispersivity, and hydraulic conductivity.

4.1.1. Background

An open and challenging problem in groundwater pollution management is the detection of unknown sources of groundwater pollution. Groundwater pollution is often detected in water supply many years after the contaminant leak. Detection of the source of groundwater pollution is a challenging task. Most of the reported pollution source identification models have been developed to estimate the unknown sources of pollution in well defined groundwater systems, where the aquifer parameters, the initial and boundary conditions, and hydraulic stresses (pumping and/or recharge) are known. Some of the important contributions are due to Gorelick

et al. (1983); Datta et al. (1989); Wagner (1992); Skaggs and Kabala (1994); Sciortino et al (2000) and Aral and Guan (1996). Gorelick et al. (1983) used a least square regression and linear programming technique to solving a hypothetical two-source groundwater contaminant problem, while Datta et al. (1989) used statistical pattern recognition technique to identify unknown sources. Response matrix approach was used by Gorelick et al. (1983) and Datta et al. (1989) and the simulation model was externally connected to identification model.

Wagner (1992) combined nonlinear maximum likelihood estimation with groundwater flow and solute simulation to simultaneously identify the aquifer parameters and a distributed pollutant source term. Skaggs and Kabala (1994) used Tikhonov regularization to recover the release history of groundwater contaminant plume in a one-dimensional groundwater system. Aral and Guan (1996) used genetic algorithms and response matrix technique to identify sources of groundwater pollution. They showed that their results are more accurate than the results obtained by using linear programming technique.

Sciortino et al (2000) solved an inverse problem to identify the location of dense non-aqueous phase liquid (DNAPL) pool in a saturated porous medium under steady flow conditions. Levenberg-Marquardt method is used to solve the least squares minimization problem for the identification of the location and the geometry of the DNAPL pool.

Mahar and Datta (1997, 2000) used nonlinear optimization models to identify the unknown groundwater pollution sources using embedding technique. The embedding technique directly incorporates the governing equations for the physical processes in the optimization model and thus eliminated the necessity of external simulation. Mahar and Datta (1997) addressed the problem of designing an optimal monitoring network for efficient source identification. Mahar and Datta (2000) presented nonlinear optimization models to simultaneously estimate aquifer parameters and identify unknown groundwater pollution sources. The model was an extension of the nonlinear optimization model for source identification presented in Mahar and Datta (1997, 2000).

Mahar and Datta (2001) considered simultaneous estimation of aquifer parameters and identification of unknown pollution sources. Datta and Chakrabarty (2003) proposed the use of linked optimization-simulation approach when the simulation model is externally linked to a classical nonlinear optimization model to solve this

source identification problem. This approach is capable of solving large-scale identification problems.

Recently, Singh and Datta (2004, 2006b), Singh et al. (2004), proposed artificial neural network (ANN) based methodologies, and a genetic algorithm (GA) based linked simulation optimization (Singh and Datta 2006a) methodology that would facilitate optimal identification for unknown groundwater pollution sources using concentration measurement data. Each methodology requires a groundwater flow and contaminant transport simulation model to simulate the physical processes in the aquifer system. The GA based simulation optimization approach uses the simulation model for fitness evaluation for the population of potential pollution sources evolved by GA. The flow and transport simulation model is externally linked to the GA based optimization model. Identification of source position could be deducted from historical data. However they are often incomplete and do not include information about leakages, or migration of residual DNAPL. Therefore, their information content is restricted. Source location can be investigated by means of partitioning trace tests. To date, these approaches are on the status to find suitable tracers, and to scale results from laboratory models to length and time scales of field applications (Brook et al. 2002; Imhoff et al. 2003; Istok et al. 2002).

In this work, we propose and evaluate a methodology to identify the unknown groundwater pollution sources.

4.1.2. Measured concentrations

Numerical models are useful when accurate input data are available. Models built using modest inputs should be updated and improved as new information becomes available. Field monitoring is an essential part of any water quality assessment. These data are needed to define the problem which is an essential step for water quality modeling. The second use for these data is in the calibration and validation stages of the model.

In the Alsatian aquifer, there are about 40 wells to monitor the groundwater quality (see Figure 3.3) 24 of which detected CCl_4 concentration greater than 0.5 μg/l. In our work, we only used these piezometers, which are the most telling, as input into our numerical model.

The total measurements in the study area for the period 1992-2004 lead to 284 data points. These data points are distributed among the 24 locations with deep CCl_4 measurements. Data set reported in 1992 had the least data gaps with respect to other years. Among these data points, 161 measurements for the piezometer named 308-1-077 were carried out in 1993.
Suitable measurements from available monitoring networks are selected. In order to obtain realistic results, a number of measurements were ignored because they appeared to be inconsistent the other measurements. Therefore, the total measurements considered in our simulation are 236 data points in 16 locations. The omitted 48 data points are:

- Five data points at the piezometers named 308-1-098, 308-1-122, 308-1-102, 308-1-103, and 308-1-104 have abnormal quantity of CCl_4 with respect to the other measurement data points (>350 mg/l) at the same period in 1992. These were interpreted as an indication of erroneous sampling.
- Eight data points were ignored because the measurements do not provide information about the locations. During the period 1992 to 2004 only one data point was recorded at these piezometers. Therefore, these data points cannot be considered as representative measurements.

It is important to note that four piezometers were eliminated, 35 data points were distributed among these four eliminated piezometers: (308-1-143, 308-1-110, 308-1-123, and 308-1-155). The four eliminated piezometers were very close to the source area. In our determination, the concentrations were considered at each grid block as the mean concentrations over the element scales. Piezometers close to the source are characterized by local concentrations which are very sensitive to small scale heterogeneities. These small-scale heterogeneities were not taken into account in the model.

The sampling locations are shown in Figure 4.1. For piezometer named 308-1-156, seven sampling depths are used ranging from 3-8 m, 15-20 m, 27-32 m, 39-44 m, 51-56 m, 63-68 m, and 75-80 m.

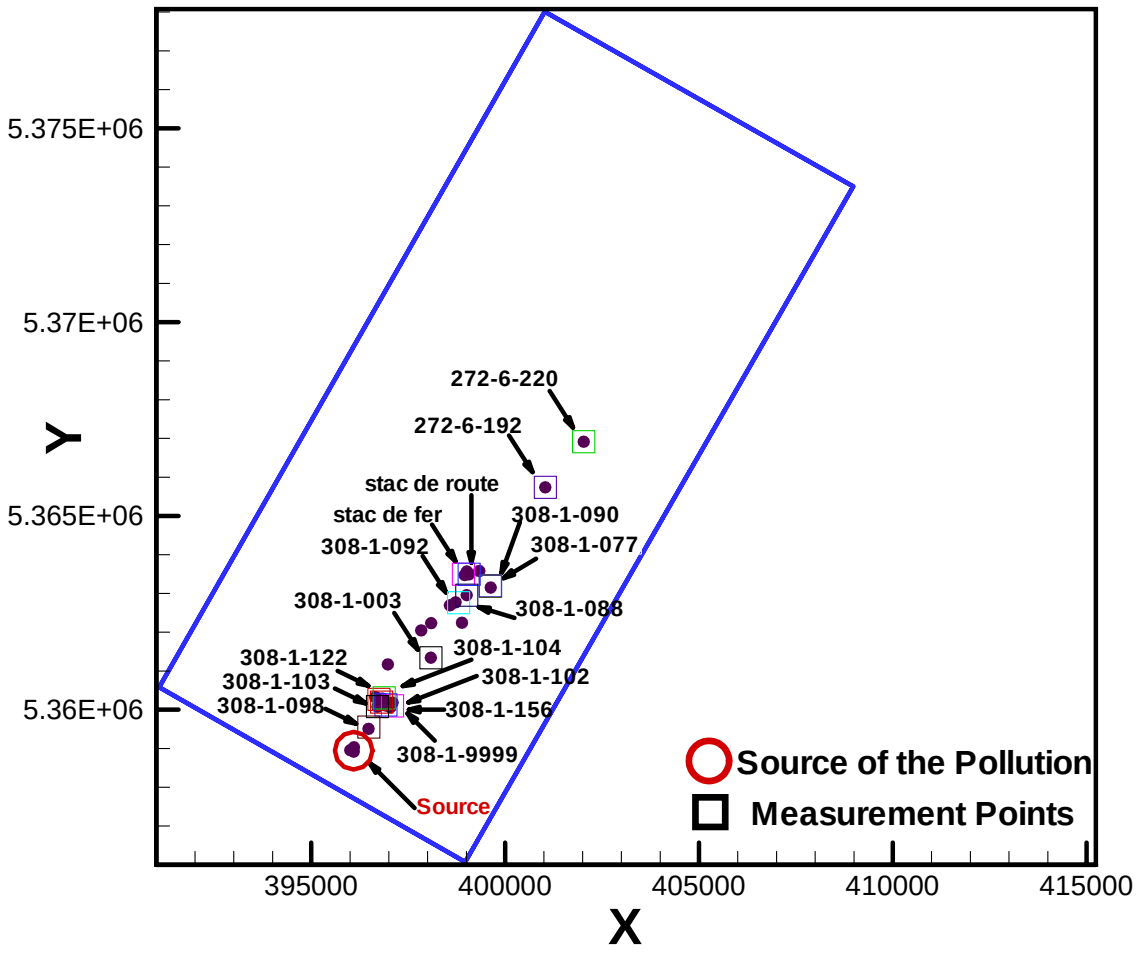

Figure 4.1 Location of the measurement points and the source of pollution.

4.1.3. Primary estimation

In order to efficiently manage the groundwater quality, a large number of response alternatives are evaluated and the best among them is selected for implementation. The pollution source characteristics (location, magnitude and duration) act as critical inputs for evaluating the response alternatives. Inaccuracies/inadequacies in determining the pollution sources may result in inefficient or unsuccessful management/remediation efforts. Therefore, to effectively and successfully manage and remediate the polluted aquifers, accurate determination of the location, magnitude and duration of pollution sources is necessary. Information regarding the

pollution sources is also necessary and useful for addressing the judicial issues of responsibility and compensation for environmental damage.

In the present study, the three dimensional model is used to study the behavior of the contaminant source at different depths. In order to estimate the source behavior, we need to recognize the source location and depth, as CCl_4 is highly volatile. The source location of CCl_4 is located in the area of the highest contaminant concentrations.

The source is discretized into four layers in the vertical direction, as previously discussed in chapter 3. The depth of the contaminated zone is about 35 m. The concentration of CCl_4 is imposed in the first eight mesh elements (each layer has two mesh elements) situated vertically beneath the accident location. The thicknesses of the layers are 16, 4, 5, and 5 m from top layer at the groundwater surface to the lowest layer, respectively. The horizontal discretization is the same for all layers.

A new methodology is proposed for optimally identifying unknown sources of groundwater pollution under a 3D convection-diffusion-dispersion model which is used to describe the transport problem. The technique assumes linear transport behavior between the concentration at the source and the distributed concentrations in the aquifer. A simplified inverse method is implemented to estimate the concentration at the source based on the measured concentrations of the aquifer at different locations and times. These concentrations are estimated by a preliminary calculation in order to determine the relationship between the source concentration and the concentration at the measurement points in the domain. The technique used to estimate the source function at the first four layers is discussed below, (see Figure 4.2):

First, we fixed the concentration of CCl_4 in each the grid cells representing the source in the four layers. The code TRACES is used to compute the concentration at the piezometers in the domain. In order to find the concentration at the cells representing the source, we matched the calculated concentrations with measured concentrations at the piezometers by using the following formula:

$$C_s\left(t-t_c\right)=C_{init}\left(t-t_c\right)\frac{C_{mes}\left(t\right)}{C_{cal}\left(t\right)} \tag{4.1}$$

where, C_{init} is the constant value (100 μg/l) at the source.

The travel time of the contaminant (t_c) between the source and the measurement-wells is estimated by the temporal moments (equation (3-5), Chapter 3), then the time at the source is given by:

$$t_s = t - t_c.$$

where t is the time of measurements.

Using the above approach, each observed datum from the measurement wells feeds back a corresponding concentration at the source. The calculated concentrations at the source in the four layers that correspond to the data measured at different time and location at the measurement wells are presented in Figure 4.3 to Figure 4.6.

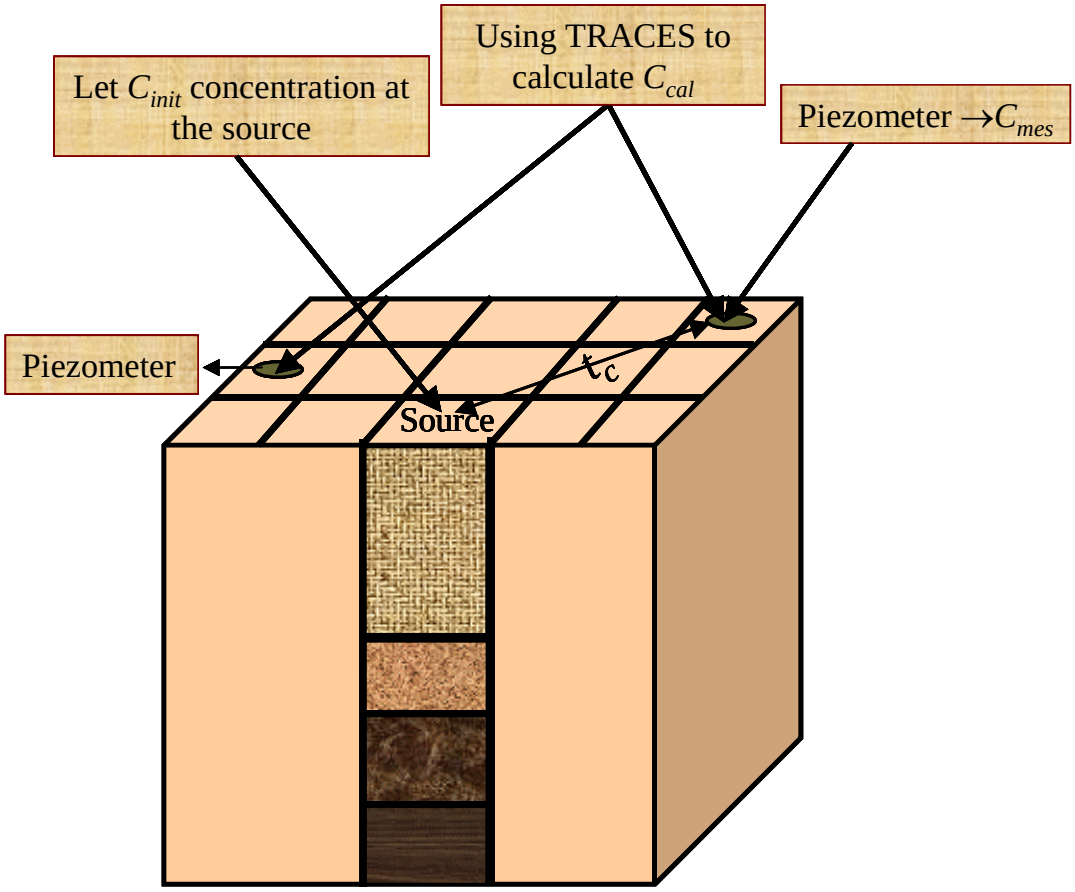

Figure 4.2 Sketch of the 3D domain with the source and the piezometers.

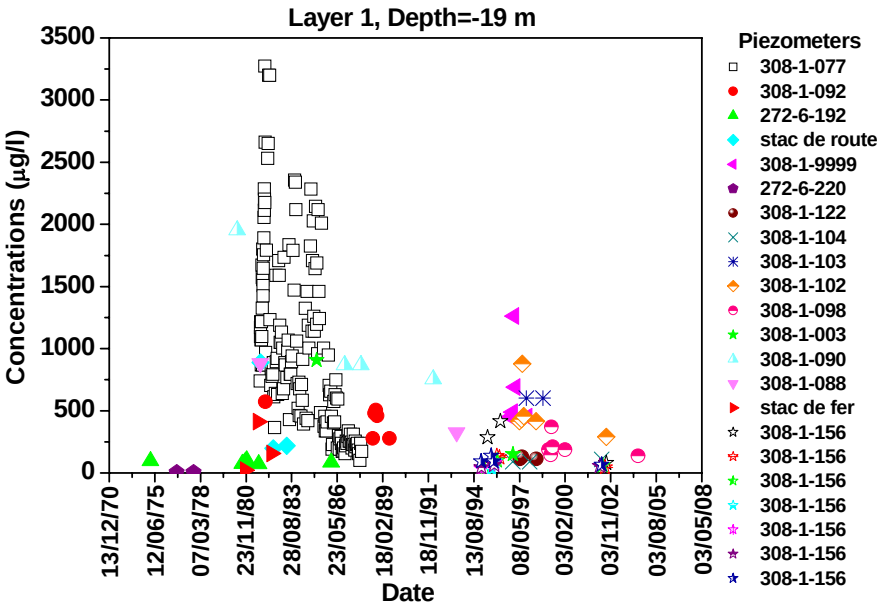

Figure 4.3 Computed concentrations at the first layer of the source.

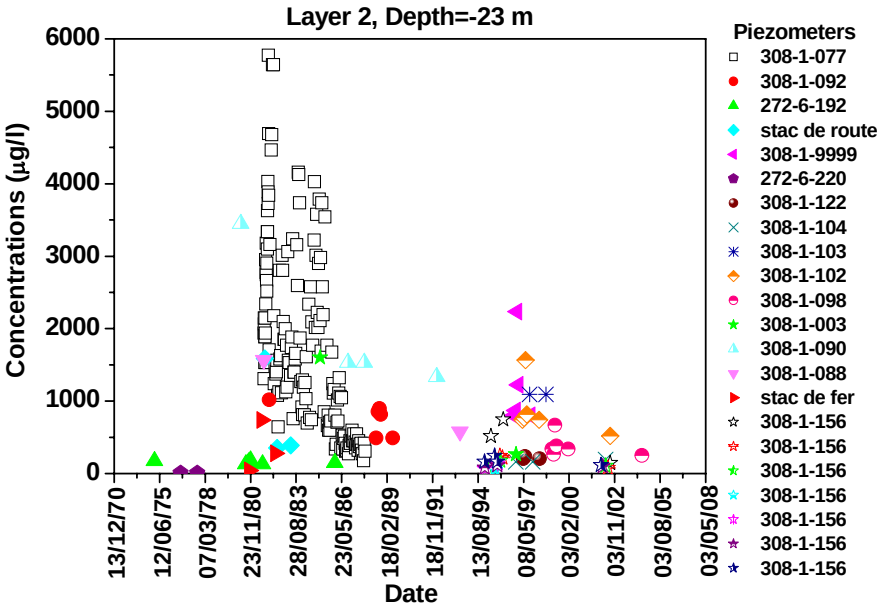

Figure 4.4 Computed concentrations at the second layer of the source.

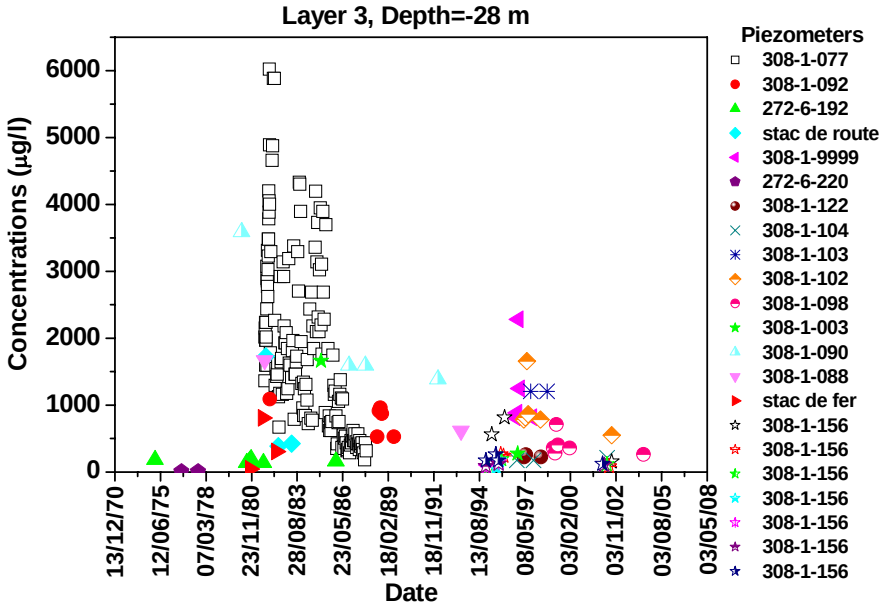

Figure 4.5 Computed concentrations at the third layer of the source.

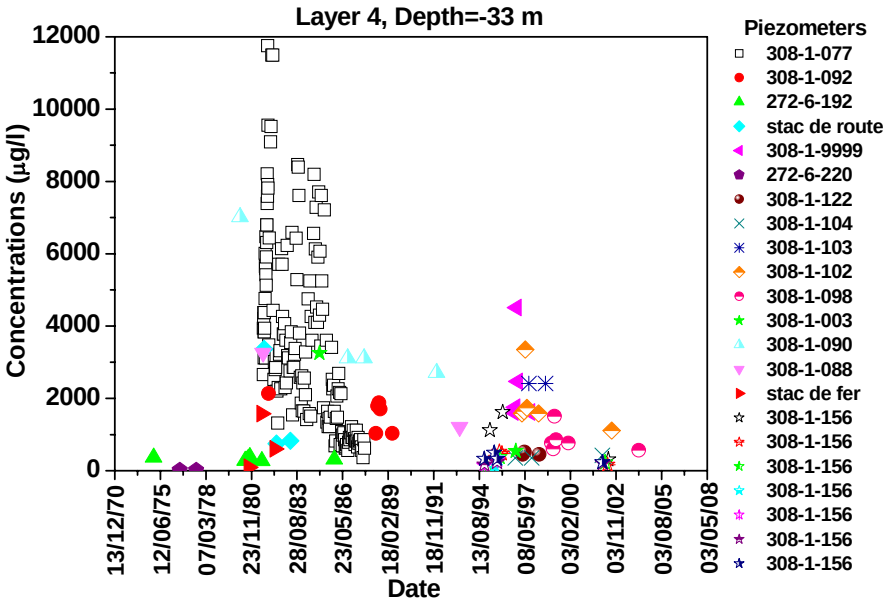

Figure 4.6 Computed concentrations at the fourth layer of the source.

4.1.4. Smoothing and interpolation of the source function

As appears in Figures 4.3-4.6, the approximated concentrations at the source term are very oscillatory due to small scale space and time which are not taken into account. Two main steps are followed to smoothen the source function in each layer. Initially we used a simple linear mean value interpolation for the source functions. Then, we used an exponential-fit interpolation, which seems to provide more reasonable results, as discussed below.

4.1.4.1. Mean value interpolation

In the first step, the computed concentrations at the source are smoothed by using a mean value interpolation. The total time interval is subdivided into a number of subintervals of uniform length (six months). In each subinterval, we replaced all given concentrations within this interval by their average value which is located at the center of the subinterval (see green curve of Figure 4.7 to Figure 4.10). If no concentrations are located within an interval, the previous concentration is considered.

Before 1992, no measurements at the contaminated zone had been carried out. Therefore, we assumed that a constant concentration at the beginning of the accident. The value of this concentration is taken from the highest concentration mean value at the early time. We found that the mean value approach did not improve the behavior of the source term at the accident location. As depicted in Figures 4.7-4.10, the obtained source term is non-monotonic and oscillatory. This approach did not provide a good approximation of the observed data and therefore it was discarded.

4.1.4.2. Exponential interpolation

In this approach the scattered data are fitted to the following exponential function:

$$C(t)=C_0\, e^{-At}$$

where $C(t)$ is a continuous concentration function describing the transient source, t is the time variable in days, and C_0 represents the initial concentration of the source at time zero and the constant A represents the rate of degradation of concentration at the source.

At first, we used the exponential fitting of the scattered concentrations plotted in Figures 4.3-4.6. The results were not as desired because of sharp jumps in the concentrations. We then used the mean values of the concentrations obtained from the previous step (Paragraph 4.1.4.1) to fit the exponential functions. The mean value interpolation is, therefore, used as a pre-smoothing step.

The obtained exponential curves with the feed data, which are the mean values, are plotted in Figures 4.7-4.10. The exponential model is used because it fit best when the spatial autocorrelation decreases exponentially with increasing distance (time), see Cressie, 1993. Figure 4.11 shows the estimated source functions in the four layers.

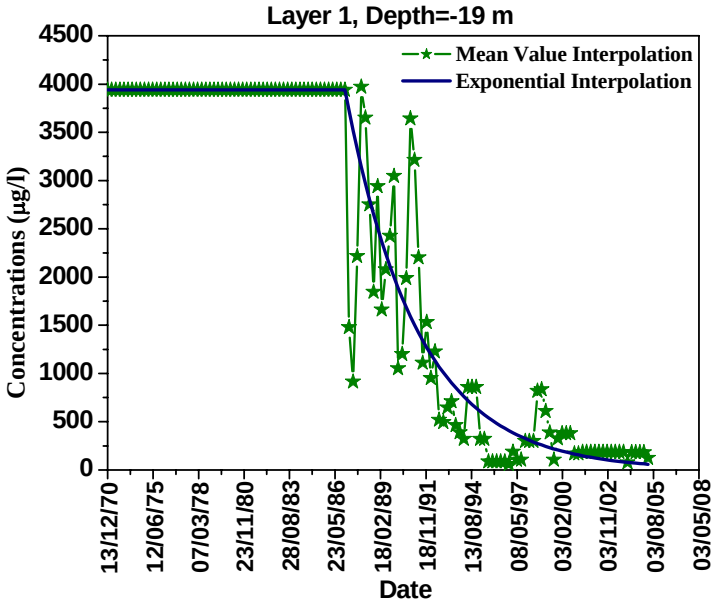

Figure 4.7 Interpolation of the concentration behavior at the source, first layer.

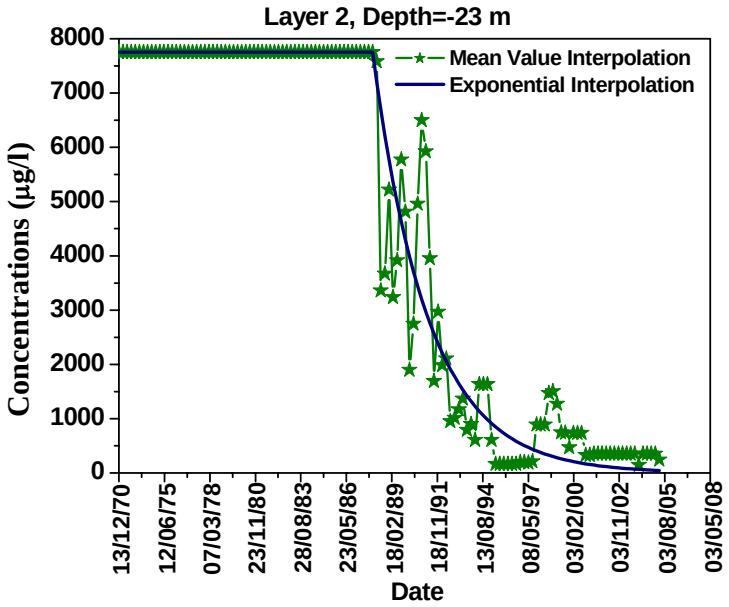

Figure 4.8 Interpolation of the concentration behavior at the source, second layer.

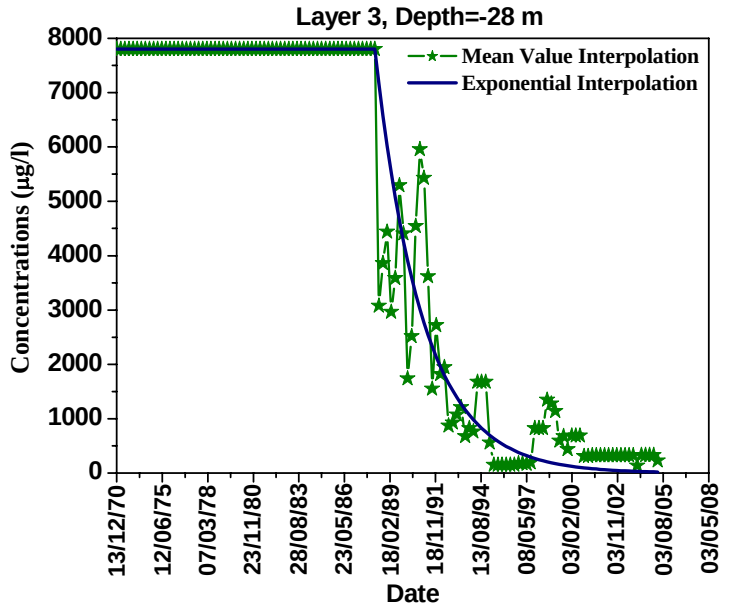

Figure 4.9 Interpolation of the concentration behavior at the source, third layer.

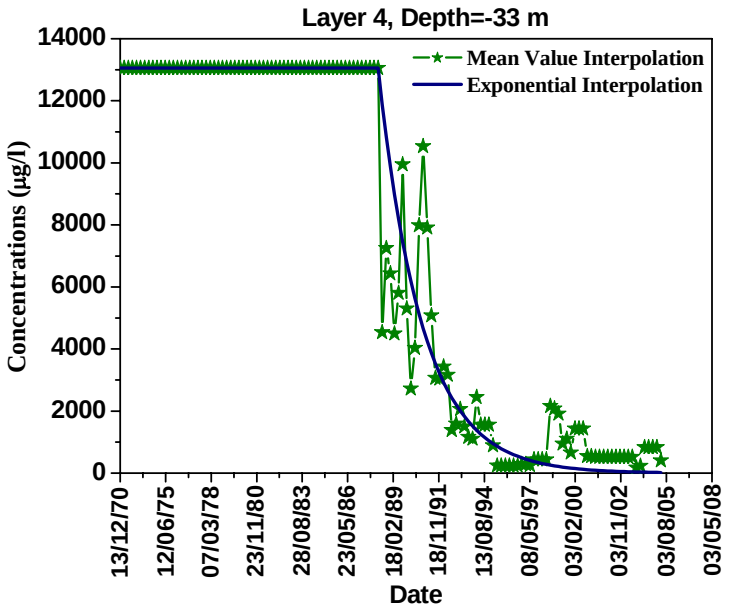

Figure 4.10 Interpolation of the concentration behavior at the source, fourth layer.

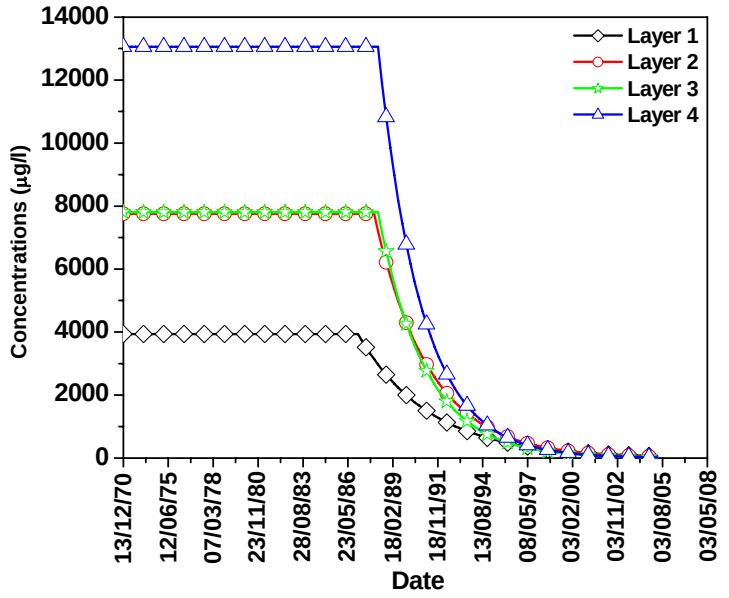

Figure 4.11 The source functions in the four layers.

4.2. Source behavior uncertainty

4.2.1. Statistical analysis

The uncertainty on the source estimation can be evaluated by analyzing mathematically or graphically the difference between observed and predicted concentrations. A scatter plot of measured against simulated concentrations was used to evaluate the effectiveness of the simulation. However, it is difficult to make a visual comparison between graphs by only visual check. The geophysical parameters, permeability, porosity, and longitudinal and transversal dispersivities, were examined in terms of mean and standard deviations.
Two different expressions of the average difference between simulated and measured CCl_4 concentrations were used:

1. The mean error (*ME*), which is the mean difference between the measured concentrations and the simulated concentrations. The mean error is defined by

$$ME = \frac{1}{n}\sum_{i=1}^{n}\left(C_{pre} - C_{obs}\right)$$

where n is the number of points, C_{pre} and C_{obs} are the simulated and measured CCl_4 concentration, respectively. Non-zero mean error indicates that the simulated values are either underestimating or overestimating the measured values. The perfect case is when the mean difference is zero.

2. The standard deviation (SD), which is the average of the square root of the variance of the difference between simulated and measured concentrations.

The standard deviation (*SD*) was calculated by:

$$SD = \sqrt{\frac{1}{n}\sum\left(D - ME\right)^2}$$

where *D* is the difference between measured and simulated CCl_4 concentrations. The standard deviation is a measure of how widely the values are dispersed from the average value.

4.2.2. Data uncertainty

The ranges of the parameter values varied in the uncertainty analysis are detailed in this section. In numerical modeling, detailed aspects of the physical system are generally unknown. An example of this is the permeability of the aquifer formation. While it is possible to determine experimentally the permeability of a soil type from a sample, it is impractical to perform this experiment in a regional scale. Parameter uncertainty is related to the fact that aquifers are heterogeneous. Yet we are only able to measure the parameters at a few points in the domain of the model. In addition, parameter measurements are imperfect, incorporating errors and the measurements themselves are dependent on the volume of the aquifer involved in the measurement, i.e. analysis of a slug test at a well will likely indicate a different hydraulic conductivity than that of three months pumping test.

In this work, each parameter has a certain range of variation, as exact value is in most cases not known or is not determined on the field. The ranges of variation of each of the parameters in this study were based on the hydrogeological investigation of the aquifer, pumping test, pervious studies, and geologic mapping.

The structure of the Alsatian aquifer can be described by seven lithological classes depending on the percentage of sand, the ratio of the shingles and gravels or their argillaceous character. Various hydrogeological studies, which were carried out for the Alsatian aquifer, showed that the hydraulic conductivity of the alluvial vary between 1 to 1000 m/day, (Hamond, 1995; Beyou, 1999). Zonation is carried out for the hydraulic conductivity. The model area is divided into eight zones based on areas of similar geology and hydrogeology. Each of these zones is characterized by minimum and maximum values of hydraulic conductivities based on geological information of the aquifer (see section 3.9.2 in Chapter 3). The ranges of values of the hydraulic conductivity used in the uncertainty analysis are given in Table 4.1.

Table 4.1. Range of hydraulic conductivity considered in the model.

Zone Number	Minimum (K_{min}) m/s	Maximum (K_{max}) m/s
1	$1.15x10^{-8}$	$1.15x10^{-7}$
2	$1.15x10^{-7}$	$1.15x10^{-6}$
3	$2.31x10^{-6}$	$2.31x10^{-5}$
4	$1.15x10^{-6}$	$1.15x10^{-}$
5	$1.15x10^{-5}$	$5.8x10^{-4}$
6	$1.15x10^{-4}$	$1.73x10^{-3}$
7	$5.8x10^{-4}$	$3.47x10^{-3}$
8	$1.15x10^{-3}$	$5.8x10^{-3}$

The porosity of sand typically range from 0.25-0.4 and for sand and gravel mixes range from 0.1-0.35 (Driscoll, 1986). The Rhine aquifer consists essentially of sands and gravels. Various hydrogeological studies, which were carried out for the Alsatian aquifer, showed that the porosity varies slightly between 10% and 20 %, (Hamond, 1995; Beyou, 1999). The porosity estimated through the uncertainty analysis ranged from 10% and 20%.

No measurements of longitudinal and transversal dispersivities are available. The longitudinal dispersivity was estimated from the scale length of the transport phenomenon. Its scale dependence has been observed for field-scale physical transport processes in many tracer experiments (Gelhar et al., 1992). The estimated longitudinal dispersivity measurements range from 10 to 20m. Transverse dispersivity is taken to be about 1/10 of the longitudinal value. The ranges of transverse dispersivity values varied between 0.5 to 3 m. See Table 4.2.

Other parameters like diffusion coefficients are not adjusted during the uncertainty analysis because their values are considered constant, or their variation is very small compared to the primary uncertain parameters.

4.2.3. Parameter uncertainty analysis

The uncertainty on the source behavior was performed by adjusting the parameters that may have influence on the source behavior. Three uncertain parameters are

estimated and used to address the effects of uncertainties associated with the source estimation. These include porosity, dispersivity, and hydraulic conductivity. No measured data of these parameters are available in the aquifer so we relied on pervious studies at Alsatian aquifer to chose the range values of these parameters. These include porosity, dispersivity, and hydraulic conductivity.

4.2.3.1. Porosity

Porosity is estimated through the trail and error technique by TRACES. The values of the porosity are manually adjusted within the range 10% to 20%. The longitudinal and transversal dispersivities coefficients are 20 m and 2 m, respectively.

4.2.3.2. Longitudinal and transversal dispersivity coefficients

The longitudinal and transversal dispersivity are estimated by trial and error technique by TRACES. Different values of the longitudinal and transversal dispersivities are used. The longitudinal dispersivity is between 10 and 20m and the transverse dispersivity is between 0.5 and 3 m.

4.2.3.3. Hydraulic conductivity

Parameter uncertainty started with the elimination of the bias by adjusting the porosity and then the dispersivity coefficients while keeping a constant zonal permeability. The domain is highly heterogeneous as depicted by hydraulic conductivity values ranging from 1 m/day to 1000 m/day.

The hydraulic conductivity was estimated within:

i) Each zone in the domain: eight zones were considered in the different geological formations of the Alsatian aquifer. The uncertainty analysis adjusts the permeability for each of these zones by changing it randomly until a reasonable fit is obtained. The longitudinal and transversal dispersivity coefficients and the porosity used in the model come from the precedent estimation for these parameters.

ii) Each grid cell in the domain: since the domain is highly heterogeneous, the numerical model requires information about the permeability in each mesh cell in the domain. Because the true hydraulic conductivity field is unknown except for local measurements, the hydraulic conductivity distribution was directly incorporated into the TRACES model by assigning a different hydraulic conductivity to each mesh cell using the Monte-Carlo method.

We use Monte Carlo method in order to generate several source scenarios. At each Monte Carlo simulation, the conductivity of each mesh is calculated by using this formula:

$$K_{i,j} = K_{min,j} + \left(K_{max,j} - K_{min,j} \right) \times z$$

where,

$K_{i,j}$: is the permeability for cell i in zone j.

$K_{min,j}$: is the minimum permeability for zone j.

$K_{max,j}$: is the maximum permeability for zone j.

z: is a random number between [0,1].

The minimum and maximum permeabilities in each zone are selected from previous studies of the aquifer geological formations, (Hamond, 1995; Beyou, 1999), see Table 4.1. Figure 4.12 shows a flowchart for generating several source scenarios by using Monte Carlo method.

The work flow is as following:

- We start with a random number z to determine the permeability of each cell by using K_{max} and K_{min} of the corresponding zone;
- The flow and transport problems are then simulated with the provided permeabilities.
- The chosen solution should give the minimum standard deviation.

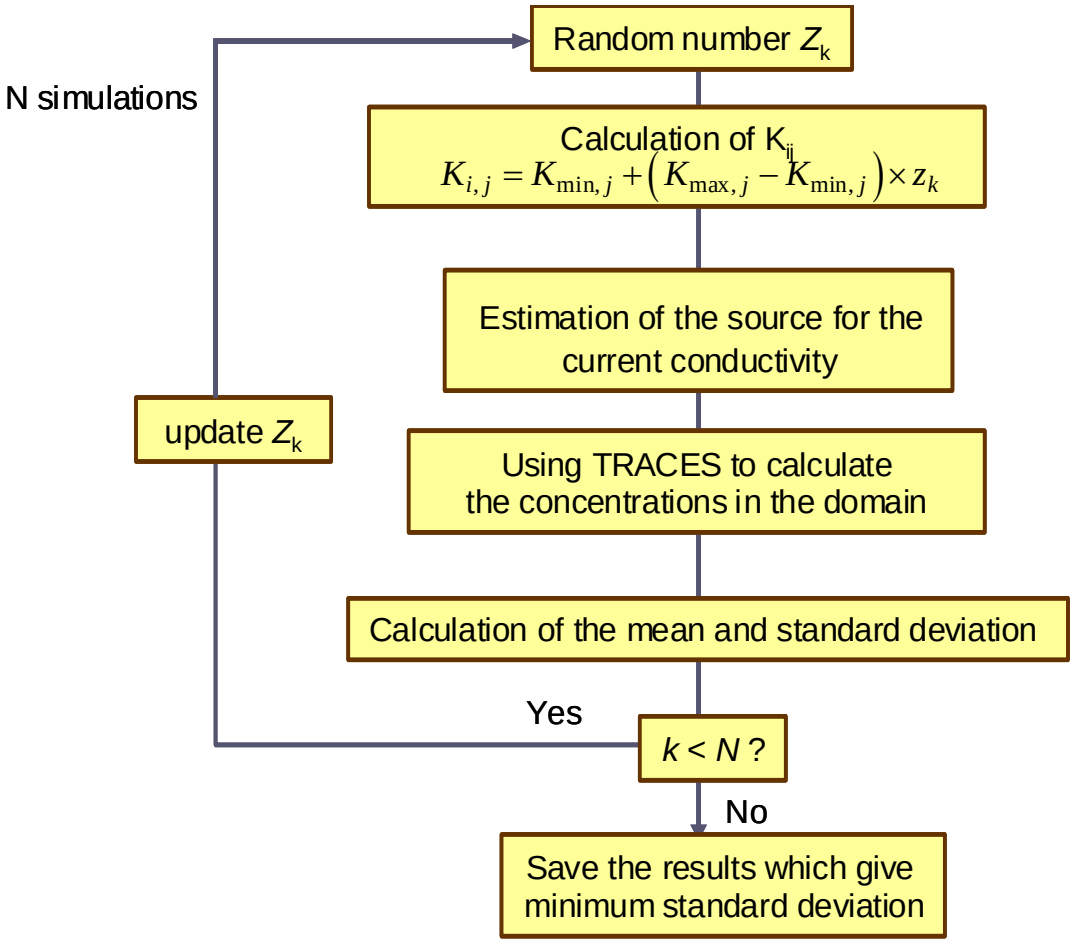

Figure 4.12 Flowchart showing the using of Monte Carlo method to generate several source scenarios

4.2.4. Procedure of estimation the Source uncertainty

The first part of this chapter focuses on the determination of the behavior of the source functions. While in this part, the uncertainty on the source term is performed by adjustment of the different parameter values. The process was performed by selecting one parameter. Then we varied the current parameter and fixed the two other parameters. For each value of the current parameter we associate a source scenario. Each source function is considered in the numerical simulator TRACES to predict the concentration in the domain. Then a comparison between calculated and observed concentration are done to select the best source scenario of the current parameter. The parameter value which obtained from the best source is considered

in the next iteration. The same procedure is repeated for the other parameters until a satisfactory match is obtained between observed and calculated concentrations. This procedure is illustrated in the Figure 4.13 which showing the flowchart of the process. The ranges of variation of each of the parameters carried out subjectively using expert knowledge. Therefore, different source scenarios were obtained by varying the parameter values (hydraulic conductivity, porosity, and longitudinal and transversal dispersivities.

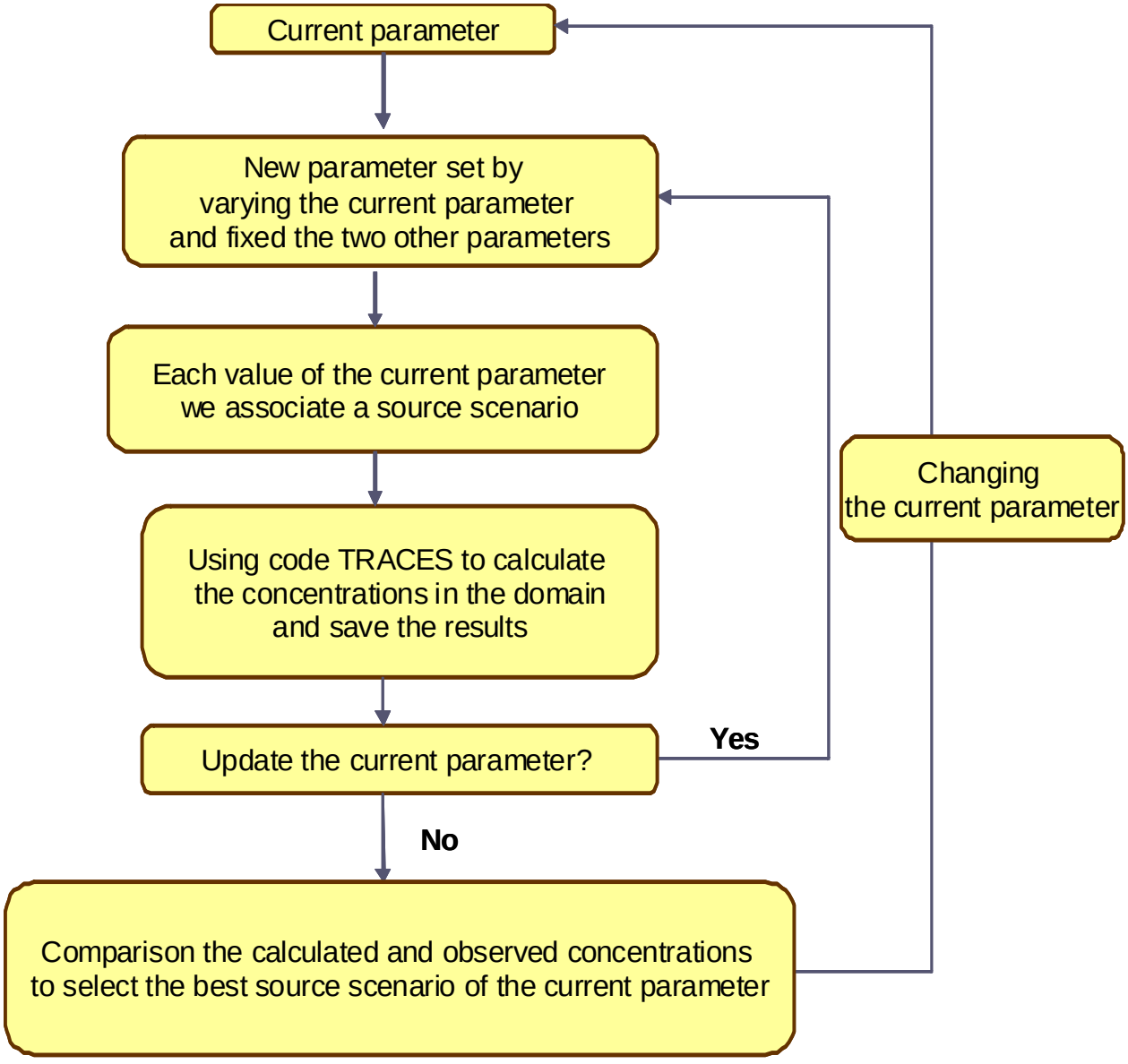

Figure 4.13 Flowchart showing the procedure of estimation the source uncertainty.

4.2.5. Source term estimation

Different source scenarios were found by varying different parameter values. In order to select the best source scenarios with an appropriate parameter values, each of the source functions are considered in the numerical simulator (TRACES) to predict the distribution of CCl_4 concentrations in the Alsatian aquifer. The degree of correspondence between model output and measured data can be analyzed graphically in scatter plots. This involves plotting observed CCl_4 concentrations versus calculated concentrations at each sampling point. The mean and standard deviation are the two performance measures used to assess model predications relative to measured data. In the following sections, we tested each source scenario by varying different parameter values (porosity, longitudinal and transversal dispersivity, and hydraulic conductivity).

4.2.5.1. Porosity

The values of porosity are adjusted within the range from 10% to 20%. Therefore, two source scenarios are obtained which corresponded to the two porosity values. These sources are considered in TRACES to predict the distribution of CCl_4 concentrations. The calculated CCl_4 concentrations are plotted versus the observed concentrations at each piezometer. Mean values and standard deviations are calculated. Mean values and standard deviations are, respectively, –15.40 μg/l and 48.40 μg/l with porosity 20% and –11.98 μg/l and 37.81 μg/l with porosity 10%. We found that the computed results are closer to the measured data with porosity 10% (see Figure 4.14 and Figure 4.15). The standard deviation is smaller with porosity 10%. The estimated source functions with porosity 10% is presented in Figure 4.16.

The plot of simulated versus observed CCl_4 concentrations for porosity 10% shows a non negligible scattering (SD=37.81 μg/l). The differences between observed and simulated concentration were used to update the simulations by changing the other parameters. The mean error is –15.40 μg/l and –11.98 μg/l for porosity 20% and 10% respectively, shows underestimation of the measured values.

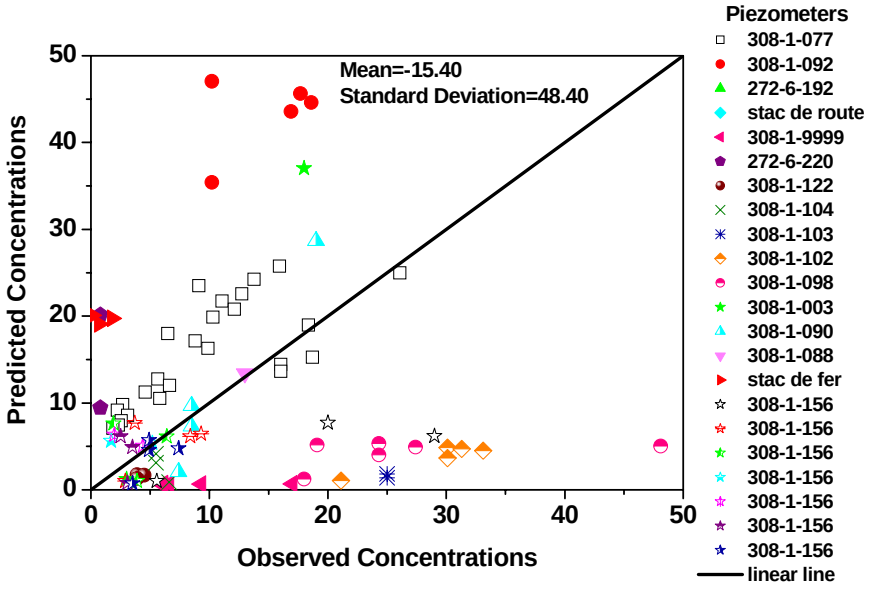

Figure 4.14 Scatter plot of predicted versus observed concentration for a porosity of 20%.

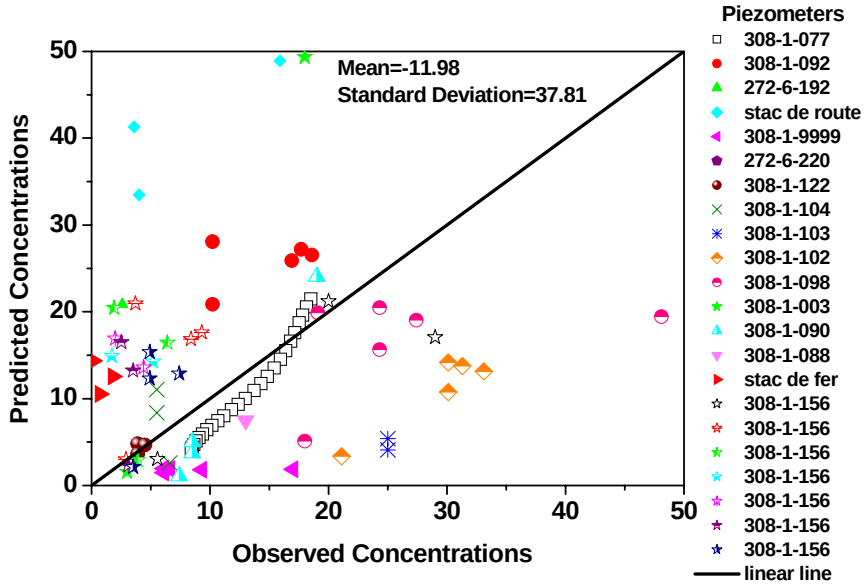

Figure 4.15 Scatter plot of predicted versus observed concentration for a porosity of 10%.

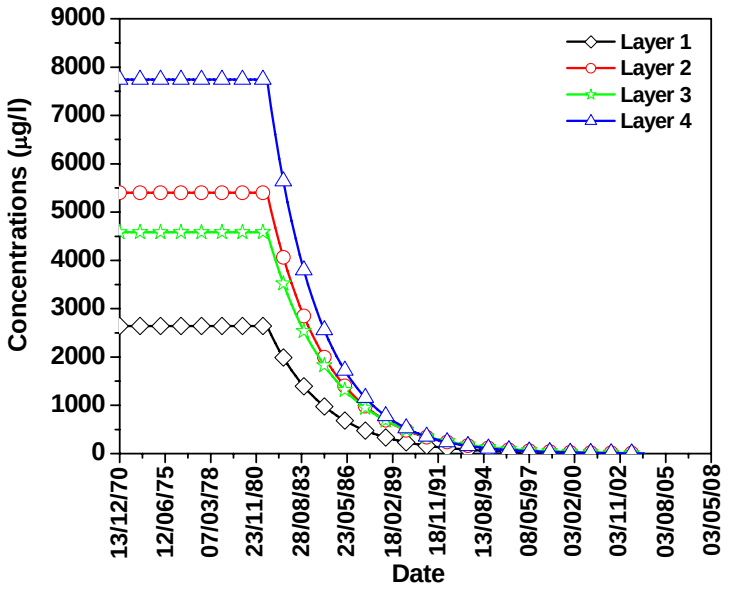

Figure 4.16 Source function in homogenous domain with: porosity=10%, longitudinal and transversal dispersivities 20 and 2 m, respectively.

4.2.5.2. Longitudinal and transversal dispersivity coefficients

The parameter uncertainty was achieved by varying longitudinal and transversal dispersivities within suggested ranges (see section 4.2.3.2) until an acceptable match between the computed and the measured concentrations was achieved. Five source scenarios are obtained which corresponded to the dispersivity values used. Each source scenario is considered in TRACES to predict the distribution of CCl_4 concentrations. The calculated CCl_4 concentrations are plotted versus the observed concentrations at each piezometer. The mean and standard deviation for different dispersivity coefficients are given in Table 4.2. In case 5 (Table 4.2), the longitudinal and transversal dispersivities coefficients are 3 m and 20 m, respectively. These values provided the best mean value and standard deviation for the present transport model, as shown in Figure 4.17. The obtained mean value and standard deviation are –7.96 µg/l and 24.53 µg/l, respectively, which indicates a reasonable matching between the computed and observed CCl_4 concentrations. The estimated source functions with longitudinal and transversal dispersivities coefficients are 3 m and 20 m, respectively is presented in Figure 4.18.

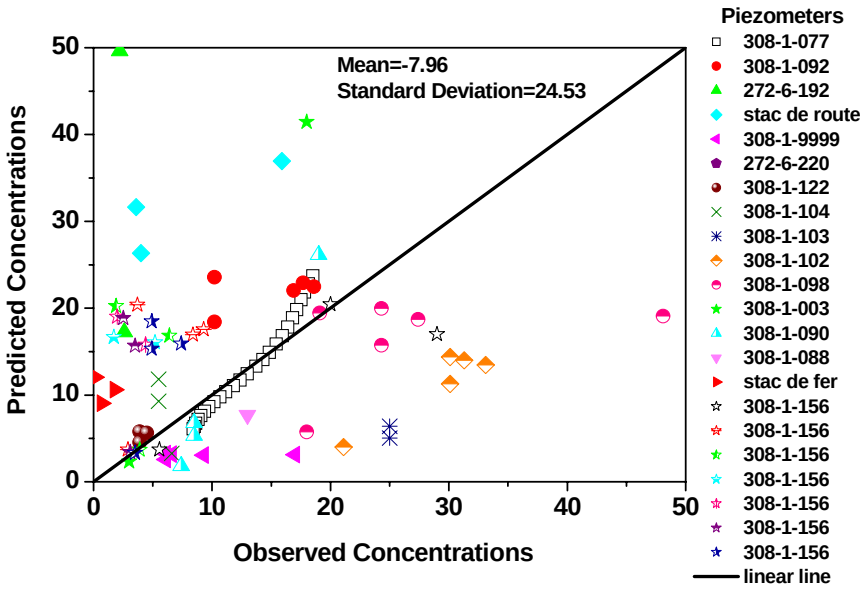

Figure 4.17 Scatter plot of predicted versus observed concentration for α_t=3 and α_l=20.

Table 4.2. Mean and standard deviation for different dispersivity coefficients

Case No.	Dispersivities Coefficients (m)	Mean (μg/l)	Standard Deviation (μg/l)
Case 1	α_t=0.5 α_l=10	-300.41	590.8
Case 2	α_t=1.0 α_l=20	-77.55	149.6
Case 3	α_t=2.0 α_l=10	-18.61	38.08
Case 4	α_t=2.0 α_l=20	-15.28	39.95
Case 5	α_t=3.0 α_l=20	-7.96	24.53

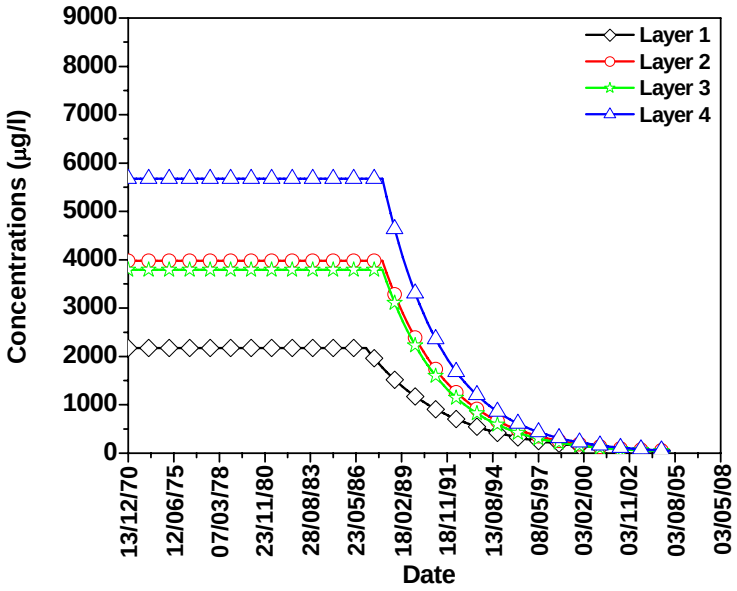

Figure 4.18 Source function in homogenous domain with: porosity=10%, longitudinal and transversal dispersivities 20 and 3 m, respectively.

4.2.5.3. Hydraulic conductivity

The hydraulic conductivity is estimated in two steps. In the first step, a constant hydraulic conductivity was assigned for different zones in the domain. Three iterations were conducted; two of them showed reasonable results. Therefore, two source scenarios are obtained which corresponded to the two iterations used. Each source scenario is considered in TRACES to predict the distribution of CCl_4 concentrations. The calculated CCl_4 concentrations are plotted versus the observed concentrations at each piezometer. The first iteration gave a mean error 1.78 µg/l and standard deviation 17.47 µg/l while with the second iteration the mean error and standard deviation are 1.50 µg/l and 19.74 µg/l, respectively. The scatter plots between observed and simulated values in Figure 4.19 show a good agreement between simulated and observed data. The estimated source functions with the second iteration is presented in Figure 4.20.

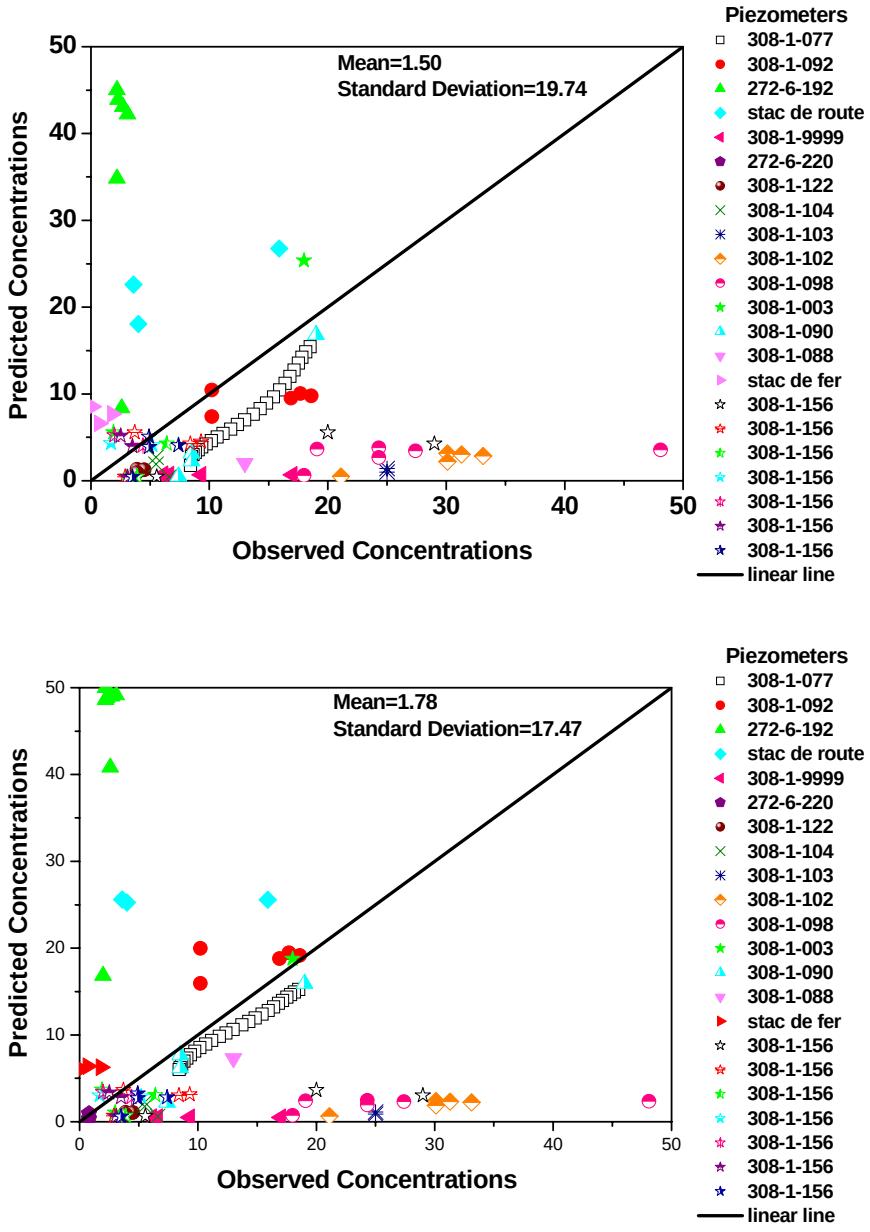

Figure 4.19 Scatter plots of predicted versus observed concentration for two iterations.

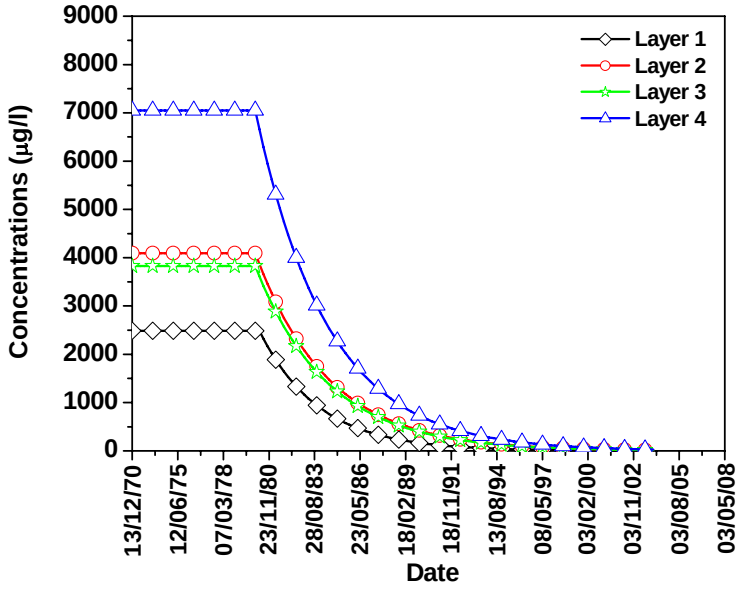

Figure 4.20 Source function with: porosity=10%, longitudinal and transversal dispersivities 20 and 3 m, respectively, and different permeabilities in each zone in the domain.

In the second step, the hydraulic conductivity is estimated by using Monte Carlo method by changing randomly the hydraulic conductivity for each grid cell within the different zones. Six iterations were performed (Table 4.3). Therefore, six source scenarios are obtained which corresponded to the six iterations used. Each source scenario is considered in TRACES to predict the distribution of CCl_4 concentrations. The calculated CCl_4 concentrations are plotted versus the observed concentrations at each piezometer. The scatter plot between observed and simulated values in Figure 4.21 shows an improvement in the simulated data when compared to the observed data (see previous results in Figure 4.14, Figure 4.15, Figure 4.17, and Figure 4.19). The scatter plot of simulated versus measured concentrations indicates that on average there is no bias in simulation results (Figure 4.21). However, the best fit was in iteration number 5. The mean error and the standard deviation were –0.41 µg/l and 15.27 µg/l, respectively. The estimated source functions, which correspond to iteration 5 is presented in Figure 22. This source is considered to predict CCl_4 concentration distribution.

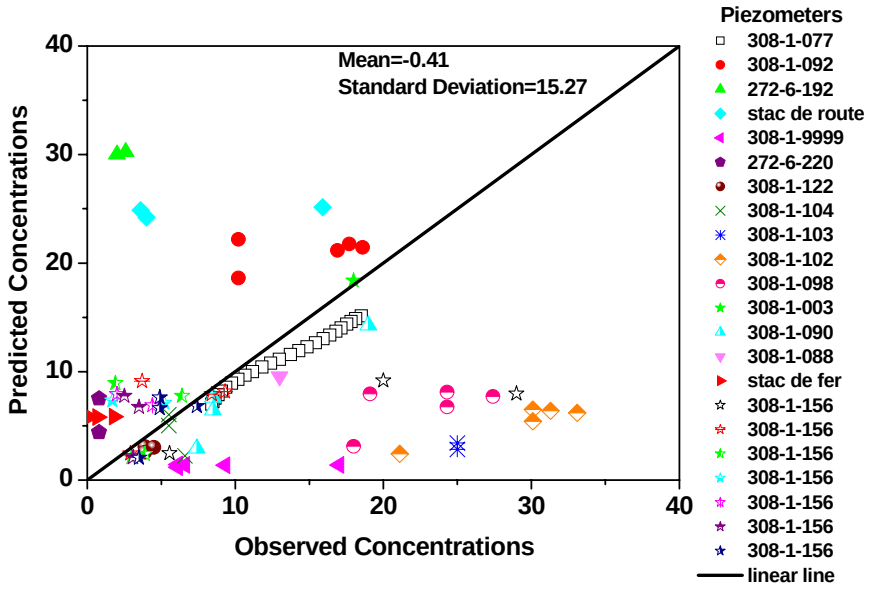

Figure 4.21 Scatter plot of predicted versus observed concentrations in iteration 5.

Table 4.3. The mean and standard deviation for six iterations.

Iteration Number	Mean (μg/l)	Standard Deviation (μg/l)
1	-1.07	17.18
2	-4.98	18.18
3	-3.64	18.80
4	-0.53	17.72
5	-0.41	15.27
6	-2.75	16.38

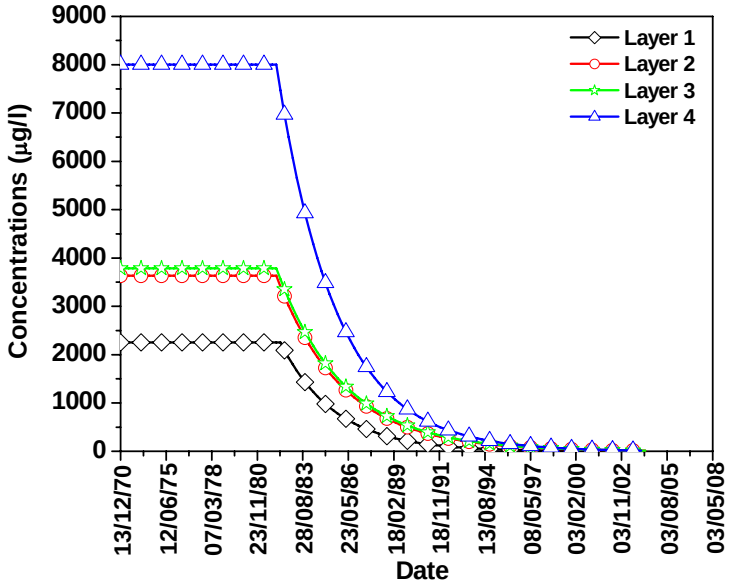

Figure 4.22 Source function in heterogeneous domain with: porosity=10%, longitudinal and transversal dispersivities 20 and 3 m, respectively.

4.2.6. Discussion

The deviations between the numerical model and the field observations can be due to conceptual errors, parameter values and their uncertainties, measuring errors of field data and errors in assumptions and approximations in the model. It is important to note that a model is only an approximation of reality and, after the parameter uncertainty analysis, its parameters may differ from the ones measured in the field or laboratory because the focus is usually on the outcome quality of the calculations rather than the accuracy of parameter.

Different source scenarios were tested by varying the parameters of the porosity, longitudinal and transversal dispersivities and permeability. The source scenario with heterogeneous assumption showed the minimum mean error and standard deviation, Figure 4.21. We reduce the standard deviation to 15.27 µg/l and the mean error to –0.41 µg/l. The various runs did not show further possibilities to reduce the error. While adjusting the permeability, the source position was displaced to allow the arrival travel time (t_c) to be shifted without changing the shape of the concentrations distributions (Figure 4.23).

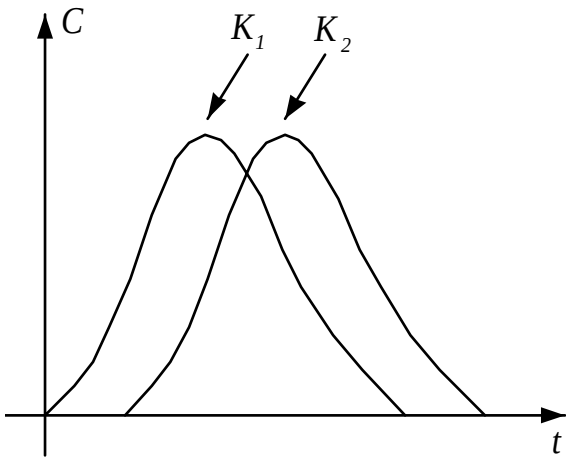

Figure 4.23 Concentration distribution of the source by varying the permeability.

4.2.7. Comparison with field data

After the adjustment of porosity, permeability, longitudinal and transversal dispersivities in the transport model, the considered source functions in the four layers, which are based on statistical results, are presented in Figure 4.22. Our predictions are conducted for a period of 20000 days, which correspond to the period between the accident time in 1970 and 2024.

Figure 4.24 to Figure 4.27 present comparisons between the numerical and experimental concentrations of CCl_4 at different locations from the source for the period between 1970 the time of accident and 2024. Overall, a good agreement between observed and simulated concentrations was achieved at different locations.

Also a comparison is done for 10 piezometers at the same date in December 1998 which show an acceptable agreement in many piezometers as see in Figure 4.28. But we can see there is high deviation in this piezometer which is far from the source location, piezometer 272-6-192 (see Figure 4.1). In addition, in these piezometers which are very close to the source location since the concentrations were considered at the source as mean concentration, while at the piezometer as local concentration. These piezometers are: 308-1-098, 308-1-102, and 308-1-103 (see Figure 4.1). Figure 4.29 shows another comparison for a multi-level piezometer 308-1-156 at the

same time (for 1997). The results show an acceptable agreement at all depths expect at the 3-8m depth, which shows high deviation. This could be because field measurement error.

Some piezometers show large deviations throughout all runs. This could be because of: groundwater samples were taken irregularly over the period from 1992 to 2004, lack of monitoring data during the period of simulation especially at early time, and limited amount of observation wells and sampling errors.

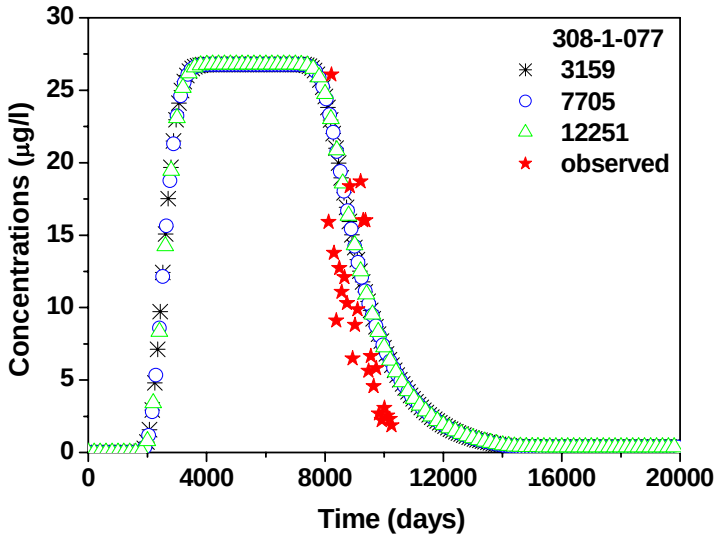

Figure 4.24 Comparison between measured and simulated concentrations at Negrodorf, 5515 m from the source.

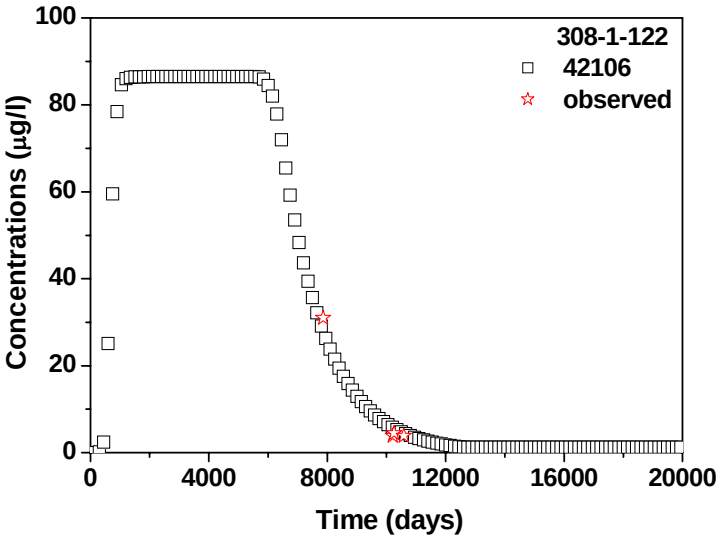

Figure 4.25 Comparison between measured and simulated concentrations at 308-1-122, 1472 m from the source.

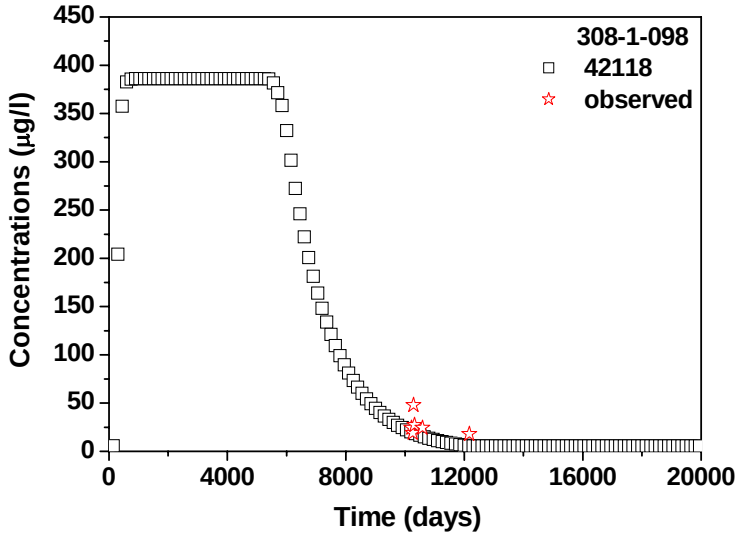

Figure 4.26 Comparison between measured and simulated concentrations at 308-1-098, 723 m from the source.

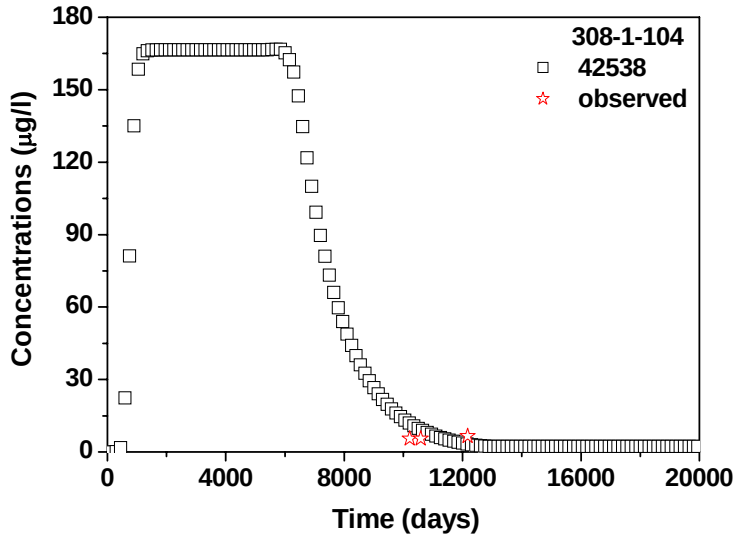

Figure 4.27 Comparison between measured and simulated concentrations at 308-1-104, 1572 m from the source.

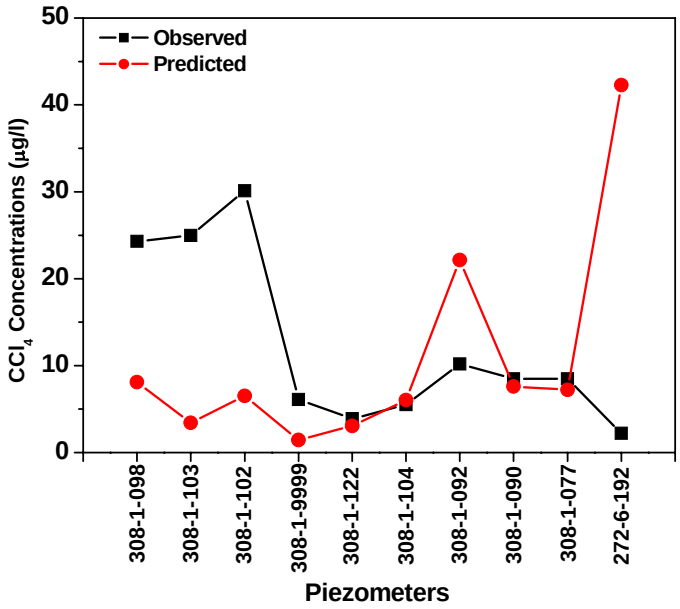

Figure 4.28 Comparison of the simulated and observed CCl_4 concentrations in 1998.

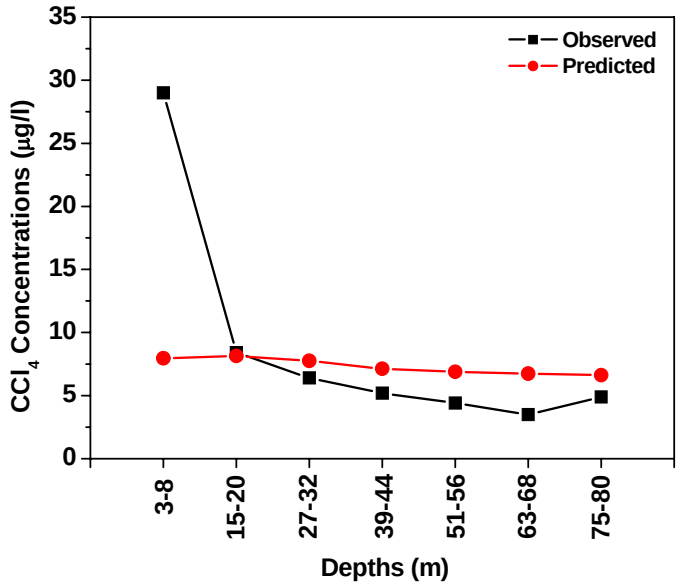

Figure 4.29 Comparison of the simulated and observed CCl_4 concentrations for multi-depth piezometer 308-1-156 in 1997.

4.2.8. Distribution of the concentration in the domain

As previously discussed, simulations were performed for the period from 1970 to 2024. Different times were set in order to monitor the change in CCl_4 concentration distribution with time. Figure 4.30 to Figure 4.34 show the simulated CCl_4 plume at 1825, 3650, 8010, 10200, and 20000 days after the accident in 1970. After 22 years (Figure 4.32), the contaminated groundwater has reach all piezometers. From these figures, one notices a wider distribution of the contaminant with time.

Figures 4.32-4.36, show distributions of CCl_4 concentrations in the aquifer after 5, 15, 22, 28, and 54 years (i.e. 1975, 1985, 1992, 1998, and 2024) with peak concentrations equal to 55, 55, 45, 35, and 25 μg/l, respectively. The peak concentrations do not decrease significantly during the early period between 1975 and 1985 because the chlorinated solvents exist in the unsaturated and saturated zone and would thus continuously feed into the groundwater. The plume initially is initially transported through a narrow zone and later appears to be more diffusive. This behavior is a result of convection and diffusion/dispersion forces. Figure 4.35 shows the hydraulic head and the streamlines in the top layer of the 3D domain. The pollutant transport is initially dominated by convection along the streamlines. Diffusion/dispersion mechanisms become predominate at later time towards the north-east boundary of the domain.

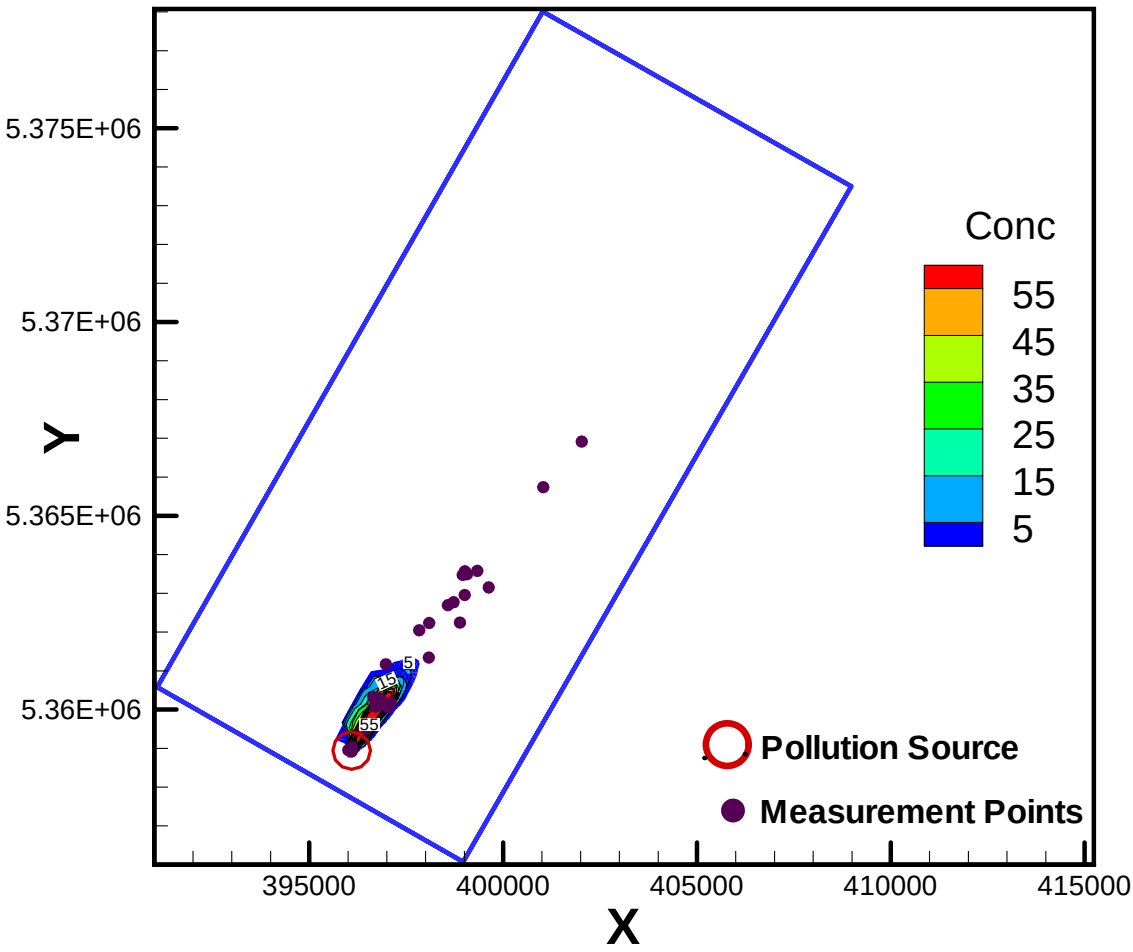

Figure 4.30 Distribution of CCl_4 concentration after 1825 days of the accident.

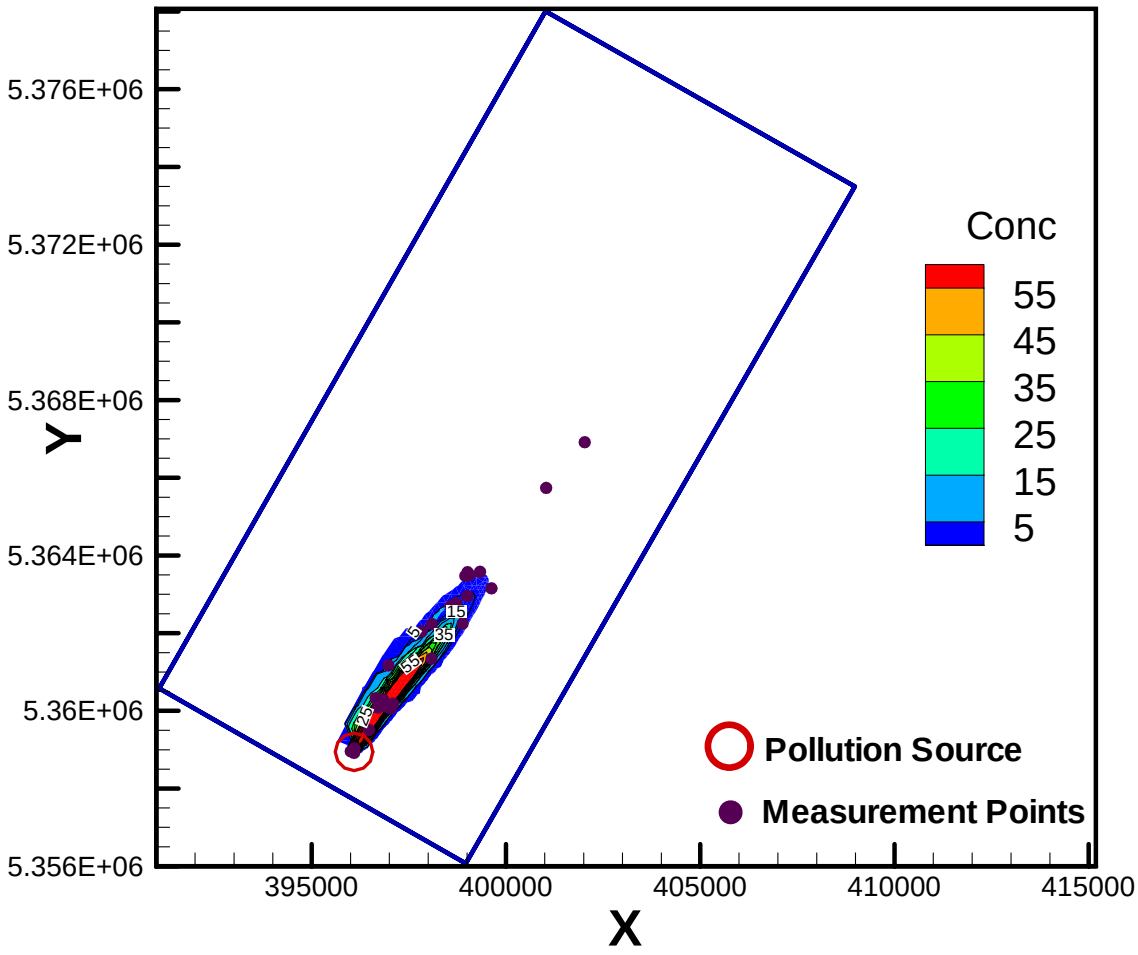

Figure 4.31 Distribution of CCl_4 concentration after 3650 days of the accident.

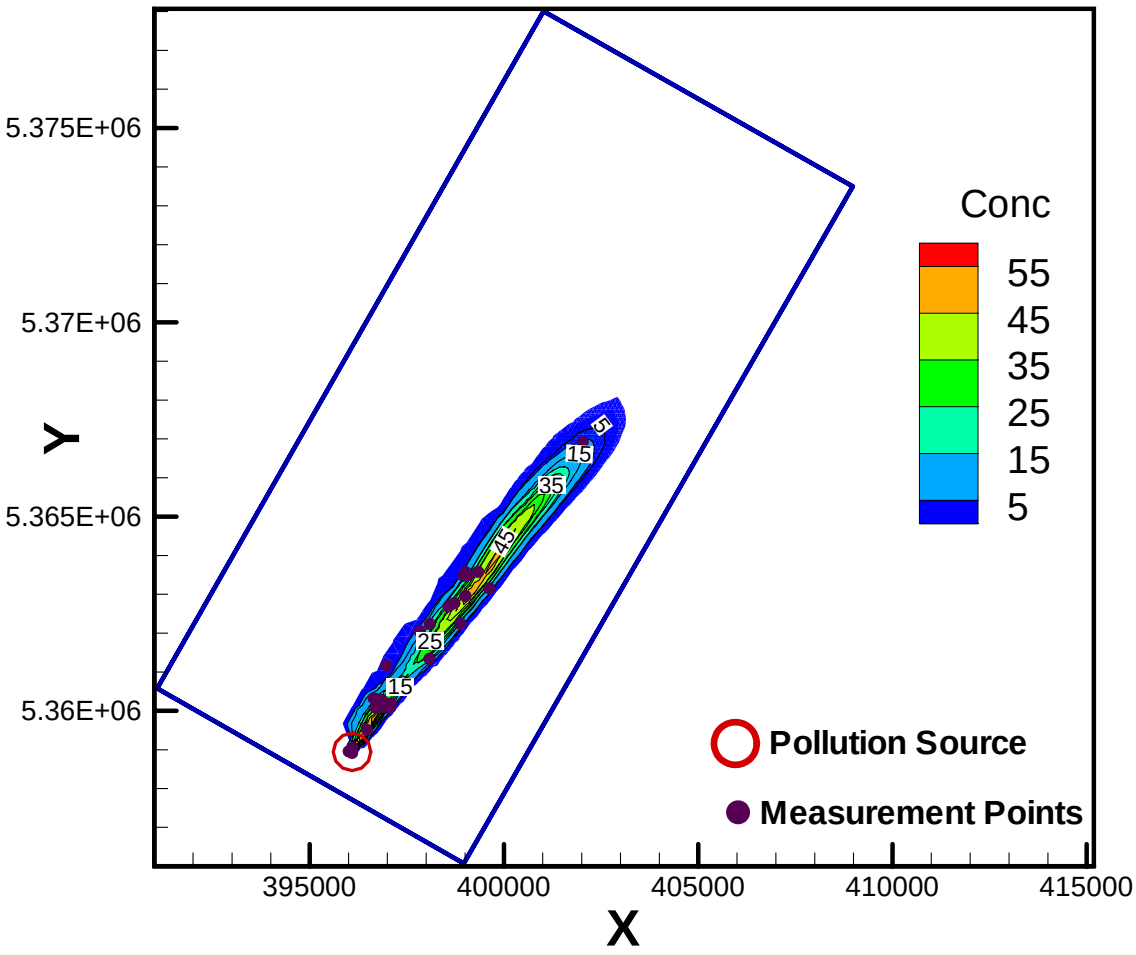

Figure 4.32 Distribution of CCl_4 concentration after 8010 days of the accident.

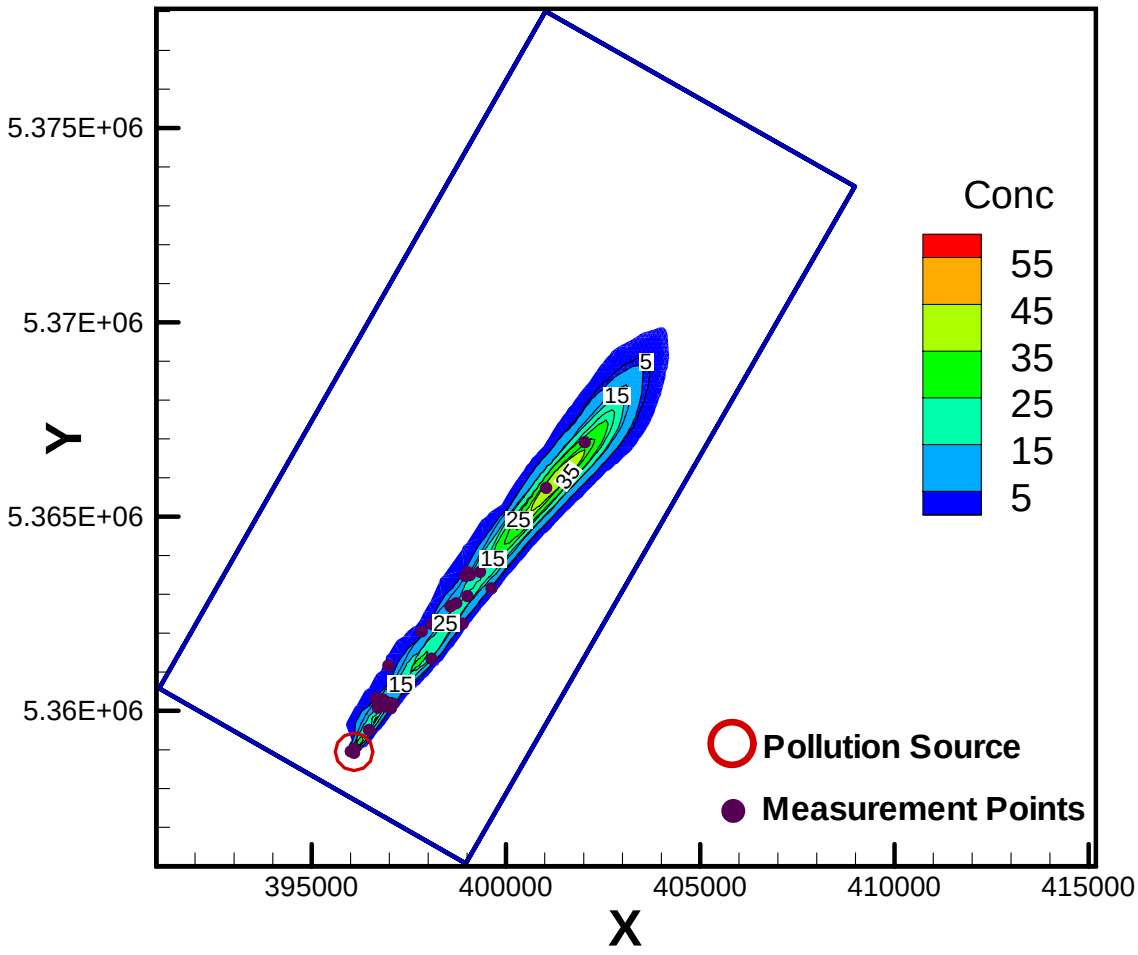

Figure 4.33 Distribution of CCl_4 concentration after 10200 days of the accident.

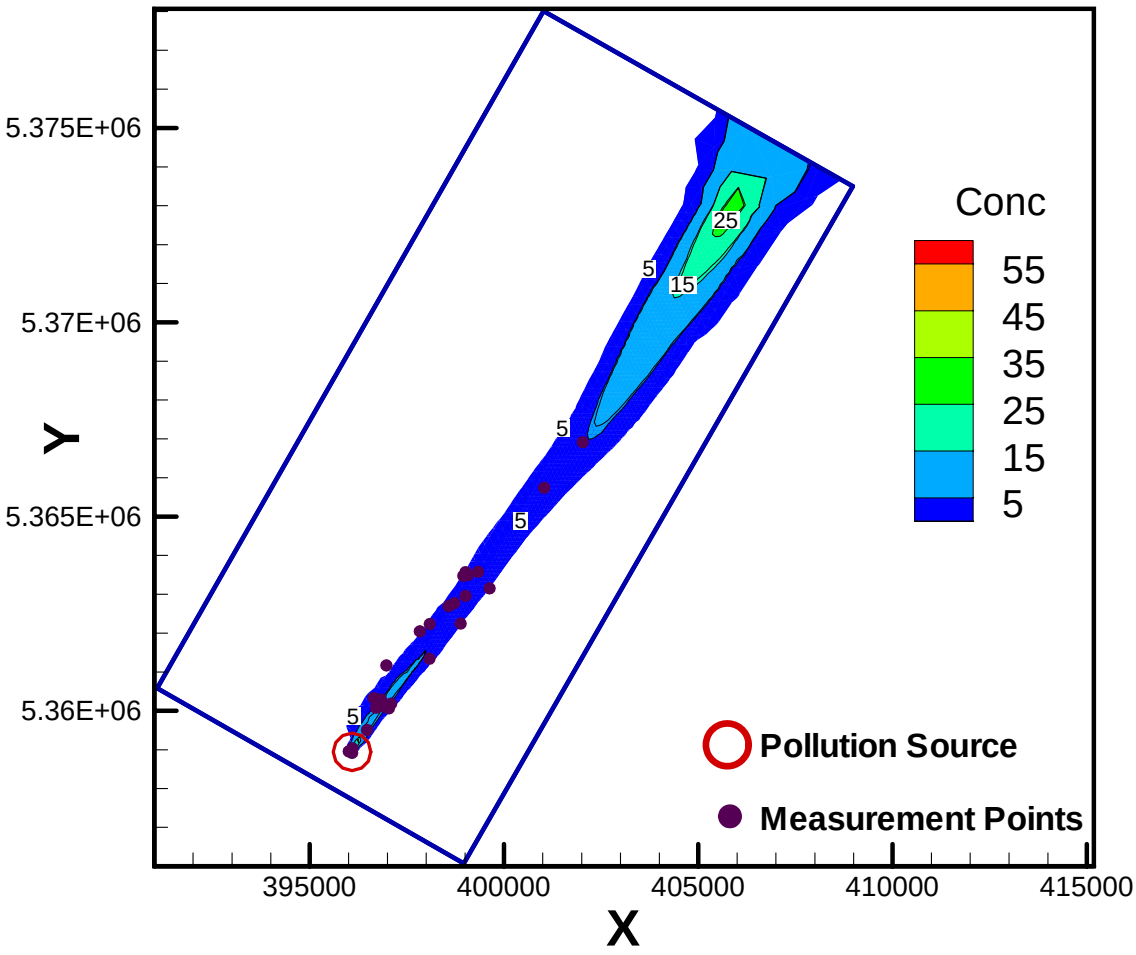

Figure 4.34 Distribution of CCl_4 concentration after 20000 days of the accident.

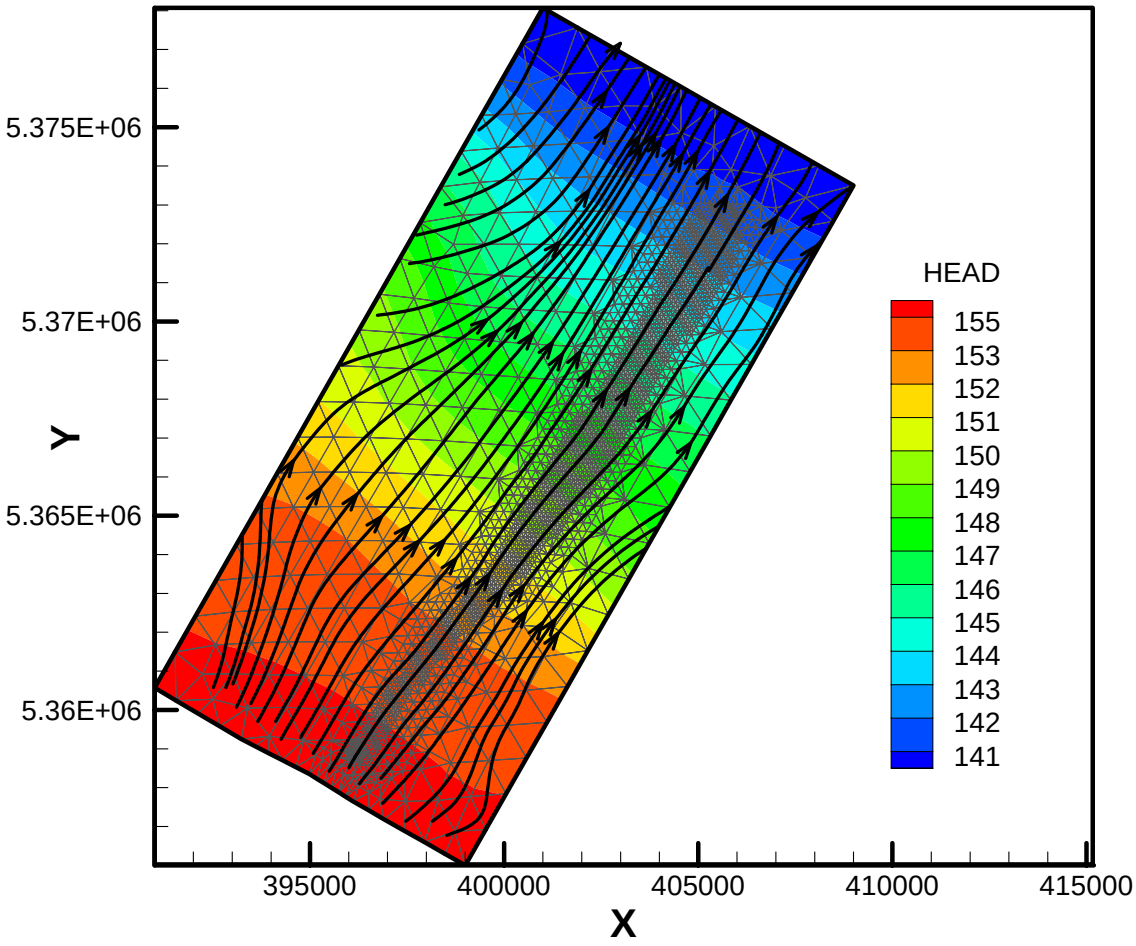

Figure 4.35 Hydraulic head and streamline profile in the top layer of the domain.

4.3. Summary

This chapter showed the detailed estimation of the source behavior and its uncertainty. The main results are summarized as follows.

- A simplified inverse method is used to estimate the source behavior at the accident location that corresponds to four layers.
- The source functions at the four layers are smoothened by using mean and exponential fitting.

- The main uncertain parameters are the porosity, permeability, and dispersivity coefficients. Each parameter is estimated at a time in a sequentially iterative procedure.
- The porosity and dispersivity coefficients are estimated by using the trail and error technique.
- The hydraulic conductivity is estimated in two steps. In the first step, a constant hydraulic conductivity was assigned for different zones in the domain by using the trial and error method. In the second step, the Monte-Carlo method is used to estimate the hydraulic conductivity in each mesh cell within the different zones.
- The uncertainty on the source behavior is performed by assuming different parameter values.
- Various source scenarios were tested by varying different parameter values.
- The source scenario with heterogeneous assumption showed the best results. This source is considered to predict CCl_4 concentration distribution.
- A good agreement between the observed and computed concentration was achieved at the different piezometers.

CONCLUSIONS AND RECOMMENDATIONS

The work presented in this thesis focuses essentially on studying the migration of carbon tetrachloride in the Alsatian aquifer that was a result of a tanker accident in 1970.

Several works in the past attempted to numerically describe and predict the pollutant migration in the aquifer by tuning different parameters to history match the data. None of the previous studies reached satisfactory results. In this work, we retook the problem and adopted different techniques to estimate the behavior of contaminant source at different depths, and we also included in our model new valuable measured data that were not available for the previous investigations.

The main assumptions in our models are illustrated in the following points:

- Only the dissolved amount of CCl_4 is considered in the flow and transport models. The pollutant is, therefore, considered as a tracer in water. The immiscible amount of CCl_4 is expected to migrate much slower than water and, therefore, the immiscible amount that can also be trapped in the neighborhood of the accident spot is accounted for in the source function. In other word, the trapped CCl_4 is assumed to act as a continuous contamination source for the underground water.
- Since inefficient degradation of CCl_4 occurs in the aquifer which has aerobic conditions (Vannelli et al., 1990), degradation mechanism is neglected.
- The adsorption reaction is neglected due to the low K_d value for CCl_4 (about 0.11 L/Kg).
- In our case, the medium is saturated in water. Volatilization is ignored since volatilization is not expected to be important unlike in unsaturated zone.

A 3D convection-diffusion-dispersion model is used to approximate the flow and transport equation. This model is used to study the behavior of the contaminant source at different depths. A methodology is proposed for optimally identifying unknown source of groundwater pollution under a 3D convection-diffusion-dispersion model. The technique primarily assumes linear transport behavior between the source and the wells in the aquifer. A simplified inverse method is implemented to estimate the concentration at the source based on the measured concentrations of the aquifer at different locations and times. These concentrations are estimated by a preliminary calculation in order to determine the relationship between the source concentration and the concentration at the measurement points in the domain. The travel time of the contaminant between the source and the measurement-wells is estimated by temporal moments method. Using the above approach, each observed datum from the measurement wells feeds back a corresponding concentration at the source. The proposed technique provides the best possible match between the observed and estimated concentrations for a selected location and time. The obtained scattered concentrations at the source, that correspond to the measured data at different locations and times, are smoothened in each of the source layers. We used a hybrid linear mean value and exponential-fit interpolation to avoid unphysical fluctuations in the data.

In order to obtain a better match between the observed and estimated concentration, source behavior uncertainty are preformed by varying the following parameters: the hydraulic conductivity, longitudinal and transversal dispersivities, and porosity. The ranges of variation of each parameters carried out subjectively using expert knowledge. The process was performed by varying one parameter at a time and fixing the two other parameters. Estimation of the model parameters carried out by ‘trial and error’ technique and Monte-Carlo method.

The porosity values estimated through the trail and error technique. The values of the porosity are manually adjusted within the range from 10% to 20%. We find that the simulated results are comparable with the measured data with porosity 10% and are less satisfactory with porosity of 20%. The longitudinal and transversal dispersivities were also estimated by trial and error technique. In order to reduce errors, different values of the longitudinal and transversal dispersivities are used. The longitudinal

and transversal dispersivity coefficients were 3 m and 20 m, respectively. Since the domain is highly heterogeneous, the permeability is estimated by using the Monte-Carlo method by changing randomly the permeability for each grid block. In the heterogeneous cases, by changing the values of permeability of each zone and of each grid cells in the domain, we got a further improvement in the results compared with those obtained from that of porosity and dispersivities coefficients. For each value of the current parameter we associate a source scenario. Therefore, various source scenarios were tested by varying the uncertain parameters, (permeability, porosity, and longitudinal and transversal dispersivities). In order to test these scenarios, the source functions are considered in the numerical simulator (TRACES) to predict the distribution of concentrations of the pollutant in the domain. During the process, parameters are gradually changed until a minimum mean difference and standard deviation are obtained between the calculated and measured data.
The considered source functions in the four layers, which are based on statistical results, were used to evaluate plausible CCl_4 migration. This was performed by running TRACES.

Our predictions are conducted for a time period of 20000 days, which corresponds to the period between the accident time in 1970 and 2024. A good agreement between observed and simulated concentrations was achieved at different locations. In some dates, however, relatively higher errors were obtained that could be because of: groundwater samples were taken irregularly over the period from 1992 to 2004, lack of monitoring data during the period of simulation especially at early time, and limited amount of observation wells, and sampling errors.

Finally, I present some perspectives of this work:

- In this work, the location of the source is given by two mesh elements, so it is important to study the effect of the discretization on the estimation of the source by refining the mesh of the source.
- As we have seen, the concentrations at the source are assumed constant at the beginning of the accident. This could be unrealistic, so it must take into account the evaluation of the source behavior at this time.

- In this work, the CCl_4 is considered as a tracer and then a single phase flow model is used. While it is interesting to use multi phases flow to study the behavior of the contaminant.
- Finally, apply the technique we used to estimate the concentrations at the source for other aquifer in order to show the reliability of the method.

REFERENCES

Abdin, A., Kaluarachchi, J., Kemblowski, M. W. and Chang, C. M.: 1996, Stochastic analysis of multiphase flow in porous media: II. numerical simulations, Stochastic Hydrology and Hydraulics, 10 (3): 231-251.

Abbaspour, K. C., Schulin, R., Schläppi, E. and H. Flühler: 1996, A Bayesian approach for incorporating uncertainty and data worth in environmental projects. Environmental Modelling and Assessment. Vol. 1, no 3/4, pp. 151-158.

Alley, W. M.: 1993, Regional groundwater quality, Van Nostrand Reynhold, New York, 634 p.

Anderson, M. P. and Woessner, W. M: 1992, Applied Groundwater Modeling, p. 381, Academic, San Diego.

Aral, M. M. and Guan, J.: 1996, Genetic algorithms in search of groundwater pollution sources, in Advances in Groundwater Pollution Control and Remediation, NATO ASI Series 2 Environment, Vol. 9, 347–369, Kluwer Academic Publishers. The Netherlands.

ASTM: 1995, Emergency Standard Guide for Risk-Based Corrective Action Applied at Petroleum Release Sites: ASTM E-1739, Philadelphia, PA.

ATSDR, Agency for Toxic Substances and Disease Registry: 1995, “Center for Disease Control”. http://www.atsdr.cdc.gov/tfacts30.html.

Banton, O. et Bangoy, L.: 1997, Hydrogéologie, Multiscience environnementale des eaux souterraines, Presse de l'Université de Québec.

Bardossy, A., and Disse, M.: 1993, Fuzzy rule-based models for infiltration, Water Resources Research, 29 (2): 373-382.

Bardossy, A. and Duckstein, L.: 1995,. Fuzzy Rule-Based Modeling with Applications to Geophysical, Biological and Engineering Systems, CRC Press Inc., New York.

Bear, J.: 1972, Dynamics of Fluids in Porous Materials, American Elsevier, New-York, 764 p.

Bear, J.: 1979, Hydraulic of groundwater, Mc Grew-Hill Series in Water Resources and Environmental Engineering, New-York.

Bear, J.: 1988, Dynamics of Fluids in Porous Media. Dover, New York.

Bertrand, G., Elsass, Ph., Wirsing, G., and Luz, A.: 2006, Quaternary faulting in the Upper Rhine Graben revealed by high-resolution multi-channel reflection seismic C. R. Geoscience 338: 574–580

Beyou, L.: 1999**,** Modélisation de l'impact d'une pollution accidentelle de la nappe phréatique d'Alsace. Cas du déversement de CCl_4 à Benfeld, projet fin d'études pour un diplôme d'ingénieur à l'ENSAIS.

Blair, A. N., Ayyub, B. M. and Bender, W. J.: 2001, Fuzzy stochastic risk-based decision analysis with the mobile offshore base as a case study, Marine Structures, 14 (1): 69-88.

Bouwer, E. J. and McCarty, P. L.: 1983a, Transformations of 1- and 2-Carbon Halogenated Aliphatic Organic Compounds under Methanogenic Conditions, Applied Environmental Microbiology, 45(4): 1286-1294.

Bouwer, E. J. and McCarty, P. L.: 1983b, Transformations of Halogenated Organic Compounds under Denitrification Conditions, Applied Environmental Microbiology, 45(4): 1295-1299.

Bouwer, E. J.: 1994, Bioremediation of chlorinated solvents using alternate electron acceptors, In: Norris RD, Hinchee RE, Brown R, McCarty PL, Semprini L, Wilson DH, Kampbell M, Reinhard EG, Bouwer R, Borden C, Vogel TM, Thomas JM, Ward CH (eds) Handbook of bioremediation, Lewis Publishers, Boca Raton, pp 149–175.

Brezzi, F. and Fortin, M.: 1991, Mixed and Hybrid Finite Element Methods. Spinger, New York.

BRGM: 1992, Captages d'alimentation en eau potable d'Erstein, Recherche de l'origine et de l'extension d'une contamination par composes organohalogénés volatils, rapport n°35862.

BRGM: 1993, Etude de la pollution de la nappe phréatique par les composés organohalogénés volatils au droit et l'aval d'Erstein, rapport n°0142 ALS 4S 93.

Brooks, M. C., Annable, M. D., Rao, P. S. C., Hatfield, K., Jawitz, J. W., Wise, W. R., Wood, A. L. and Enfield C. G.: 2002, Controlled release, blind tests of DNAPL characterization using partitioning tracers, J. Contam. Hydrol, 59: 187–210.

BUA: 1990, [Tetrachloromethane, Report of the German Chemical Society Advisory Committee on Existing Chemicals of Environmental Relevance.] Stuttgart, S. Hirzel Wissenschaftliche Verlagsgesellschaft (BUA Report 45), (in German).

Chavent, G., Cockburn, B., Cohen, G. and Jaffré, J.: 1985, Une méthode d'élémnets finis pour la simulation dans un réservoir de déplacements bidimensionnel d'huile par de l'eau, rapport INRIA, No 353.

Chavent, G. and Jaffre, J.: 1986, Mathematical models and finite elements for reservoir simulation, North Holland Publishing Company, Amsterdam, 376p.

Chavent, G. and Roberts, J. E.: 1991, A unified physical presentation of mixed, mixed-hybrid finite elements and standard finite difference approximations for the determination of velocities in waterflow problems, *Advances in Water Resources,* 14, 329-348.

Chen, S. Q.: 2000, Comparing probabilistic and fuzzy set approaches for design in the presence of uncertainty, Ph.D. Dissertation, Virginia Polytechnic Institute and State University, Blacksburg, Virginia, U.S.A.

Chiou, C. T., Porter, P. E. and Schmedding, D. W.: 1983, Partition Equilibria of Nonionic Organic Compounds Between Soil Organic Matter and Water, Environmental Science and Technology, Vol.17, pp.227-231.

Christakos, G., Hristopulos, D. T. and Li, X. Y.: 1998, Multiphase flow in heterogeneous porous media from a stochastic differential geometry viewpoint, Water Resources Research, 34 (1): 93-102.

CIENPPA: 1984, La nappe phréatique de la plaine d'Alsace, plaquette d'information, 24p.

Cirpka, O. A. and Kitanidis, P.K.: 2000, Sensitivity of temporal moments calculated by the adjoint-state method, and joint inversing of head and tracer data*,* Advances in Water Resources, 24(1):89.103, 2000.

Clement, T. P., Gautam, T. R., Lee, K. K. and Truex, M. J.: 2004, Modeling coupled NAPL-dissolution and rate-limited sorption reactions in biologically active porous media, Bioremediation Journal 8, no. 1–2: 1–18.

Cobb, G. D. and Bouwer, E. J.: 1991, Effects of electron acceptors on halogenated organic compound biotransformations in a biofilm column, Environ., Sci. Technol, 25: 1068-1074.

Cochran, J. W., Yates, M. V. and Henson, J. M.: 1988, A modified fuge-and-trap gas chromatography method for analysis of volatile halocarbons in microbiological degradation studies, J. Microbiol Methods, 8: 347-354.

Connell, L. D.: 1995, An analysis of perturbation based methods for the treatment of parameter uncertainty in numerical groundwater models, Transport in Porous Media, 21 (3): 225-240.

Copty, N. K. and Findikakis, A. N.: 2000, Quantitative estimates of the uncertainty in the evaluation of ground water remediation schemes. Ground Water. Vol. 38, no. 1, pp. 29-37.

CPHF: 1998, Health risk assessment of carbon tetrachloride (CTC) in California drinking water, State of California Contract No. 84-84571 to the California public health foundation.

Dagan, G. and Nguyen, V.: 1989, A comparison of travel time and concentration approaches to modeling transport by groundwater. J. Contam. Hydrol. 4: 79-91.

Datta, B., Beegle, J. E., Kavvas, M. L. and Orlob, G. T.: 1989, Development of an Expert System Embedding Pattern Recognition Techniques For Pollution Source Identification, National Technical Information Service, Springfield, Virg., U.S.A.

Datta, B. and Chakrabarty, D.: 2003, Optimal identification of unknown pollution sources using linked optimization simulation methodology, Proc. of Symposium on Advances in Geotechnical Engg, (SAGE 2003), I.I.T. Kanpur India , 368-379.

Davis, T. J. and Keller, C. P.: 1997, Modeling uncertainty in natural resource analysis using fuzzy sets and Monte Carlo simulation: slope stability prediction, International Journal of Geographical Information Science, 11 (5): 409-434.

Davis, G. B., Trefry, M. G. and Patterson, B. M.: 2004, Petroleum and solvent Vapours: quantifying their behaviour, assessment and exposure, a report to the Western Australian Department of Environment, G.B., CSIRO Land and Water.

DDASS Bas-Rhin/ Service santé et environnement: 1992, Ville d'Erstein-Contamination des captages d'eau potable par du tétrachlorure de carbone et du trichloroethylene, rapport du conseil départemental d'hygiène, 8p. et annexes.

De Marsily, G.: 1981, Hydrologie Quantitative, Masson, Paris, 215 p.

Domenico, P. A. and Schwartz, F. W.: 1990, Physical and chemical hydrogeology, New York, John Wiley and Sons, p. 824.

Domenico, P.A. and Schwartz, F. W.: 1998, Physical and chemical hydrologeology. 2nd Edition, John Wiley & Sons, New York, N.Y. 528p.

Doong R. A., Wu, S. C. and Chen, T. F.: 1996, Effects of electron donor and microbiol concentration on the enhanced dechlorination of carbon tetrachloride by anaerobic consortia, Appl Microbiol Biotechnol 46: 183-186.

Driscoll, Fletcher G.: 1986, Groundwater and wells, St. Paul, Minnesota.

Durlofsky, L. J.: 1994, Accuracy of mixed and control volume finite element approximations to Darcy velocity and related quantities. Water Resources Research, 30, 965–73.

EAT : 1997, Etude de l'évolution de la pollution de la nappe d'Alsace par les organochlorés au droit et à l'aval de Benfeld : suivi de forage, Rapport no° 71-2-0400/3.

Egli, C., Scholtz, R., Cook, A. M. and Leisinger, T.: 1987, Anaerobic dechlorination of tetrachloromethane and 1,2-dichloroethane to degradable products by pure cultures of desulfobacterium sp. and methanobacterium sp. FEMS, Microbiol Lett., 43, 257-261.

Eikenberg, J., Tricca, A., Vezzu, G., Stille, P., Bajo, S. and Ruethi, M.: 2001, $^{228}Ra/^{226}Ra/^{224}Ra$ and $^{87}Sr/^{86}Sr$ isotope relationships for determining interactions between ground and river water in the upper Rhine valley, Journal of Environmental Radioactivity, 54, 133-163.

Feenstra, S., Cherry, J. A. and Parker, B. L.: 1996, Conceptual models for the behaviour or dense non-aqueous phase liquids (DNAPLs) in the subsurface, in Dense Chlorinated Solvents and other DNAPLs in Groundwater, eds J. F. Pankow and J. A. Cherry, Waterloo Press, Portland, OR, pp. 53-88.

Feenstra, S. and Guiguer, N.: 1996, Dissolution of dense non-aqueous phase liquids in the subsurface, in Dense Chlorinated Solvents and other DNAPLs in Groundwater, eds J. F. Pankow & J. A. Cherry, Waterloo Press, Portland, OR, pp. 203-229.

Ferrante, D.: 1996, Sorption processes, Groundwater Pollution Primer, CE 4594: Soil and Groundwater Pollution. Civil Engineering Dept, Virginia Tech.

Fetter, C. W.: 1993, Contaminant hydrogeology, Macmillan Publishing Company. New York.

Freeze, R. A. and Cherry, J. A.: 1979, Groundwater, Prentice Hall, Inc., Englewood Cliffs, New Jersey, 604 p.

Freeze, R. A., Massmann, J., Smith, L., Sperling, J. and James, B.: 1990, Hydrogeological decision analysis, 1, a framework, Ground Water, 28 (5): 738-766.

Gelhar, L. W., Welty, C. and Rehfeldt, K. R.: 1992, A critical review of data on field-scale dispersion in aquifers, Water Resources Research 28(7):1955-1974.

Gelhar, L. W.: 1993, Stochastic subsurface hydrology, Prentice Hall, Englewood Cliffs, NJ, U.S.A.

Gorelick, S. M., Evans, B. and Remson, I.: 1983, Identifying sources of groundwater pollution: An optimization approach, Water Resources Research, 19, 779–790.

Graham, W. D. and Mclaughlin, D. B.: 1991, A stochastic model of solute transport in groundwater: application to the Borden, Ontario, tracer test, Water Resources Research, 27 (6): 1345-1359.

Cressie, Noel A. C.:1993, Statistics for Spatial Data. John Wiley & Sons, New York, New York.

Guiguer, N. and Frind, E. O.: 1994, Dissolution and mass transfer processes for residual organics in the saturated groundwater zone, In *Proceedings of the* International Symposium on Transport and Reactive Processes in Aquifers*:* International Association for Hydraulic Research, Zurich, April 11-15.

Guilley, F.: 2004, l'emploi des huiles biodegradables dans les ecosystemes forestiers en remplacement des huiles minerales polluantes, projet fin d'études pour un diplôme d'ingénieur de l'ENSTIB.

Hamond, M. C.: 1995, Modélisation de l'extension de la pollution de la nappe phréatique d'Alsace par le tétrachlorure de carbone au droit et à l'aval de Benfeld, mémoire pour le DESS sciences de l'environnement à l'IMFS.

Harvey, C. F. and Gorelick, S. M.: 1995, Temporal moment-generating equations: Modeling transport and mass-transfer in heterogeneous aquifers, *Water Resources Research*, 31(8):1895.911.

Hoogeweg, C. G.: 1999, Impact of uncertainty in model input data on predicted pesticide leaching, Ph.D. Dissertation, University of Florida, FL.

Hoteit, H. and Acherer, Ph.:2003, TRACES user's guide V 1.00, Institut mécanique des fluides et des solides de Strasbourg.

Hoteit, H., Acherer, Ph., Mose, R., Erhel, J. and Philippe, B.: 2004, New two dimensional slope limiters for discontinuous Galerkin methods on arbitrary

meshes. International Journal of Numerical Methods in Engineering, 61 (14), 2566-2593.

HSG 108: 1998, IPCS International programme on chemical safety health and safety, Guide No. 108 carbon tetrachloride health and safety guide**.**

Hu, B. X. and Huang, H.: 2002, Stochastic analysis of reactive solute transport in heterogeneous, fractured porous media: a dual permeability approach, *Transport in Porous Media,* 48 (1): 1-39.

Hu, B. X., Huang, H. and Zhang, D.: 2002, Stochastic analysis of solute transport in heterogeneous, dual-permeability media, *Water Resource Research,* 38 (9): 14-1-14-16.

IMFS-BURGEAP: 1999, Etude de l'evolution de la pollution de la nappe d'Alsace par des organochlores volatils au droit et à l'aval de Benfeld, Rapport IMFS-BURGEAP ave annexes.

Imhoff, P. T., Jaffe, P. R. and Pinder, G. F.: 1994, An experimental study of complete dissolution of nonaqueous phase liquid in saturated porous media, Water Resources Research, 30 (1): 307-320.

Imhoff, P. T., Mann, A. S., Mercer, M. and Fitzpatrick, M.: 2003, Scaling DNAPL migration from the laboratory to the field, Journal of Contamination Hydrology, 64: 73–92.

IPCS: 1999, Carbon Tetrachloride, Geneva, World Health Organization, International Programme on Chemical Safety, pp. 1-177 (Environmental Health Criteria 208).

Istok, J. D., Field, J. A., Schroth, M. H., Davis, B. M. and Dwarakanath, V.: 2002, Single-well 'Push–Pull' partitioning tracer test for NAPL detection in the subsurface. Environ. Sci. Technol. 36: 2708–2716.

James, A. L. and Oldenburg, C. M.: 1997, Linear and Monte Carlo uncertainty analysis for subsurface contaminant transport simulation, *Water Resources Research*, 33 (11): 2495-2508.Kosugi, K. : 1996, Lognormal distribution model for unsaturated soil hydraulic properties, *Water Resources Research*, 32, 2697-2703.

Jeffers, P. M., Ward, L. M., Woytowitch, L. M. and Wolfe, N. L.: 1989, Homogeneous Hydrolysis Rate Constants for Selected Chlorinated Methanes, Ethenes, and Propanes, Environ. Sci. Technol. 23(8): 965-969.

Jeffers, P. M., Brenner, C. and Wolfe, N. L.: 1996, Hydrolysis of carbon tetrachloride, Environ. Toxicol. Chem. 15(7): 1064-1065.

Kaluarachchi, J. J., Cvetkovic, V. and Berglund, S.: 2000, Stochastic analysis of oxygenand nitrate-based biodegradation of hydrocarbons in aquifers, *Journal of Contaminant Hydrology*, 41 (3-4): 335-365.

Karickhoff, S. W., Brown, D. S. and Scott, T. A.: 1979, Sorption of Hydrophobic Pollutants on Natural Sediments, Water Res., Vol.13, pp. 241-248.

Kinzelbach, W.: 1986, Groundwater Modelling, Developments in Water Science 25, Elsevier Science Publishers, Amsterdam

Knox, R. C., Sabatini, D. A. and Canter, L. W.: 1993, Subsurface Transport and Fate Processes, Lewis Publishers, Boca Raton, Florida, 430 p.

Kucera, E.: 1965, Contribution to the theory of chromatography: linear non-equilibrium elution chromatography. J. Chromatogr. 19, 237–248.

Kueper, B. H., Redman, J. D., Starr, R. C., Reitsma, S. and Mah, M.,: 1993, A field experiment to study the behaviour of tetrachloroethylene below the water table: spatial distribution of residual and pooled DNAPL. Journal of Ground Water, Vol. 31, No. 5, pp. 756-766.

Kueper, B. H., Wealthall, G. P., Smith, J. W. N., Leharne, S. A. and Lerner, D. N.: 2003, An Illustrated handbook of DNAPL fate and transport in the subsurface, R&D Publ., vol. 133, Environment Agency, UK, 63 pp.

Lahkim, M. B., and Garcia, L. A.: 1999, Stochastic modeling of exposure and risk in a contaminated heterogeneous aquifer, 1: Monte Carlo uncertainty analysis, Environmental Engineering Science, 16 (5): 315-328.

Larsen, T., Kjeldsen, P. and Christensen, T. H.: 1992, Sorption of hydrophobic hydrocarbons on three aquifer materials in a flow through system, Chemosphere 24:439-451.

Larson, R. A. and Weber, E. J.: 1994, Reaction mechanisms in environmental organic chemistry: Lewis Publishers, Boca Raton, FL, 433 p.

Lasatoskie, C.: 1999, Cell and contaminant migration in heterogeneous porous media: implications for In situ bioremediation, Michigan State University Department of Chemical Engineering.

Lerner, D. N.: 2003, Surface water-groundwater interactions in the context of groundwater resources, In Xu, Y.; Beekman, H. E. (Eds.), Groundwater recharge estimation in Southern Africa, Paris, France: UNESCO, pp.91-107.

Levy, J. and Ludy, E. E.: 2000, Uncertainty quantification for delineation of wellhead protection areas using the Gauss- Hermite Quadrature approach. Ground Water. Vol. 38, no. 1, pp. 63-75.

Lyman, W. J., Reehl, W. F., and Rosenblatt, D. H.: 1990, Handbook of chemical property estimation methods, American Chemical Society, Washington, D.C.

Macdonald, T. L.: 1982, Chemical mechanisms of halocarbon metabolism, Crit. Rev. Toxicol. 11, pp. 85-120.

Mackay, D. M., Freyberg, D. L., Goltz, M. N.: 1983, A field experiment of ground water transport of halogenated organic solutes (Preprint Extended Abstract), American Chemical Society 196th National Meeting of Division of Environmental Chemists 23:368-371.

Mackay, D., Shiu, W. Y., Maijanen, A. and Feenstra, S.: 1991, Dissolution of nonaqueous phase liquids in groundwater, J. Contam. Hydrol. 8(1), pp. 23-42.

Mahar, P. S. and Datta, B.: 1997, Optimal monitoring network and ground-water pollution source identification, Journal of Water Resources Planning and Management-ASCE, 123 (4): 199-207.

Mahar, P. S., and Datta, B.: 2000, Identification of pollution sources in transient groundwater systems, Water Resources Management, 14 (3): 209-227.

Mahar, P.S., and Datta, B.: 2001, Optimal identification of groundwater pollution sources and parameter estimation, ASCE Journal of Water Resources Planning and Management, 27(1), 20-29.

McCarty, P. L. and Semprini, L.: 1994, Ground-water treatment for chlorinated solvents. p. 87-116. In R. D. Norris et al. (eds.) *Handbook of Bioremediation*, Lewis Publishers, Boca Raton.

Mendoza, C. A. and McAlary, T. A.: 1990, Modeling of ground-water contamination caused by organic solvent vapors, Ground Water, Vol. 28, No. 2.

Middelkoop, H.: 1998, Twice a river, Rhine and Meuse in the Netherlands, RIZA report 98.041 Arnhem: RIZA.

Miller, C. T., Poirier-McNeill, M. M. and Mayer, A. S.: 1990, Dissolution of trapped nonaqueous phase liquids: mass transfer characteristics, *Water Resources Research*, 26(11): 2783-2796.

Mosé, R., Siegel, P., Ackerer, P. et Chavent, G.: 1994, Application of the mixed hybrid finite element approximation in a groundwater flow model: Luxury or necessity, *Water Resources Research*, 30 (11), 3001-3012.

Naff, R. L., Haley, D. F. and Sudicky, E. A.: 1998a, High-resolution Monte Carlo simulation of flow and conservative transport in heterogeneous porous media, 1. methodology and flow results, Water Resources Research, 34 (4): 663-677.

Naff, R. L., Haley, D. F. and Sudicky, E. A.: 1998b. High-resolution Monte Carlo simulation of flow and conservative transport in heterogeneous porous media, 2. transport results, Water Resources Research, 34 (4): 679-697.

Newell, C. J., Rifai, H. S., Wilson, A. J., Connor, J. A., Aziz, C. E. and Suarez, M. P.: 2002, Calculation and use of first-order rate constants for monitored natural attenuation studies, US EPA Ground Water Issue, EPA/540/S-02/500.

NIOSH: 1994, Pocket Guide to Chemical Hazards, U. S. Dept. of Health and Human Services, National Institute for Occupational Safety and Health, NIOSH publication #94-116.

Nyer, E. K. and Duffin, M. E.: 1997, The state of the art of bioremediation, Ground Water Monitoring and Remediation, Spring, 64-69.

Oldenhuis, R., Vink, R. L., Janssen, D. B. and Witholt, B.: 1989, Degradation of Chlorinated Aliphatic Hydrocarbons by Methylosinus Trichosporium OB3b Expressing Soluble Methane Monooxygenas, Appl. Environ. Microbiol, 55: pp.2819-2826.

Pankow, J. F. and Cherry, J. A.: 1996, Dense chlorinated solvents and other DNAPLs in groundwater, Waterloo Press, Canada, pp. 522.

Parsons F., Barrio Lage, G. and Rice, R.: 1985, Biotransformation of chlorinated organic solvents in static microcosms, Environ. Toxicol Chem., 4: 739-742.

Peaudecerf, P. and Sauty, J. P.: 1978, Application of a mathematical model to the characterization of dispersion effects of groundwater quality, Prog. Water Technol. 10(5/6): 443-454.

Picardal, F. W., Arnold, R. G. and Huey, B. B.: 1995, Effects of electron donor and acceptor conditions on reductive dehalogenation of tetrachloromethane by Shewanella putrefaciens 200, Appl. Environ. Microbiol. 61: 8–12.

Pickens, F. J. and Grisak, E. G.: 1981, Scale dependent dispersion in stratified granular aquifer, Water Resources Research, 17(4): 1191-1211.

Powers, S. E., Abriola, L. M. and Weber, W. J.: 1992, An experimental investigation of nonaqueous phase liquid dissolution in saturated subsurface systems: steady state mass transfer, Water Resour. Res. 28 (10), 2691– 2705.

Raviart, P. A. and Thomas, J. M., 1977: A mixed finite element method for second order elliptic problems. In Mathematical Aspects of the finite elements method, Vol. 606, Magenes E, Springer, New York.

Ragion Alsace: 1997, étude de l'évolution de la pollution de la nappe d'Alsace par des organochlorés au droit et a l'aval de Benfeld, rapport final, No. 71-2-0400/3.

Rifai, H. S., Borden, R. C., Wilson, J. T. and Ward, C. H.: 1995, Intrinsic Bioattenuation for Subsurface Restoration, in R. E. Hinchee and others (eds.), Intrinsic Bioremediation, Columbus, Ohio, Battelle Press, p. 1-29.

Rivett, M. O. and Allen-King, R. M.: 2003, A controlled field experiment on groundwater contamination by a multicomponent DNAPL: dissolved-plume retardation, J. Contam Hydrol., 66, 117-146.

Rivett, M. O., Drewes, J., Barrett, M., Appleyard, S., Chilton, J., Dieter, H., Wauchope, D., Kerndorff, H. and Fastner, J.: 2004, World Health Organization Technical Report 02683, Chemicals: health relevance, transport and attenuation.

Schafer, W.: 2001, Predicting natural attenuation of Xylene in groundwater using a numerical model, Journal of Contaminant Hydrology, 52, p 57-83.

Schulz, K., Huwe, B. and Peiffer, S.: 1999, Parameter uncertainty in chemical equilibrium calculations using fuzzy set theory, Journal of Hydrology, 217 (1): 119-134.

Schwille, F.: 1988, Dense chlorinated solvents in porous and fractured media: model experiments (Engl. Transl.), Lewis Publishers, Ann Arbor, MI, pp. 146.

Sciortino, A., Harmon, T. C. and Yeh, W-G: 2000, Inverse modeling for locating dense nonaqueous pools in groundwater under steady flow conditions, Water Resources Research, 36(7), 1723-1735.

Shiu, W. Y., Ng, A .L. Y. and Mackay, D. M.: 1988, Preparation of aqueous solutions of sparingly soluble organic substances: ii. Multicomponent systems-hydrocarbon mixtures and petroleum products, Environmental Toxicology and Chemistry, 7, 125–137.

Siegel, P., Mosé, R., Ackerer, Ph. and Jaffré, J.: 1997, Solution of the advection-diffusion equation using a combination of discontinuous and mixed finite elements. International Journal For Numerical Methods in Fluids, 24:595-613.

Simler, L.: 1979, La nappe phréatique de la plaine du Rhin en Alsace, these collective de sciences géologiques, mémoire n°60, Université Louis Pasteur, Strasbourg, p. 266.

Singh, R. M. and Datta, B.: 2004, Groundwater pollution source identification and simultaneous parameter estimation using pattern matching by artificial neural network, Environmental Forensics , Vol 5, No.3, 143-159.

Singh, R. M., Datta, B. and Jain, A.: 2004, Identification of Unknown groundwater pollution sources using artificial neural networks, Journal of Water Resources Planning and Management, ASCE, Vol.130, No.6, 506-514.

Singh, R. M., and Datta, B.: 2006a, Identification of groundwater pollution sources using GA based linked simulation optimization, Journal of Hydrologic Engineering, ASCE.

Singh, R. M. and Datta B.: 2006b, Artificial neural network modeling for identification of unknown pollution sources in groundwater with partially missing concentration observation data, Water Resources Management, doi: 10.1007/s11269-006-9029-z.

Skaggs, T. H. and Kabala, Z. H.: 1994, Recovering the release history of a groundwater contaminant, Water Resour. Res. 30(1), 71–79.

Sleep, B. E. and Sykes, J. F.: 1989, Modeling the transport of volatile organics in variably saturated media, Water Resources Research, 25 (1): 81-92.

Stenger, A. and Willinger, M.: 1998, Preservation value for groundwater quality in a large aquifer: a contingent-valuation study of the Alsatian aquifer, Journal of Environmental Management, 53, 177–193.

Suarez, P. M. and Rifai, S. H.:1999, Biodegradation rates for fuel hydrocarbons and chlorinated solvents in groundwater, Bioremediation Journal, 3(4), pp. 337-362.

Sudicky, E. A. and Cherry, J. A.: 1979, Field observations of tracer dispersion under natural flow conditions in an unconfined sandy aquifer. Water Pollut. Res. Can. 14:1-17.

Thomas, J. : 1977, Sur l'analyse numérique des méthodes d'elément finis hybrides et mixtes, Thèse de Doctorat d'Etat, Université de Pierre et Marie Curie.

Truex, M. J., Murray, C. J., Cole, C. R., Cameron, R. J., Johnson, M. D., Skeen, R. S. and Johnson, C. D.: 2001, Assessment of carbon tetrachloride groundwater transport in support of the Hanford carbon tetrachloride innovative technology

demonstration program, Pacific Northwest National Laboratory, US Department of Energy.

UNEP: 1996, The 1987 Montreal protocol on substances that deplete the ozone layer as adjusted and amended by the Second, Fourth and Seventh Meeting of the Parties. In: Handbook for the international treaties for the protection of the ozone layer, 4th ed. Nairobi, Kenya, United Nations Environment Programme, pp 18-39.

U.S. EPA: 1986, Background Document for the Ground-Water Screening Procedure to Support 40 CFR Part 269 - Land Disposal: EPA/530-SW-86-047.

U.S. EPA: 1997, Guiding Principles for Monte Carlo Analysis, USEPA EPA/630/R-97/001, U.S. Environmental Protection Agency, Risk Assessment Forum, Washington, DC, 35 pp.

U.S. EPA: 1998, Technical fact sheet on Carbon Tetrachloride, National Primary Drinking Water Regulations, www://epa.gov/OGWDW/dwh/t-voc/carbonte.html.

Valocchi, A. J.: 1985, Validity of the local equilibrium assumption for modeling sorbing solute transport through homogenous soils. Water Resour. Res. 21 (6), 808– 820.

Vanderborght, J., Mallants, D. and Feyen, J.: 1998, Solute transport in a heterogeneous soil for boundary and initial conditions: evaluation of first-order approximations, Water Resources Research, 34 (12): 3255-3269.

Vannelli, T., Logan, M., Arciero, D. M. and Hooper, A. B.: 1990, Degradation of halogenated aliphatic compounds by the ammonia-oxidizing bacterium nitrosomonas europaea, Appl. Environ. Microbiol, 56: pp.1169-1171.

Vigouroux, P., Vançon, J. P. and Drogue, C. : 1983, Conception d'un model de propagation de pollution en nappe aquifer-Exemple d'application à la nappe du Rhin, Journal of Hydrology 64, Issues 1-4, p. 267– 279.

Villemin, T. and Bergerat, F. : 1987, L'évolution structurale du fossé rhénan au cours du Cénozoïque: un bilan de la de´ formation et des effets thermiques de l'extension, Bull Geol. France 8:245–255.

VILLIGER-Sytemtechnik report: 2004, l'échantillonnage multiniveaux, PZ Benfeld/Sand, avec annexes.

Vogel, T. M.: 1994, Natural bioremediation of chlorinated solvents, In: Handbook of Bioremediation, Lewis Publishers, Boca Raton, FL.

Wagner, B. J.: 1992, Simultaneous parameter estimation and contaminant source characterization for coupled groundwater flow and contamiant transprot modelling, J. Hydrol. 135, 275–303.

Walton, B. T., Hendricks, M. S., Anderson, T. A., Griest, W. H., Merriweather, R., Beauchamp, J. J. and Francis, C. W.: 1992, Soil sorption of volatile and semivolatile organic compounds in a mixture, J. Environ. Qual. 21: 552-558.

Wiedemeier, T. H., Rifai, H. S., Newell, C. J. and Wilson, J. T.: 1999, Natural attenuation of fuels and chlorinated solvents in the subsurface, John Wiley & Sons, Inc., New York.

Wolfe, W. J., Haugh, C. J., Webbers, A., and Diehl, T. H.: 1997, Preliminary conceptual models of the occurrence, fate and transport of chlorinated solvents in Karst regions of Tennessee, U.S. Geological Survey Water Resources Investigations, Report 97-4097.

Zhu, J. and Sykes, J. F.: 2000a, Stochastic simulations of NAPL mass transport in variably saturated heterogeneous porous media, Transport in Porous Media, 39 (3): 289-314.

Zhu, J. and Sykes, J. F.: 2000b, The influence of NAPL dissolution characteristics on field-scale contaminant transport in subsurface, Journal of Contaminant Hydrology, 41: 133-154.